A Decade of Lessons Learned from the 2011 Tohoku-oki Earthquake

N. Uchida[1], and R. Bürgmann[2]

[1]Graduate School of Science and International Research Institute of Disaster Science, Tohoku University

[2] Department of Earth and Planetary Science, University of California, Berkeley

Corresponding author: Naoki Uchida (naoki.uchida.b6@tohoku.ac.jp)

Key Points:

- The lessons learned in the last decade highlight more realistic estimation of seismic hazard and importance of interdisciplinary study.
- Pre-2011 studies based on a variety of evidence did not result in a consensus assessment of the great-earthquake hazard.
- Despite the precursory foreshocks and slow slip and improved monitoring capabilities, prediction of such events still appears impossible.

Abstract

The 2011 Mw 9.0 Tohoku-oki earthquake is one of the world's best-recorded ruptures. In the aftermath of this devastating event, it is important to learn from the complete record. We describe the state of knowledge of the megathrust earthquake generation process before the earthquake, and what has been learned in the decade since the historic event. Prior to 2011, there were a number of studies suggesting the potential of a great megathrust earthquake in NE Japan from geodesy, geology, seismology, geomorphology, and paleoseismology, but results from each field were not enough to enable a consensus assessment of the hazard. A transient unfastening of interplate coupling and foreshock activity were recognized before the earthquake, but did not lead to alerts. Since the mainshock, follow-up studies have (1) documented that the rupture occurred in an area with a large interplate slip deficit, (2) established large near-trench coseismic slip, (3) examined structural anomalies and fault-zone materials correlated with the coseismic slip, (4) clarified the historical and paleoseismic recurrence of M~9 earthquakes, and (5) identified various kinds of possible precursors. The studies have also illuminated the heterogeneous distribution of coseismic rupture, aftershocks, slow earthquakes and aseismic afterslip, and the enduring viscoelastic response, which together make up the complex megathrust earthquake cycle. Given these scientific advances, the enhanced seismic hazard of an impending great earthquake can now be more accurately established, although we do not believe such an event could be predicted with confidence.

Plain Language Summary

The Mw 9 Tohoku-oki earthquake was one of the most disastrous earthquakes in recent history. In this review, we first clarify the knowledge of the earthquake and tsunami potential before the earthquake. Pre-Tohoku-oki studies partly recognized the potential of Mw 8 or larger earthquakes. However, the knowledge based on different types of observations was incomplete and the occurrence of such a great event was not considered in the official earthquake probabilities. The improved understanding of earthquake-cycle and rupture processes since the Tohoku-oki earthquake advanced the leading edge of efforts to characterize megathrust earthquake hazards. We can summarize the lessons as follows. 1) The incorporation of interdisciplinary research is essential to advance our understanding of the processes underlying the occurrence of earthquakes. 2) The recognition of earthquake potential informed by geologic evidence extending beyond available instrumental records is essential for assessing the largest possible earthquake in a subduction zone. 3) The development of advanced scientific infrastructure, especially ocean-bottom observations is necessary to evaluate earthquake potential and monitor dynamic megathrust fault-zone processes. 4) Although post-Tohoku-oki studies have better characterized the hazard and a number of possible precursors have been identified, the confident prediction of such events appears impossible in the near future.

1 Introduction

The Mw 9.0 Tohoku-oki earthquake occurred off the Pacific coast of the Tohoku region of Japan, on March 11, 2011 (Fig. 1). A M7-8 earthquake with rupture dimensions of about ~100km was expected along this segment of the subduction zone but it was far larger with a rupture area of about 300 x 200 km (Fig. 2). The strong shaking and tsunami from the event caused devastating damage. The loss of life was as large as 19,729 and more than 121,996

houses were completely destroyed [*Fire and disaster management agancy*, 2020]. Earthquake early warning and tsunami warnings were issued by the Japan Meteorological Agency (JMA) as part of the routine operation of Japan's earthquake monitoring system, but the initial warnings underestimated the impending shaking and tsunami [*Hoshiba and Iwakiri*, 2011].

The earthquake is probably one of the most scientifically important recent subduction zone ruptures. There have been many studies on the earthquake, including several review papers focused on various aspects of the earthquake. Previous reviews illuminate the observations and characteristics of the coseismic rupture [*Lay*, 2018; *Satake and Fujii*, 2014; *Tajima et al.*, 2013], provide insights gained from geodetic deformation measurements [*Nishimura et al.*, 2014], examine the environment, structure and mechanical properties of the shallow megathrust from ocean bottom drilling [*Brodsky et al.*, 2020], describe preseismic processes from seismicity and geodetic observations [*Hasegawa and Yoshida*, 2015], summarize the tsunami source mechanism [*Pararas-Carayannis*, 2014], and assess post-earthquake changes in earthquake hazard [*Somerville*, 2014]. There are also early overviews of broad knowledge about the earthquake gained within a few years following the mainshock [*Hino*, 2015; *Tajima et al.*, 2013]. However, there are no comprehensive reviews that summarize the advancement of knowledge across a broad range of scientific disciplines after a decade of investigations of the earthquake. Our review targets the whole earthquake-cycle process (before, during and after the earthquake), draws on evidence from a wide range of disciplines (seismology, geodesy, geology, geomorphology, and paleoseismology), and covers up-to-date information based on research up to ~10 years after the earthquake.

While there had been many studies of this subduction zone before the earthquake, the knowledge did not lead to awareness of the potential of an M~9 earthquake and scenarios considering large near-trench slip in official hazard assessments at Tohoku. One of the missing pieces was an interdisciplinary understanding of the potential of great megathrust earthquakes based on the wide range of available evidence. Here, we integrate the lessons learned from this event and review insights about the earthquake occurrence process derived from various disciplines. We summarize and evaluate retrospective investigations of pre-earthquake processes and highlight new ocean bottom observations established after the earthquake, which are another missing piece of the pre-Tohoku-oki level of understanding. We believe that such an assessment is also important to make good use of the lessons in scientific studies and hazard mitigation efforts in other subduction zones around the world, where there is a great need to better understand the potential of future damaging earthquakes.

2 Knowledge before the earthquake

2.1 Seismic and geodetic coupling

Since megathrust ruptures occur to release accumulated stress due to the coupling on the plate interface, it is important to know the distribution of coupled areas to identify the potential source areas of interplate earthquakes. There are two primary methods to infer the interplate coupling, which rely on the slip of known historic interplate seismic events and the interseismic surface deformation of the upper plate. We refer to the coupling derived from seismic and geodetic data as seismic and geodetic coupling, respectively. The seismic coupling is the ratio of the rate of slip released by observed earthquakes to the rate of relative plate motion and associated slip-deficit accumulation across the seismogenic depth extent of the megathrust. For offshore Tohoku, the seismic coupling ratio was estimated to be 0.18-0.24 [*Pacheco et al.*, 1993;

Peterson and Seno, 1984] from just under one hundred years of data. On the other hand, the geodetic coupling was estimated to be substantially higher off Tohoku (0.5 – 1.0) [*C Hashimoto et al.*, 2009; *Loveless and Meade*, 2010; *Nishimura et al.*, 2000; *Suwa et al.*, 2006] (Fig. 3). This indicates a factor of two to five discrepancy between the estimates of seismic and geodetic coupling.

The major source of uncertainty for the seismic coupling estimates is the limited observation period. If the observation period does not include occurrences of the largest earthquakes, the estimation becomes very uncertain. On the other hand, major uncertainties of the geodetic estimates based on on-land data are due to the possibility of temporal coupling changes during the interseismic period, low resolution of the degree of coupling near the trench, and unknown mechanisms in the release of the slip deficit (i.e., by earthquakes or slow slip events). Nevertheless, the evaluation of the interplate locking state represents a fundamental objective to infer the potential of large earthquakes and the discrepancy in seismic and geodetic coupling estimates was not thoroughly discussed in most studies. One important discussion of the discrepancy, which was made before the Tohoku-oki earthquake, is that by *Kanamori et al.* [2006]. Based on their estimate of much smaller seismic coupling (~0.25) than geodetic coupling (~1) in the central part (offshore Miyagi, Fig. 2a) of the future Tohoku-oki earthquake rupture, they proposed the possibility that the accumulated slip deficit will eventually be released by large megathrust events. However, *Kanamori et al.* [2006] also considered other possibilities, including resolution problems in the estimates from geodetic data, and strain release by slow tsunami earthquakes or silent earthquakes. The recognition of silent earthquakes and afterslip, which can release moments comparable to that of large earthquakes [e.g., *K. Heki et al.*, 1997; *Kawasaki et al.*, 2001], was behind the consideration of such aseismic process. Offshore observation of ocean-bottom geodetic observations using GPS-Acoustic ranging had just started in 2005, 6-years before the Tohoku-oki earthquake [*Sato et al.*, 2011b], however the number of stations was small and the data had not yet been used to formally reassess the degree of coupling in the wide near-trench area.

2.2 Geologic and historic evidence of megathrust earthquakes

The geologic and historic evidence of past M>8 earthquakes provides one of the most direct ways to document the possibility of such great events. Written records of a very large earthquake and tsunami in the Tohoku area exist for the 869 Jyogan and 1611 Keicho earthquakes [*H Abe et al.*, 1990; *T Usami*, 1996]. In addition, oral legends pertaining to the 869 Jyogan earthquake and tsunami persisted along the coast of Miyagi prefecture to Ibaraki prefecture (Fig. 4a, [*H Watanabe*, 2001]), although it is difficult to assign accurate timing and size of the earthquake from this type of information. Importantly, tsunami deposits of the Jyogan earthquake were found in the Sendai plain [*H Abe et al.*, 1990; *Minoura and Nakaya*, 1991], suggesting the occurrence of a large interplate earthquake and tsunami that carried water several kilometers inland. The distribution of young tsunami deposits that are possibly associated with the 869 and 1611 Keicho earthquakes was found to extend over a wide area of the Sendai [*Minoura and Nakaya*, 1991; *Sawai et al.*, 2007] and Ishinomaki [*Shishikura et al.*, 2007] plains, years before the Tohoku-oki earthquake (Fig. 4a). Some of the tsunami deposits initially attributed to the 1611 Keicho earthquake were later associated with the 1454 Kyotoku earthquake [*Sawai et al.*, 2012]. These studies also found additional tsunami deposits older than the 869 event and estimated the recurrence interval to be 600 -1400 years [*Sawai et al.*, 2007] and 500 - 1000 years [*Shishikura et al.*, 2007]. *Satake et al.* [2008], *Namegaya et al.* [2010] and

Sugawara et al. [2011] used numerical simulations to infer the source fault of the 869 Jyogan earthquake from the tsunami deposit data and estimated a rupture of Mw >8.4, 8.4 and 8.3, respectively.

The discrepancy between the long-term deformation at geological time scales and short-term deformation measured by geodetic methods in the land area of Tohoku provides additional constraints on the probability of rare very large events. The geodetic observations in the last 100 years have revealed strain accumulation rates as high as 10^{-7} per year. However, geologically observed strain rates, based on slip rates on active faults and folding are as low as 10^{-8} per year [*Ikeda*, 1996; *Kaizuka and Imaizumi*, 1984]. This suggests that while the elastic rebound is likely incomplete, it still accounts for most of the geodetically observed deformation in this area. Thus, *Ikeda* [1996] suggested that the strain accumulated at high rates in the last 100 years will be released by big earthquake(s) with magnitude 8 or greater, rather than by distributed deformation away from the plate interface.

In summary, studies of the distribution of tsunami deposits, written records and oral legends, and the discrepancy in the deformation rate at geodetic and geologic time scales all suggested the occurrence of megathrust events much larger than the instrumentally observed earthquakes offshore Tohoku (Fig. 5), although the detailed nature of such earthquakes remained unclear.

2.3 Other indicators of earthquake potential

There are other approaches to assess the potential of very large megathrust earthquakes. *Ruff and Kanamori* [1980] investigated correlations between variations in coupling and other physical features of subduction zones and suggested that fast plate convergence rates and young plate ages are correlated with the occurrence of great earthquakes. Since the convergence rate at Tohoku-oki region is relatively high (~9 cm/yr) but the subducting Pacific slab is old (~130 Ma), the relationship suggested by *Ruff and Kanamori* [1980] would suggest a maximum earthquake of roughly M 8.2. However, the 2004 Sumatra earthquake (Mw 9.1), which occurred in a slow subduction zone with an old slab, had already clearly violated such a general relationship [e.g., *McCaffrey*, 2008]. The earthquake size distribution, such as the Gutenberg–Richter frequency-magnitude law, can also be used to statistically infer the maximum earthquake size in a region. For example, *Kagan* [1997] estimated M8.6 as the maximum size for the Japan-Kurile-Kamchatka region, a relatively high value close to the magnitude of the eventual Tohoku-oki earthquake. Other attempts for estimating earthquake probabilities prospectively were based on a variety of methods, and efforts by the Collaboratory for the Study of Earthquake Predictability (CSEP) to assess such efforts had started before the Tohoku-oki earthquake [*Nanjo et al.*, 2011]. A total of 35 forecast models had been submitted before the Tohoku-oki earthquake, but they did not intend to estimate the potential of very large earthquakes.

2.4 Long-term earthquake forecast

Figure 6 shows the segments offshore Tohoku considered in the official assessment of the long-term subduction earthquake probabilities, which was effective at the time of the 2011 Tohoku-oki earthquake [*Headquarters of Earthquake Research Promotion*, 2002]. The offshore Tohoku area was divided into source regions based on 11 earthquakes since 1611 (Fig. 5). The maximum considered magnitude was M8.2 in the near-trench area off northern Sanriku to off-Boso and southern Sanriku-oki. The earthquake probabilities were estimated for each individual segment. In the near-trench area from northern Sanriku-oki to Boso-oki, compound hazard from

interplate and normal-faulting earthquakes in the Pacific plate were also considered. The possibility of earthquakes with larger rupture areas was not considered, with one exception; in the off Miyagi area, simultaneous rupture was allowed for the Miyagi-ken oki and southern Sanriku-oki regions (pink shaded area), and the size of the compound rupture was estimated to be M8.2. The considered segment failures were too small compared to the eventual rupture area of the 2011 Tohoku-oki earthquake, which ruptured a wide area that encompassed at least five segments considered in the long-term forecast (Fig. 6).

There was evidence that earthquake ruptures had occurred repeatedly in some of the smaller segments. Figure 5a shows the distribution of the slip areas for Mw≥7 earthquakes in 1930-2002 from *Yamanaka and Kikuchi* [2004] and *Murotani et al.* [2003]. They show that some of the slip areas appear to be overlapping and may represent repeat failures. The compilation of aftershock areas and tsunami source areas from instrumental data spanning 85 and 118 years, respectively, (Fig. 5b and c) also shows that some of the sources are located in the same area. The evidence for repeating ruptures was established for M~7 [*Yamanaka and Kikuchi*, 2004] and much smaller repeating earthquakes [*Igarashi et al.*, 2003] in the same subduction zone, as well as for some other historical plate boundary earthquakes [e.g., *Murray and Langbein*, 2006]. Therefore, it came natural to infer that the same fault area repeatedly produces characteristic earthquakes of nearly the same size [*Hasegawa et al.*, 2009; *Schwartz and Coppersmith*, 1984]. However, there was also evidence of multisegment ruptures and partial rupture of previous large megathrust slip zones in the Aleutian subduction zone [*Shennan et al.*, 2009], Kuril subduction zone [*Nanayama et al.*, 2003], Sumatra subduction zone [*Konca et al.*, 2008], and Nankai subduction zone [*M Ando*, 1975]. In addition, there were indications that smaller sized earthquakes occur within the slip areas of larger ruptures, including frequent partial ruptures of a middle-sized (M~5) off-Kamaishi repeating earthquake sequence [*Uchida et al.*, 2007], suggesting a hierarchical structure of the slip area. Heterogeneous frictional parameters or multi-scale heterogeneity may explain such observations [*Hori and Miyazaki*, 2010; *Ide and Aochi*, 2005]. This means that if we define likely rupture segments based only on the so far observed, smaller-sized events, even if they had occurred repeatedly, we neglect the real possibility of much larger earthquakes. In any case, the official long-term forecast and most individual studies before 2011 did not consider the occurrence of M~9 earthquakes offshore Tohoku, largely because of insufficient evidence for ruptures of that size.

2.5 Reported anomalies before the earthquake

The central part of Tohoku-oki, the Miyagi-oki area where M~7.5 earthquakes occurred every ~30 years, was considered as one of the most probable locations of pending earthquakes and the long-term forecast suggested a 90% or larger probability of rupture before 2030 [*Headquarters of Earthquake Research Promotion*, 2000]. Therefore, the area received special attention, although the expected magnitude of the earthquake was moderate. Notably, a M 7.3 earthquake occurred 2 days before the Tohoku-oki earthquake just updip of the expected Miyagi-oki earthquake (Figs 2 and 5). However, there were no pre-Tohoku-oki reports on the foreshock and related monitoring results or forecasting attempts.

Changes in interplate coupling offshore Tohoku were being investigated based on Global Positioning System (GPS) time series and repeating earthquake data sets. The 2009 report of a project “Research and Observation of the Miyagi-Oki Earthquake” under The Headquarters for Earthquake Research Promotion (HERP), which aimed to quantify coupling and its temporal changes, indicated that both the GPS and repeating earthquake data show relative uncoupling in

the south Tohoku area since 2008 [*Headquarters for Earthquake Research Promotion, Ministry of Education, Culture, Sports, Science and Technology, Japan,,*, 2009] (Fig. 7). The underlying observations were clear, but the results were not published in peer-reviewed journals until after the earthquake (see section 4.2) and the report did not include discussions of potential future earthquakes.

The moderate seismic activity during February of 2011 in the off Miyagi area, which included a M5.5 earthquake, was reported on March 9 (2 days before the Tohoku-oki earthquake) at the monthly meeting of HERP. It was considered to be similar to previous periods of seismic activity including M5-6 earthquakes that occur sometimes in the area [*Headquarters for Earthquake Research Promotion, Ministry of Education, Culture, Sports, Science and Technology, Japan,* 2011]. The M7.3 foreshock that occurred later on March 9 (Fig. 2a) did not get evaluated by the HERP but several institutes published information on their webpages, mostly on the general information on the earthquake type and previous seismic activity near the source. One detailed posting with interpretation was posted by Tohoku University, which also commented on the apparent uncoupling that had occurred since around 2008 [*Research Center for Prediction of Earthquakes and Volcanic Eruptions*, 2011]. However, again there was no discussion of possible future large earthquakes. To the contrary, since the M 7.3 slip area was considered to be located in southern Sanriku-oki, where simultaneous rupture with the Miyagi-oki region had been considered (Fig. 6), other researchers considered that the occurrence of the M7.3 earthquake decreased the possibility of large multi-segment earthquakes [e.g., *Kahoku-shinpo*, 2011]. The fact that these geodetic and repeating earthquake anomalies over the last several years and the early 2011 foreshock activity were not investigated in detail and discussed as a potential anomaly related to enhanced megathrust earthquake hazard before the Tohoku-oki earthquake probably reflects the still limited level of knowledge of the subduction zone before the Tohoku-oki earthquake. Other kinds of potential precursory anomalies were, as far as we know, only pointed out retrospectively after the Tohoku-oki earthquake had occurred.

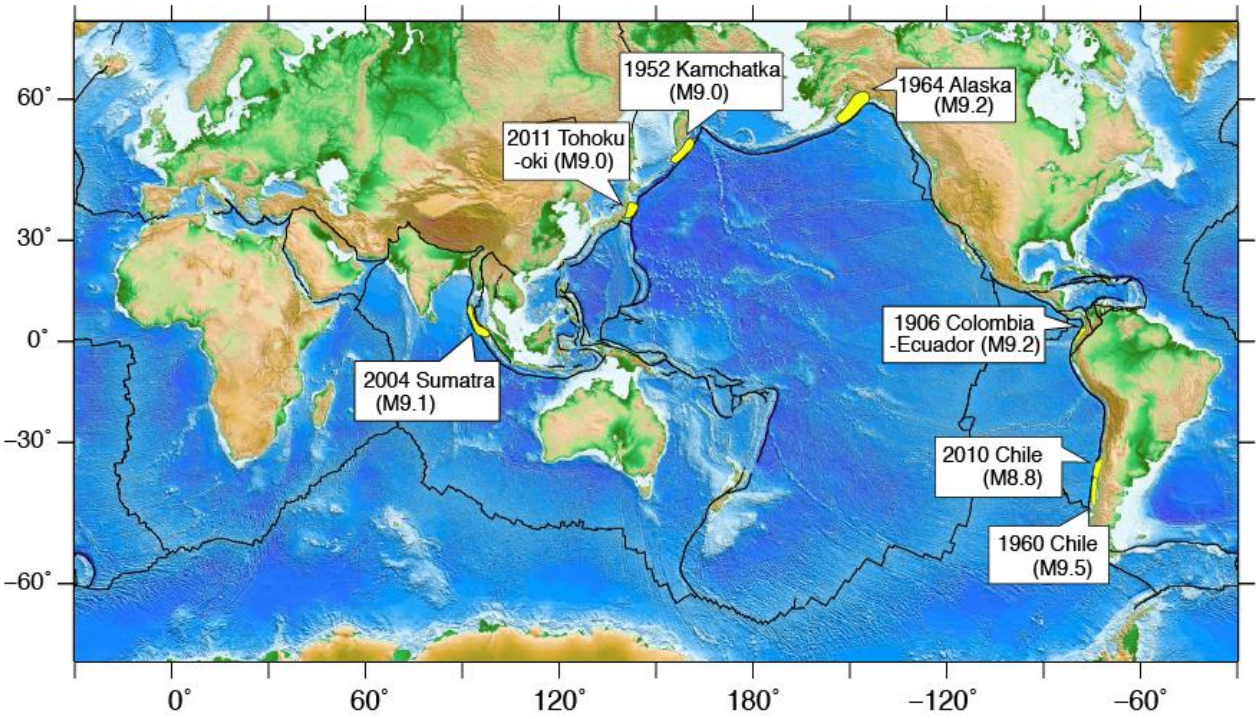

Figure 1 Global distribution of instrumentally recorded M>8.8 earthquakes. The rupture areas are schematically shown by yellow polygons. The moment magnitudes are based on U. S. Geological Survey except for the Tohoku-oki earthquake which is based on JMA.

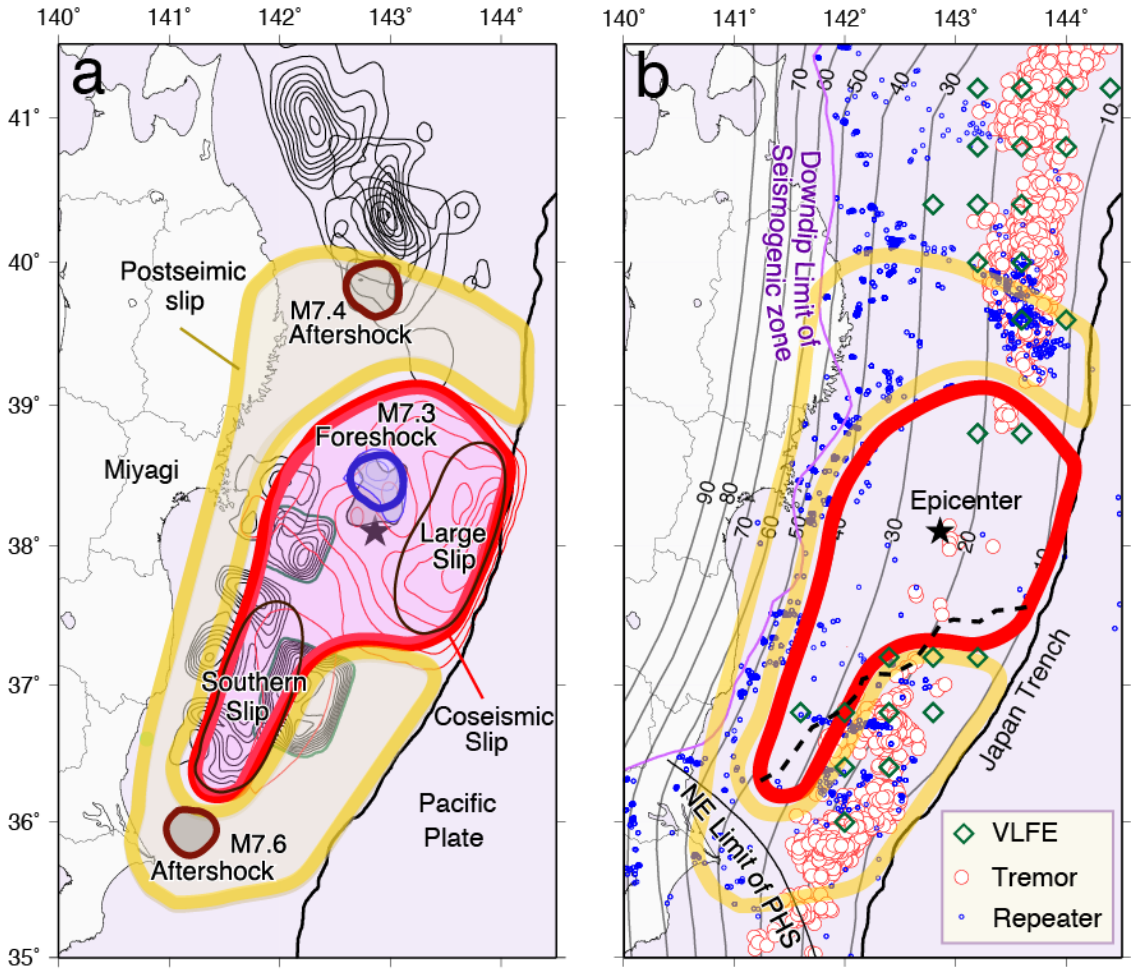

Figure 2 A schematic model showing the coseismic (red) and postseismic slip areas (orange) of the 2011 Tohoku-oki earthquake with observed slip areas of previous earthquakes (a) and postseismic distribution of Very Low Frequency Earthquakes (VLFEs, green diamonds, Baba et al. 2020), tremors (red circles, *Nishikawa et al.* [2019]) and repeating earthquakes (small blue circles, *Nishikawa et al.* [2019]) (b). In (a), the slip distribution of the 2011 Tohoku-oki earthquake is shown with 10 m intervals [*Iinuma et al.*, 2012]. The slip distribution of other M>=7 earthquakes by *Yamanaka and Kikuchi* [2004] and *Murotani et al.* [2003] are shown with 0.5 m and 1 m contour intervals, respectively, to the north and south of 37.7°N in black. In (b) the gray contour lines show the depth of the plate boundary and a magenta line indicates the downdip limit of the seismogenic zone [*Igarashi et al.*, 2001; *Kita et al.*, 2010a; *Uchida et al.*, 2009]. The dashed black line show forearc segment boundary from residual topography and gravity anomalies data [*Bassett et al.*, 2016]. The northeastern limit of the Philippine Sea plate (PHS) on the subducting Pacific plate is from [*Uchida et al.*, 2009].

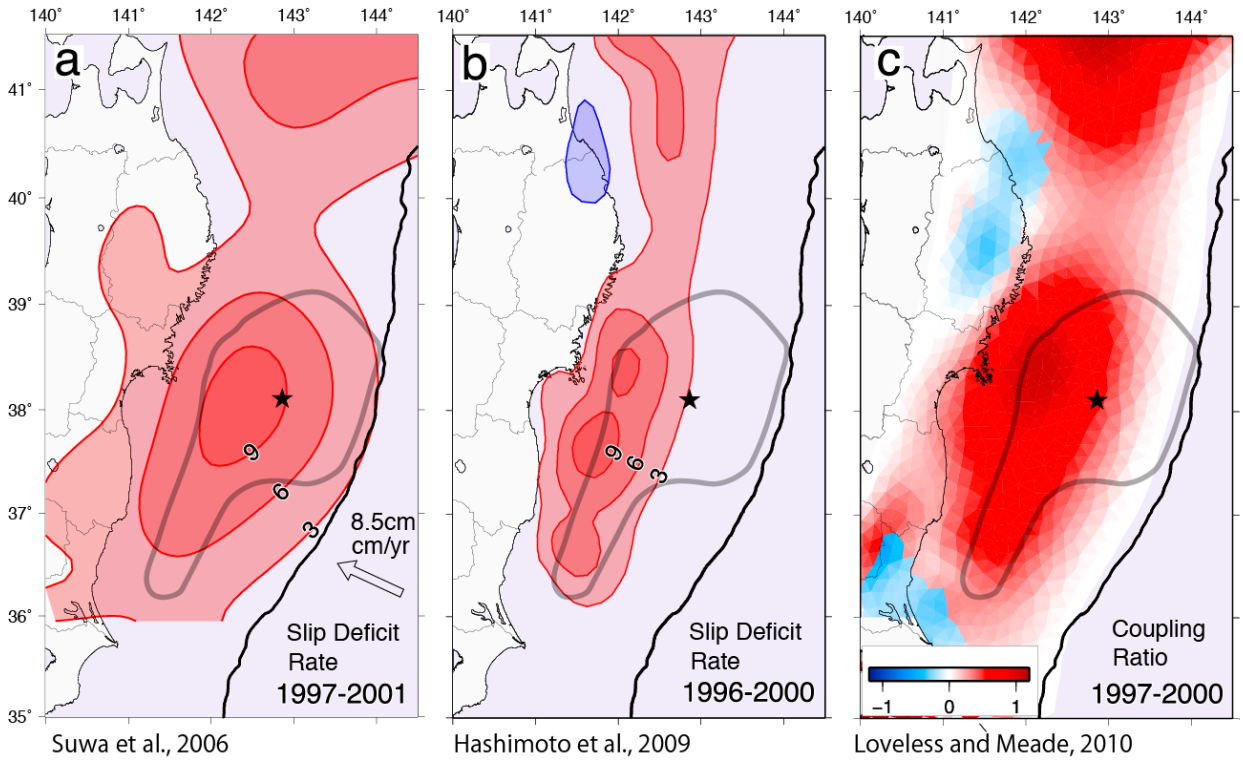

Figure 3 Distribution of slip deficit rate (a, b) and coupling ratio (c) from model inversions of interseismic on-land GPS velocities. (a) The distribution of slip deficit rate from 1997 to 2001 [*Suwa et al.*, 2006]. (b) The distribution of slip deficit rate from 1996 to 2000 [*C Hashimoto et al.*, 2009]. The contour interval for (a) and (b) is 3 cm/year. (c) The distribution of coupling ratio from January 1997 to May 2000 [*Loveless and Meade*, 2010] . The stars show the epicenter of the 2011 Tohoku-oki earthquake. Note that there are wide areas of large slip deficit or coupling ratio offshore southern Tohoku in all three models, which correspond to the approximate slip area of the Tohoku-oki earthquake (gray line, the same area as shown in Fig. 2). Note also that the model resolution in the near-trench area is poor and largely depends on the assumed boundary conditions.

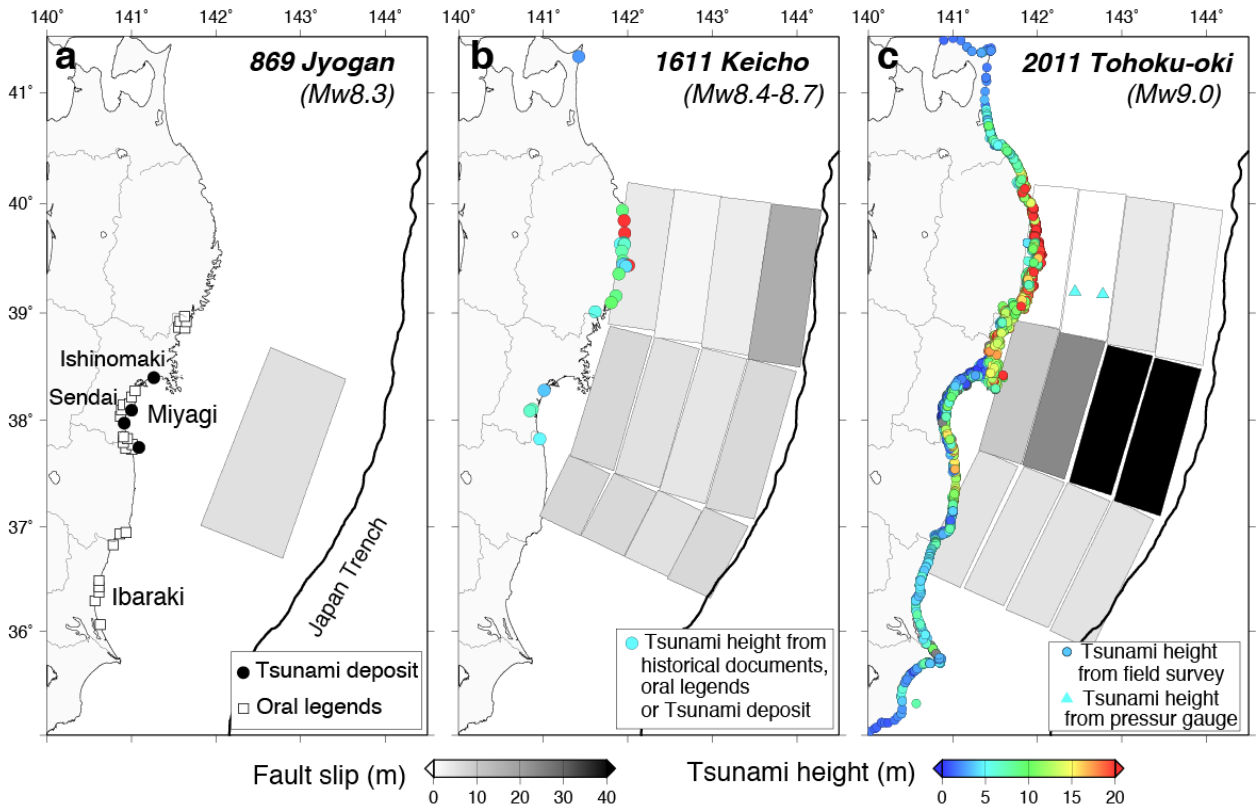

Figure 4. The tsunami observations and source models for the (a) 869 Jyogan, (b) 1611 Keicho and (c) 2011 Tohoku-oki earthquakes. The symbols along the coast and triangles in (c) show the locations of tsunami data. The data in (a) represent oral legends of tsunami at locations shown by squares [*H Watanabe*, 2001] and excavated tsunami deposits at black circles [*H Abe et al.*, 1990; *Minoura et al.*, 2001; *Minoura and Nakaya*, 1991; *Sawai et al.*, 2008; *Sawai et al.*, 2007; *Shishikura et al.*, 2007; *Sugawara et al.*, 2010; *Sugawara et al.*, 2001]. These data do not provide tsunami run-up height values. The historical observation data in (b) represent written documents and oral legends except for the northernmost point that is based on the absence of tsunami deposits attributed to the 1611 event. The data are from *Ebina and Imai* [2014], *Hatori* [1975], [*Yoshinonu Tsuji and Ueda*, 1995], Tsuji and Ueda [1995], *Yoshinomu Tsuji et al.* [2011] and [*Yoshinobu Tsuji et al.*, 2012]. The observation data in (c) show field survey measurements of tsunami height by the *Tsunami Joint Survey Group* [2011]. Please note both run-up heights and inundation heights are shown. The rectangles show the tsunami source models based on these observations except for (c), which is only based on the waveforms of the two offshore pressure gauges (cyan triangles). The data source are (a) *Sugawara et al.* [2011] (b) *Imai et al.* [2015] and (c) *Maeda et al.* [2011].

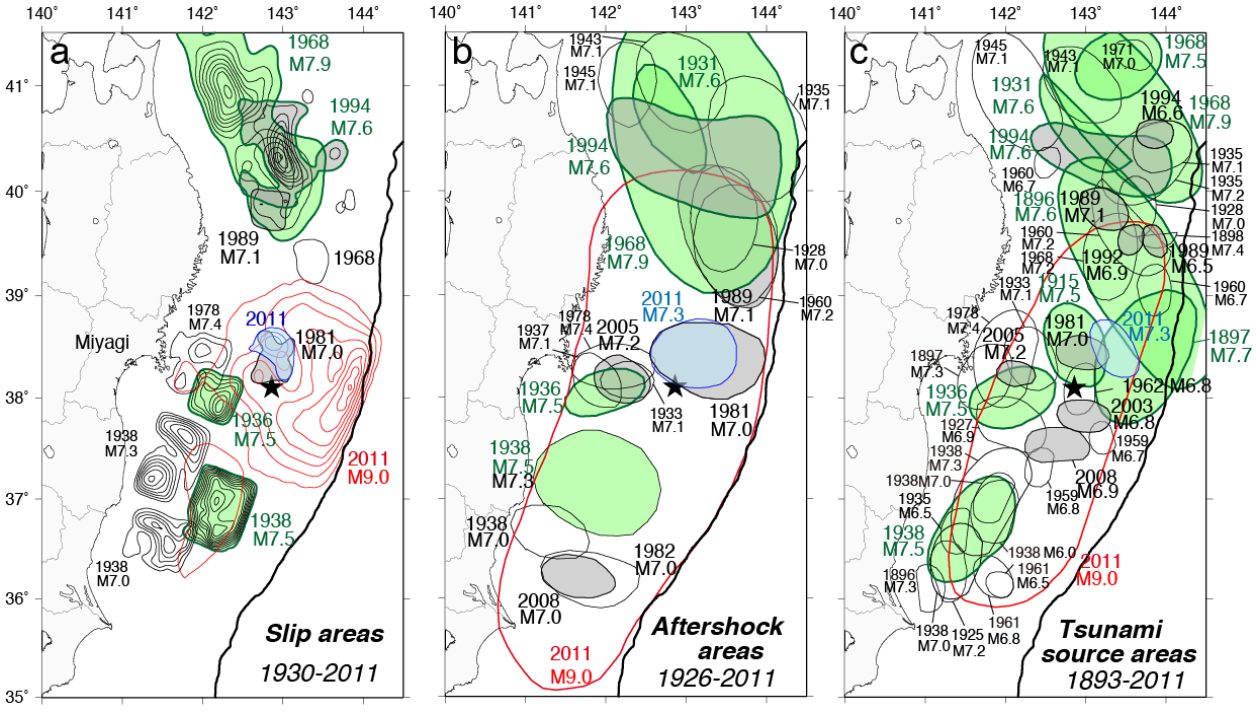

Figure 5 The distribution of interplate earthquake source areas from instrumental records. Green, gray and blue lines show M7.5 or larger earthquake, 1980 or more recent earthquakes, and the March 9, 2011 foreshock, respectively. Red lines and black star show the source area and epicenter of the 2011 Tohoku-oki earthquake. (a) Slip distributions based on seismic waveform inversions. The slip area of the 2011 Tohoku-oki earthquake in 10 m intervals [*Iinuma et al.*, 2012] is shown in red and was obtained from terrestrial and seafloor geodetic data. The slip distribution of other M≧7 earthquakes by *Yamanaka and Kikuchi* [2004] and *Murotani et al.* [2003] are shown with 0.5 m and 1 m contour intervals, respectively, to the north and south of 37.7°N. The foreshock slip is by *Ohta et al.* [2012a] with 0.5 m contour intervals. (b) Aftershock areas that are thought to delineate the extent of source ruptures for M≧7 earthquakes. The data are *Hasegawa et al.* [1985] and *Uchida et al.* [2009]. The foreshock and aftershock areas for the 2011 Tohoku-oki earthquake were added in blue and red in this study based on the distribution of aftershocks from the first 24 hours. (c) The tsunami source areas of interplate earthquakes that produced coseismic ocean bottom deformation. The red line shows the 2011 Tohoku-oki earthquake [*Hatori*, 2012]. The other data are [*Hatori*, 1972; 1974; 1975; 1976; 1978; 1989; 1996].

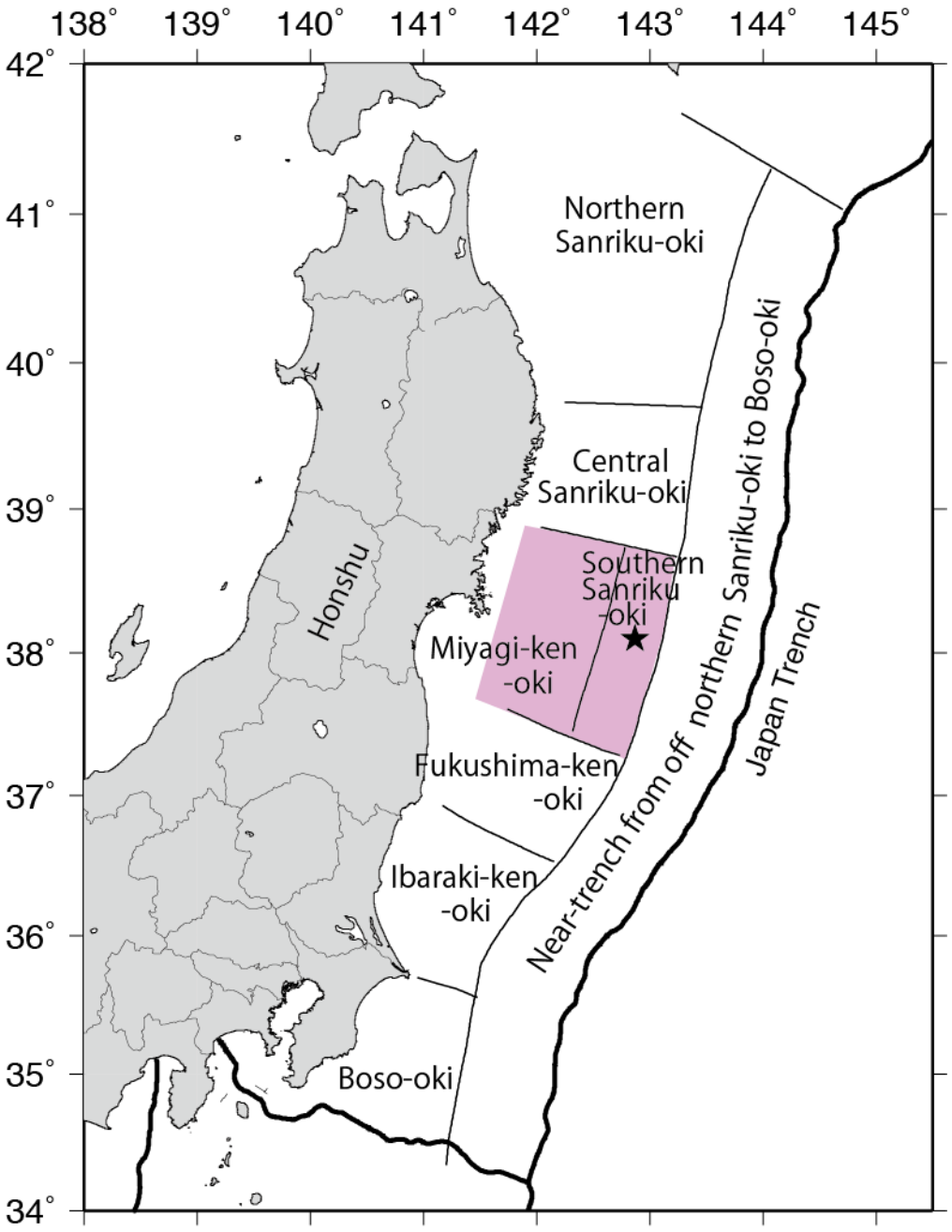

Figure 6 Inferred rupture segmentation along the Japan trench for which long-term earthquake probabilities were estimated by the Earthquake Research Committee of the Headquarters for Earthquake Research Promotion. The colored patches represent the segments for which multi-segment rupture was considered. For the near-trench segment, both interplate and intraplate earthquakes are considered and are not assumed to rupture the whole area simultaneously. The star shows the epicenter of the Tohoku-oki earthquake. Modified from *Headquarters of Earthquake Research Promotion* [2002].

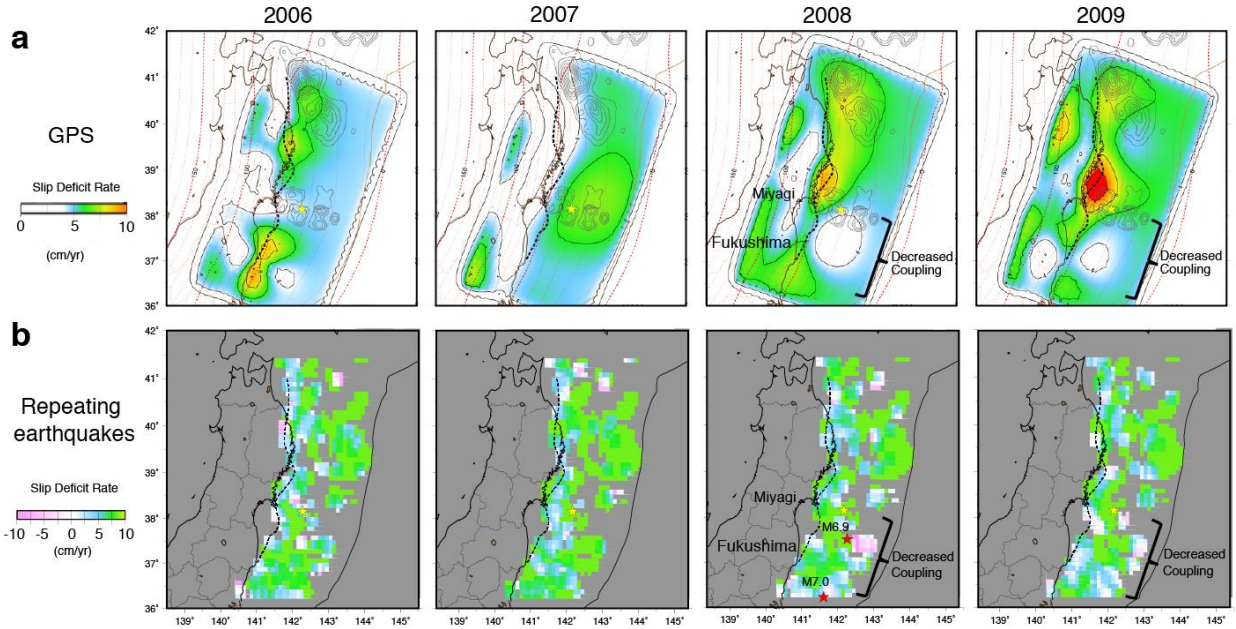

Figure 7 The distribution of slip deficit rate from GPS data and repeating earthquakes from 2006 to 2009. The years are shown a the top of each panel (after Figs 6 and 14 of section 3.1, *Headquarters for Earthquake Research Promotion, Ministry of Education, Culture, Sports, Science and Technology, Japan,*, [2009]). As the repeating earthquake analysis estimates slip rate, it was converted to slip deficit rate using the plate convergence rate of 8.5 cm/year. Please also note that the GPS and repeater data suggest zero or negative (slip in excess of long-term rates) slip deficit off Fukushima after 2008.

3 The features of the Tohoku-oki earthquake

3.1 Co- and postseismic observations of the earthquake

The characteristics of the coseismic and postseismic slip processes of the Tohoku-oki earthquake were constrained with better spatio-temporal resolution than previous M~9 earthquakes, benefitting from on-land and offshore geophysical observations. The data that were available in real time or near-real time are mostly from land stations and include geodetic observations (high sampling rate GPS, tilt meter, strain meter) and seismic data (broad band seismometer, strong motion, short period seismometer) and far-field geodetic and seismic data. The on-land area (Honshu Island) is one of the most densely instrumented areas in the world but located outside of the slip area. Nonetheless, the real time seismic data were valuable for rapid estimation of seismic intensity and magnitude (for earthquake early warning) and tsunami heights based on the seismic source model, although the station density is of limited advantage for initial source characterization. The tsunami waveforms collected at coastal tide gauges are also available for source parameter studies, but most of the gauges are clipped by the large tsunami (Fig. 8). Two cabled pressure gauges off Sanriku [*Hino et al.*, 2001; *Maeda et al.*, 2011]) and GPS buoys [*Satake et al.*, 2013] were also available to obtain data of the sea surface height (tsunami, Fig 9c).

The geophysical data acquired by permanently operating networks in the Japanese islands also contributed to more detailed analysis. The seismic network allowed for the detection of local triggered earthquakes [e.g., *Lengliné et al.*, 2012; *Miyazawa*, 2011; *Okada et al.*, 2015], and changes in elastic earth structure [e.g., *Sawazaki et al.*, 2015; *Takagi and Okada*, 2012]. The global broadband seismic network and arrays contributed to understand the source process and offshore seismicity immediately after the earthquake [e.g., *Kiser and Ishii*, 2013; *Lay et al.*, 2011b]. Data from the dense GPS network revealed details of the heterogeneous co- and postseismic surface deformation fields in the land area, which contributed to better understanding of the rheological structure beneath the arc [*Meneses-Gutierrez and Sagiya*, 2016; *Muto et al.*, 2016; *Ohzono et al.*, 2013].

The offshore geophysical measurement capabilities that were developed in recent decades [e.g., *Bürgmann and Chadwell*, 2014] provided unprecedented data for this earthquake soon after the earthquake. The horizontal movements of the seafloor around the main slip area were measured by seven GPS-Acoustic (combined geodetic technique of GPS and acoustic ranging) stations (Fig. 9a, [*Kido et al.*, 2011; *Sato et al.*, 2011a]. The campaign style repeat observations collected 17-31 days after the Tohoku-oki earthquake revealed as much as 31 m horizontal coseismic sea bottom displacement [*Kido et al.*, 2011; *Sato et al.*, 2011a]. The vertical coseismic movement of the seafloor was also constrained at some of the stations by the GPS-Acoustic system [*Kido et al.*, 2011] as well as by ten campaign-style seafloor pressure gauges near the epicenter that had been deployed before the Tohoku-oki earthquake ([*Iinuma et al.*, 2016; *Y Ito et al.*, 2011b], Fig. 9c). The Deep-ocean Assessment and Reporting of Tsunamis (DART) buoys east of the Japan trench and nearshore GPS-buoys (Fig. 9c) also recorded the tsunami [e.g., *Satake et al.*, 2013].

The geophysical and geological surveys conducted (before and) after the earthquake on land and the ocean bottom also provided new constraints on the coseismic rupture process. Multi-beam active source surveys of the bathymetry were performed within 11 days to 5 years after the Tohoku-oki earthquake and compared with data collected before the earthquake. Similarly, a seismic reflection survey was completed 3-20 days after the earthquake to compare

with pre-earthquake data [*Kodaira et al.*, 2012]. These data provided unprecedented constraints on the seafloor and frontal-wedge deformation near the trench (Fig. 10) [*Fujiwara et al.*, 2017; *Fujiwara et al.*, 2011; *Kodaira et al.*, 2020; *Kodaira et al.*, 2012]. An ocean bottom survey of the distribution of coseismic turbidites near the trench was also performed after the earthquake in 2012, 2013 and 2016 [*Ikehara et al.*, 2016; *McHugh et al.*, 2016; *Molenaar et al.*, 2019]. The Japan Trench Fast Drilling project in 2012 (JFAST) retrieved fault material from 820 m below the seafloor (location in Fig. 10) and recorded temperature time series for ~6 months around the recently ruptured fault, suggesting a very low frictional strength [e.g., *Brodsky et al.*, 2020; *Chester et al.*, 2013; *Fulton et al.*, 2013; *Ujiie et al.*, 2013]. Emergency observations of land areas by the phased-array-type L-band SAR (PALSAR) on Japan's ALOS satellite allowed for repeat image acquisitions 4 – 38 days after the Tohoku-oki earthquake, which provided centimeter-level crustal deformation at 10s of meter spatial resolution [*Kobayashi et al.*, 2011; *Y Takada and Fukushima*, 2013]. The large-scale coseismic and postseismic deformation of the lithosphere also produced permanent changes in the Earth's gravity field that were captured by the pair of Gravity Recovery And Climate Experiment (GRACE) satellites [*Matsuo and Heki*, 2011; *Lei Wang et al.*, 2012b]. Along the coast, post-earthquake field surveys revealed details of the spatial distribution of tsunami run up, inundation heights and area (*H Nakajima and Koarai* [2011]; *Sugawara et al.* [2013]; *Tsunami Joint Survey Group* [2011] Fig. 3c). The distribution of sandy tsunami deposits and long-lasting geochemical tracers of seawater in flooded areas provided new insights into the nature of tsunami inundation processes and allowed for more accurate estimation of the tsunami inundation area of paleo-tsunamis from sand and geochemical signatures [*Chagué-Goff et al.*, 2012; *K Goto et al.*, 2011].

In 2013, the deployment of a 5800 km-long cable hosting a network of seismometers and pressure gauges at 150 observation points (the S-net) was initiated, and S-net now provides seismic and geodetic data directly from above the megathrust fault [*Aoi et al.*, 2020; *National Research Institute for Earth Science and Disaster Resilience*, 2019]. In 2012, the GPS-Acoustic network measuring sea-bottom deformation was also enhanced to 26 stations, capturing the enduring postseismic deformation transients of the Tohoku-oki earthquake along the trench (Fig. 9b) [*Honsho et al.*, 2019; *Tomita et al.*, 2017; *S-i Watanabe et al.*, 2014].

3.2 Coseismic slip and tsunami

Early knowledge of the magnitude and location of the Mw9.0 Tohoku-oki earthquake was provided and disseminated in real time. An earthquake early warning was issued during this earthquake on the basis of coastal seismic records and successfully delivered to people in the Tohoku area [*Hoshiba and Iwakiri*, 2011]. The warning was issued before the S wave arrival and more than 15 s earlier than the strongest ground motion (intensity 5-lower or greater on the JMA scale) everywhere in the Tohoku area. The estimated magnitude, which was estimated from maximum displacement amplitudes, was only 7.2 for the first warning to the public. 116.8 s after the first trigger, the estimated magnitude was raised to 8.1 [*Hoshiba and Iwakiri*, 2011]. This is lower than the estimates from long-period or geodetic data analysis (Mw 9.0) provided later but comparable to the upper limit of the JMA displacement magnitude, which saturates for earthquakes Mw≧8. The initial tsunami warning was issued around three minutes after the earthquake based on the earthquake location and magnitude (M7.9) available at that time [*Japan Meteorological Agency*, 2013]. This first warning was only for 6 m, 3 m and 3 m run-up for the coast along the Miyagi, Fukushima and Iwate prefectures, respectively (Fig. 8), which was too

small compared with the observed heights of 10-20 m, 15-40 m and 8-15 m in the three prefectures (Fig. 4c) [*Tsunami Joint Survey Group*, 2011]. JMA upgraded its estimate of the maximum tsunami height twice based on observations on a GPS buoy 10 km offshore the coast and at coastal tide gauges. The final estimate issued 44 minutes after the earthquake was for a ≥10 m tsunami along a ≥200 km extent of the coast [*Japan Meteorological Agency*, 2013] (Fig. 8). JMA determined a magnitude of Mw 8.8 around 50 minutes after the earthquake by analyzing global seismic data which was not used to update the local warning because of the late timing (Fig. 8).

The coseismic slip of the Mw 9.0 Tohoku-oki earthquake was estimated from seismic waveform data [*Ammon et al.*, 2011; *Hayes*, 2011; *Ide et al.*, 2011; *Satriano et al.*, 2014; *Shao et al.*, 2011; *Suzuki et al.*, 2011; *Uchide*, 2013; *Yagi and Fukahata*, 2011; *Kunikazu Yoshida et al.*, 2011], geodetic surface deformation measurements [*Iinuma et al.*, 2012; *T Ito et al.*, 2011a; *Kyriakopoulos et al.*, 2013; *Ozawa et al.*, 2012; *Perfettini and Avouac*, 2014; *Pollitz et al.*, 2011; *Silverii et al.*, 2014; *Zhou et al.*, 2014], high-rate GPS time series [*Z Wang et al.*, 2016; *H. Yue and Lay*, 2011], tsunami wave observations [*Fujii et al.*, 2011; *Hossen et al.*, 2015; *Maeda et al.*, 2011; *Saito et al.*, 2011; *Satake et al.*, 2013], InSAR, and various combinations of these data [*Bletery et al.*, 2014; *Gusman et al.*, 2012; *Hooper et al.*, 2013; *Koketsu et al.*, 2011; *Kubo and Kakehi*, 2013; *Lee et al.*, 2011; *Melgar and Bock*, 2015; *Minson et al.*, 2014; *Romano et al.*, 2012; *Romano et al.*, 2014; *C Wang et al.*, 2012a; *R Wang et al.*, 2013; *Shengji Wei et al.*, 2012; *Yamazaki et al.*, 2018; *Yokota et al.*, 2011; *Han Yue and Lay*, 2013] (Fig. 11). Resolution tests of models constrained by individual datasets indicate that the strong motion data alone have limited resolution of slip updip from the hypocenter, while inversions of on-land static geodetic data can resolve slip out to the hypocenter but have no resolution of slip near the trench [*Shengji Wei et al.*, 2012]. On the other hand, Tsunami data and seafloor geodetic data are important to constrain shallow slip near the trench [*Koketsu et al.*, 2011; *Shengji Wei et al.*, 2012; *Yokota et al.*, 2011]. The seafloor deformation data off Miyagi provide resolution in the shallow updip area off Miyagi (central part of the peak-slip area and near the hypocenter) but the northern and southern regions remain unresolved due to the lack of stations [*Iinuma et al.*, 2016] (Fig. 9a).

According to the large number of studies, the overall feature of the coseismic slip can be summarized as follows. The Tohoku-oki earthquake rupture initiated in the Miyagi-oki area to the south of the foreshock (Fig. 5a). During the initial 20 second, the rupture first propagated to the north and then changed direction to the west (downdip) after the rupture reached the foreshock slip area [*Uchide*, 2013]. The downdip part of the coseismic slip includes the slip area of recurrent M~7.5 Miyagi-oki earthquakes [*Iinuma et al.*, 2012; *Pollitz et al.*, 2011]. Then, substantial slip continued for more than 100 seconds in the updip shallow part of the plate boundary [*Z Wang et al.*, 2016]. Some studies suggest repeated rupture of some sections occurred in this shallow updip area [*Ide et al.*, 2011; *Lee et al.*, 2011; *Z Wang et al.*, 2016]. The large slip area reaching to the trench produced seafloor uplift that caused the tsunami and led to the high tsunami run up along the Sanriku Coast and wide inundation in the Sendai plane [*Mori et al.*, 2011; *H Nakajima and Koarai*, 2011]. A deep southern expansion of the rupture with modest slip occurred after 110s [*Han Yue and Lay*, 2013]. In this downdip area, high-frequency radiation was prominent [e.g., *Koketsu et al.*, 2011; *Kurahashi and Irikura*, 2011; *Yokota et al.*, 2011; *Kunikazu Yoshida et al.*, 2011] (Fig. 12d). The existence of this southern extension of the rupture is consistent with the zone of reduced interplate seismicity extending from the northern large-slip area, as well as with the surrounding enhanced aftershock activity, indicative of stress drop in the coseismic slip area and stress increase in the surrounding areas (Fig. 2, Fig. 12a-c,

[*Kato and Igarashi*, 2012; *W Nakamura et al.*, 2016]. This southern extension corresponds to the location of many previous M~7 earthquakes, including the 1938 sequence (Fig. 5).

The duration of the rupture was estimated to be 171 s from high-frequency energy radiation [*Hara*, 2011] and 150 s from the joint inversion of seismic and geodetic data [*Minson et al.*, 2014]. The mean stress drop is 2.3 ± 1.3 MPa, based on the area within the 5 m slip contour from 40 published slip models and assuming a uniform rigidity of 40 GPa. However, locally the stress drop well exceeds 20 MPa for the majority of models [*Brown et al.*, 2015]. Some models using tsunami data or joint inversion suggest a northern extension of slip near the trench to ~40.0°N [e.g., *Hossen et al.*, 2015; *Satake et al.*, 2013; *Yokota et al.*, 2011]. However, slip models constrained by other data and aftershocks [*W Nakamura et al.*, 2016], differential seafloor bathymetry [*Kodaira et al.*, 2020], and near-trench turbidities [*Ikehara et al.*, 2016] (Fig. 10) suggest that the main coseismic slip is limited to the south of 39.2N. The higher-frequency tsunami waves [*Tappin et al.*, 2014] and seismic profiles of shallow structure [*Y Nakamura et al.*, 2020] showed that gravitational slope failures of the trench inner wall can also explain the proposed tsunami source around 39-40°N.

3.3 Implications of the coseismic slip

An especially important feature of the coseismic slip, we think, is that the main slip occurred in the area where a large slip deficit had been estimated from the GPS data before the earthquake [e.g., *C Hashimoto et al.*, 2012; *Loveless and Meade*, 2010; *Suwa et al.*, 2006]. The repeating earthquake data had also indicated a large slip deficit in the coseismic slip area before the earthquake [*Uchida and Matsuzawa*, 2011] and the trend of the compressional axis in the upper plate before the Tohoku-Oki earthquake also supported strain accumulation in the near-trench large-slip area [*Hasegawa et al.*, 2012]. Therefore, to first order the Tohoku-oki earthquake compensated the slip deficit that had accumulated in the wide area off Tohoku. There were arguments that other processes, such as slow slip events or tsunami earthquakes, could make up the slip deficit inferred from the discrepancy between geodetic and seismic coupling discussed in Section 2.1 [*Kanamori et al.*, 2006]; however, such events did not occur. This suggests that it is important to understand the variability of slip mode of the fault surface. Obviously, the instrumental record of ~100 years was insufficiently long to evaluate seismic coupling that is dominated by the largest earthquake. *Scholz and Campos* [2012] re-estimated the seismic coupling ratio to be 0.59 by considering M~9 Tohoku-oki earthquakes and assuming the a recurrence interval of 1000 years, based on the tsunami deposit observation of the 869 Jyogan earthquake. Despite the great uncertainties involved in either estimate, this updated value is consistent with the coupling from geodetic data (0.54 - 0.65).

The large near-trench slip was the second important feature of the Tohoku-oki earthquake that heightened the devastating tsunami and causalities. Although the variability of the slip models is large especially in the near-trench areas (Fig. 13), *Sun et al.* [2017] confirmed that $\geq$ 62 m slip reached to the trench by modeling the high-resolution bathymetry-change data of *Fujiwara et al.* [2011] (track MY101 and MY102 of Fig. 10) observed above the large-slip area. Closest to the trench, the change in shallow structure from seismic reflection data obtained before and after the earthquake, differential bathymetry, and sediment core data suggest that the slip reached to the seafloor at the trench axis [*Kodaira et al.*, 2012; *Strasser et al.*, 2013]. The near-trench slip in coseismic slip models occurred along a ~120-km-long section of the trench off Miyagi, which is consistent with the distribution of turbidite deposits in the trench [*Ikehara et*

583 *al.*, 2016; *Ikehara et al.*, 2018] and the along-trench extent of the bathymetry change [*Kodaira et*
584 *al.*, 2020] (Fig. 10). Due to the unconsolidated nature of fault-zone material in the shallow
585 megathrust, many studies assumed the area closest to the trench represents an aseismic slip zone
586 [e.g., *Bilek and Lay*, 2002; *Hyndman and Wang*, 1993; *Oleskevich et al.*, 1999]. Therefore, the
587 very large, near-trench seismic slip and resulting tsunami were a surprise to many, even though
588 the area was considered by some to be capable of generating tsunami earthquakes or sometimes
589 participating in larger ruptures [e.g., *Kanamori*, 1972; *Lay et al.*, 2012; *Tanioka and Satake*,
590 1996]. Dynamic weakening mechanisms [e.g., *Noda and Lapusta*, 2013; *Shengji Wei et al.*,
591 2012] and dynamic overshoot [e.g., *Fukuyama and Hok*, 2015; *Ide et al.*, 2011; *Kozdon and*
592 *Dunham*, 2013] may help explain the large slip all the way to the trench. Various models, for
593 example considering thermal pressurization [*Shibazaki et al.*, 2019], and rate- and state-
594 dependent friction with two state variables that lead to strong velocity weakening properties at
595 high slip velocities [*Shibazaki et al.*, 2011], have been proposed to explain such large shallow
596 slip. In addition, laboratory experiments on fault-zone material retrieved from the shallow
597 Tohoku plate-boundary by drilling suggest very low friction due to the presence of smectite
598 [*Ujiie et al.*, 2013]. The laboratory-derived properties of fault materials in combination with
599 dynamic rupture simulations of fault weakening and rupture propagation contribute to a more
600 realistic estimation of the near-trench slip mode [*Hirono et al.*, 2016]. The determination of near-
601 trench coupling and slip is now possible thanks to the recent addition of more GPS-Acoustic
602 stations [*Honsho et al.*, 2019]. As the shallow coseismic slip is directly linked to the height of the
603 resulting tsunami, it is generally important to accurately quantify the near-trench slip deficit in
604 all subduction zones.
605 In addition to the near-fault material, the large-scale structure was also examined to infer
606 the structure related to the Tohoku-oki earthquake. *Zhao et al.* [2011] used seismic tomography
607 and found that a high-velocity body exists above the plate boundary in the Miyagi-oki region
608 where the peak coseismic slip occurred. *K Wang and Bilek* [2014] suggest that relatively smooth
609 subducting seafloor is responsible for large megathrust earthquakes, including the 2011 Tohoku-
610 oki earthquake, from the global review of seismic and geodetic studies. *Bassett et al.* [2016]
611 found that the slip area of the Tohoku-oki earthquake is located to the north of a geologic
612 boundary revealed by residual topography and gravity anomalies (Fig. 2b), suggesting some
613 control of coseismic slip by the upper plate. *Kubo et al.* [2013] also found that the coseismic slip
614 and largest aftershock at the southern end of the coseismic rupture stopped to the north of the
615 area where the upper plate is the Philippine Sea plate (not the North America or Okhotsk plate
616 where the main slip occurred) (Fig. 2b). *Satriano et al.* [2014] interpreted the broadband
617 characteristics of the slip to along-dip differences of material properties and structure, including
618 the material of the overlying plate (crust/mantle), thermal structure and plate geometry. *Hua et*
619 *al.* [2020] used offshore seismometers (S-net) to find weak material above the shallow large slip
620 area from seismic tomography. *Lay et al.* [2012] related often-observed along-dip changes in
621 rupture characteristics of megathrust ruptures to first-order changes in material properties and
622 structure, including the Tohoku-oki earthquake (Fig. 12d). The material properties of the
623 overriding plate, morphology of the plate interface and fault zone and along-dip segmentation
624 may all contribute to the characteristics and size of the coseismic rupture. These observations
625 support an important influence of structural heterogeneities on the megathrust rupture mode.
626

3.4 Postseismic deformation and seismicity

Substantial postseismic deformation and seismicity were observed starting immediately following the Tohoku-oki earthquake, as captured by land and ocean bottom stations. The land GPS stations showed seaward movement (Fig. 9b) that can be explained by aseismic afterslip downdip of the coseismic slip area and near the coastline (Fig. 14) [e.g., *Iinuma et al.*, 2016; *Yamagiwa et al.*, 2015] as well as viscoelastic relaxation in the mantle wedge above the subducting slab [e.g., *Hu et al.*, 2016; *Sun et al.*, 2014]. The offshore geodetic data [*Honsho et al.*, 2019; *Tomita et al.*, 2017] again provided important constraints on the spatial distribution of offshore afterslip and allowed for the characterization of the viscoelastic response of the mantle above and below the Pacific plate. The offshore GPS-Acoustic stations above the large coseismic slip area showed landward movement (Fig. 9b) and subsidence, which can only be explained by relaxation of stresses induced by the thrust earthquake in the mantle below the downgoing plate [*Hu et al.*, 2016; *Sun et al.*, 2014]. On the other hand, the GPS-Acoustic stations to the north and south of the coseismic slip zone exhibit postseismic seaward motions caused by the rapid afterslip on the adjacent, poorly coupled sections of the plate boundary [*Honsho et al.*, 2019; *Tomita et al.*, 2017].

The afterslip of the Tohoku-oki earthquake was estimated by *Diao et al.* [2014]; *Hu et al.* [2016]; *Iinuma et al.* [2016]; *Johnson et al.* [2012]; *Ozawa et al.* [2012]; *Ozawa et al.* [2011]; *Shirzaei et al.* [2014]; *Silverii et al.* [2014]. In most studies, the contribution of viscoelastic relaxation was first removed to estimate postseismic slip on the plate boundary [e.g., *Diao et al.*, 2014; *Iinuma et al.*, 2016]. The postseismic slip area showed a complementary distribution with the coseismic slip (Fig. 14a, c) [*Iinuma et al.*, 2016; *Ozawa et al.*, 2012]. The distribution of accelerated repeating earthquakes on the plate interface also confirmed near-trench afterslip to the north of the coseismic rupture in addition to downdip and the shallow portion of the megathrust to the south (Fig. 14b) [*Uchida and Matsuzawa*, 2013]. The repeating earthquake data also indicated delayed acceleration in the afterslip at larger distances from the coseismic slip area, suggesting spatio-temporal propagation of the afterslip. The repeating earthquake data was also used with GNSS data to better constrain the interplate postseismic slip [*Shirzaei et al.*, 2014] and to improve the discrimination of interplate afterslip and viscoelastic response of the earth [*Hu et al.*, 2016].

Most of the interplate aftershocks occurred near the edge of the coseismic slip and can be considered as a proxy of afterslip. Two large, M7.4 and M7.6 aftershocks occurred just beyond the northern and southern edges of the coseismic slip area, on the day of the Tohoku-oki earthquake [*Kubo and Nishikawa*, 2020; *W Nakamura et al.*, 2016] (Fig. 2). The slip areas of the 2011 Tohoku-oki earthquake and these immediate aftershocks don't appear to overlap with the inferred areas of postseismic repeating earthquakes, earthquake swarms, tremors, and very low-frequency earthquakes on the plate interface (Fig. 2). Conversely, these seismic phenomena were strongly enhanced in the area surrounding the coseismic slip, which suggests the occurrence of aseismic slip there. The spatial distribution of tremors, very low-frequency earthquakes and repeating earthquakes in the subduction thrust before the Tohoku-oki earthquake are largely the same as in the postseismic period but they may have been more active near the large slip area [*Baba et al.*, 2020; *Katakami et al.*, 2018; *Takanori Matsuzawa et al.*, 2015; *Takahashi et al.*, 2020; *Uchida and Matsuzawa*, 2013]. The northern M 7.4 aftershock rupture area overlaps with the slip zones of previous M~7 earthquakes (Fig. 2) [*Kubo and Nishikawa*, 2020; *Nishikawa et al.*, 2019]. In the downdip plate interface and along the updip edge of the rupture, no large

interplate aftershocks occurred and the near-trench plate-boundary was especially silent after the Tohoku-oki earthquake [*Asano et al.*, 2011].

The aftershock focal mechanisms away from the plate interface were also consistent with the stress changes due to the coseismic slip of the Tohoku-oki earthquake and the postseismic slip [*Diao et al.*, 2014; *W Nakamura et al.*, 2016]. Seismicity on the updip side of the coseismic rupture was characterized by normal faulting earthquakes in the subducting plate (outer-rise and near-trench area) while the downdip side of the coseismic slip area was characterized by reverse-faulting earthquakes in the subducting plate and normal-faulting earthquakes are prominent in the upper plate [*W Nakamura et al.*, 2016]. On the downdip side, a significant rate increase of intermediate-depth earthquakes in the upper plane of the double seismic zone was observed [*Delbridge et al.*, 2017]. The upper plane of the double seismic zone is in downdip compression [*Hasegawa et al.*, 1978; *Kita et al.*, 2010b], and the increase of the stress due to coseismic and postseismic slip of the seismogenic plate interface apparently accelerated the deep intraplate seismicity [*Delbridge et al.*, 2017]. A relatively large reverse faulting earthquake (M7.1 on April 7, 2011), consistent with the coseismic stress change, occurred in the subducting slab and near the downdip end of the coseismic rupture. Based on a low-velocity feature observed by seismic tomography and the dip of the fault plane of this event, *J Nakajima et al.* [2011] suggested reactivation of a fault that was produced by the normal faulting in the outer-rise area. On the updip side, *Kubota et al.* [2019] examined an earthquake doublet (Mw 7.2 and 7.1 on December 7, 2012) in the subducting plate consisting of shallow normal- and deep reverse-faulting subevents near the trench, and pointed to the role of intraplate stress state changes due to the Tohoku-oki earthquake. In the outer-rise region of the incoming plate, many normal-faulting events, including a Mw7.7 event, were triggered. *Obana et al.* [2012] argued that the increase in the depth extent of normal-faulting events in the outer-rise area can be explained by the increased tensile bending stresses in the Pacific plate after the earthquake. Large interplate thrust events and outer-rise normal-faulting earthquakes produce slip-encouraging stress changes on each other, and paired interplate and outer-rise earthquakes are quite commonly observed in global subduction zones [*Lay et al.*, 2011a; *Lay et al.*, 2010].

Seismicity rates also significantly changed in the inland seismogenic upper crust (Fig. 16a) [*Okada et al.*, 2011; *Uchida et al.*, 2018]. The seismicity sometimes started few days to few weeks after the Tohoku-oki earthquake and many areas showed swarm activity and upward migrations [e.g., *Okada et al.*, 2015; *Okada et al.*, 2011; *Keisuke Yoshida and Hasegawa*, 2018; *Keisuke Yoshida et al.*, 2019](Fig. 16 c, d). Areas that were dominated by active thrust faulting prior to the Tohoku-oki earthquake showed reduced postseismic seismicity rates. Dynamic triggering of seismicity was also evident especially in the western part of Japan, consistent with triggering by surface waves out to a distance of nearly 1,350 km [*Kato et al.*, 2013; *Miyazawa*, 2011]. Small events and tremors triggered by the passage of seismic waves from the Tohoku-oki earthquake were also recognized globally [*Chao et al.*, 2013; *Gonzalez-Huizar et al.*, 2012].

3.5 Implications of the postseismic deformation and triggered seismicity

One of the most important features of the postseismic deformation revealed by the Tohoku-oki earthquake is the immediate and far-reaching viscoelastic response of the earth. This deformation represents the relaxation of coseismic stress changes by the flow of mantle and crustal material below the brittle-ductile transition zone. Since the postseismic deformation is caused by a combination of afterslip on the plate boundary, viscoelastic relaxation and

poroelastic rebound in the surrounding media, it is important to distinguish the contributions from these processes. *Sun and Wang* [2015] suggest that immediately after large megathrust earthquakes (Mw>8.0), viscoelastic deformation should always lead to opposing motion of inland and trench areas. Neglecting viscoelastic relaxation results in overestimation of postseismic slip downdip of the coseismic rupture and an underestimate of the afterslip at shallower depths [*Sun et al.*, 2014], because the contribution of the viscoelastic relaxation is trenchward in the land area and landward in the near-trench area (Fig. 15 a, b). Consideration of contributions of viscoelastic relaxation in the mantle above and below the downgoing slab (Fig. 15 a, b) together with independent constraints on afterslip from repeating earthquakes (Fig. 14 b & 15 c) improve the characterization of the different relaxation mechanisms following large subduction earthquake [*Hu et al.*, 2016].

The post-mainshock seismicity also provided important insights into the ambient state of stress and the frictional strength of the megathrust and surrounding faults. Prior to 2011, the stress field of the Tohoku region reflected east-west compression and earthquakes with reverse mechanisms dominated in the area. The coseismic Coulomb stress changes on the reverse faults were negative (Fig. 17), including on many known active faults in the area [*Toda et al.*, 2011a]. A large number of normal-faulting aftershocks suggests that the stress change during the mainshock was large enough, relative to the pre-earthquake ambient stress levels, to reverse the dominant style of faulting close to the large slip area [*Chiba et al.*, 2013; *Hardebeck*, 2012; *Hardebeck and Okada*, 2018; *Hasegawa et al.*, 2012; *Hasegawa et al.*, 2011]. A low background differential stress, on the order of the earthquake stress drop, is also supported by the analysis of ocean bottom borehole breakouts at the JFAST site (Fig. 10b) [*Brodsky et al.*, 2017; *Lin et al.*, 2013]. As the fault materials and temperature data collected at JFAST [e.g., *Brodsky et al.*, 2020; *Chester et al.*, 2013; *Fulton et al.*, 2013; *Ujiie et al.*, 2013], the low regional heat flow [*Gao and Wang*, 2014] and a forearc force-balance model [*K Wang et al.*, 2019] all suggest a weak fault, the Tohoku-oki earthquake can be characterized as the rupture of a weak fault in a low-stress environment [*Hardebeck*, 2015; *K Wang et al.*, 2019].

In the inland area, earthquakes with a variety of focal mechanisms were activated after the earthquake (Fig. 16a). They can potentially be explained by small faults with highly variable fault orientations [*Toda et al.*, 2011b], a heterogeneous local deviatoric stress field [*Keisuke Yoshida et al.*, 2019] and/or the upward movement of fluids into the fault zone that can reduce the effective normal stress on the faults (Fig. 16c) [*Keisuke Yoshida and Hasegawa*, 2018; *Keisuke Yoshida et al.*, 2019]. The role of fluid migration as an important mechanism of earthquake triggering is supported by the observation that many earthquake clusters only inititated after a few days to few weeks after the Tohoku-oki earthquake (Fig. 16d) [*Keisuke Yoshida et al.*, 2019]. Substantial spatial heterogeneity of stress orientations in the inland area before the 2011 Tohoku-oki earthquake was identified from focal-mechanism data and the anomalous areas corresponded to areas of increased seismic activity after the Tohoku-oki mainshock [*Imanishi et al.*, 2012; *Keisuke Yoshida et al.*, 2019]. One of the areas with anomalous stress orientations is located in region D of Fig. 16a. In this area, not only strong seismicity occurred but also a repeating earthquake pair of ~M6 that recurred within an anomalously short interval (5 years), suggesting that the postseismic deformation of the Tohoku-oki earthquake rapidly reloaded the shallow inland fault segment [*Fukushima et al.*, 2018].

Both postseismic deformation and aftershocks provide indirect evidence of the extent and magnitude of coseismic slip. There have been efforts to improve constraints on the spatial distribution of the coseismic slip by incorporating the postseismic seafloor geodetic (GPS-

763 Acoustic) time series and the inferred viscoelastic relaxation [*Tomita et al.*, 2020; *Yamagiwa et*
764 *al.*, 2015]. The concentration of aftershocks near the edges of the coseismic slip area helps
765 delineate details of the extent of coseismic rupture (Fig. 12 a-c). In turn, the interplate seismicity
766 was diminished in some areas due to the stress drop on the rupture and stress shadow effects (Fig.
767 12 a-c) [*Asano et al.*, 2011; *Kato and Igarashi*, 2012; *W Nakamura et al.*, 2016]. Thus,
768 postseismic observations can also be valuable to constrain the coseismic slip, independent of the
769 data obtained coseismically.
770
771
772
773

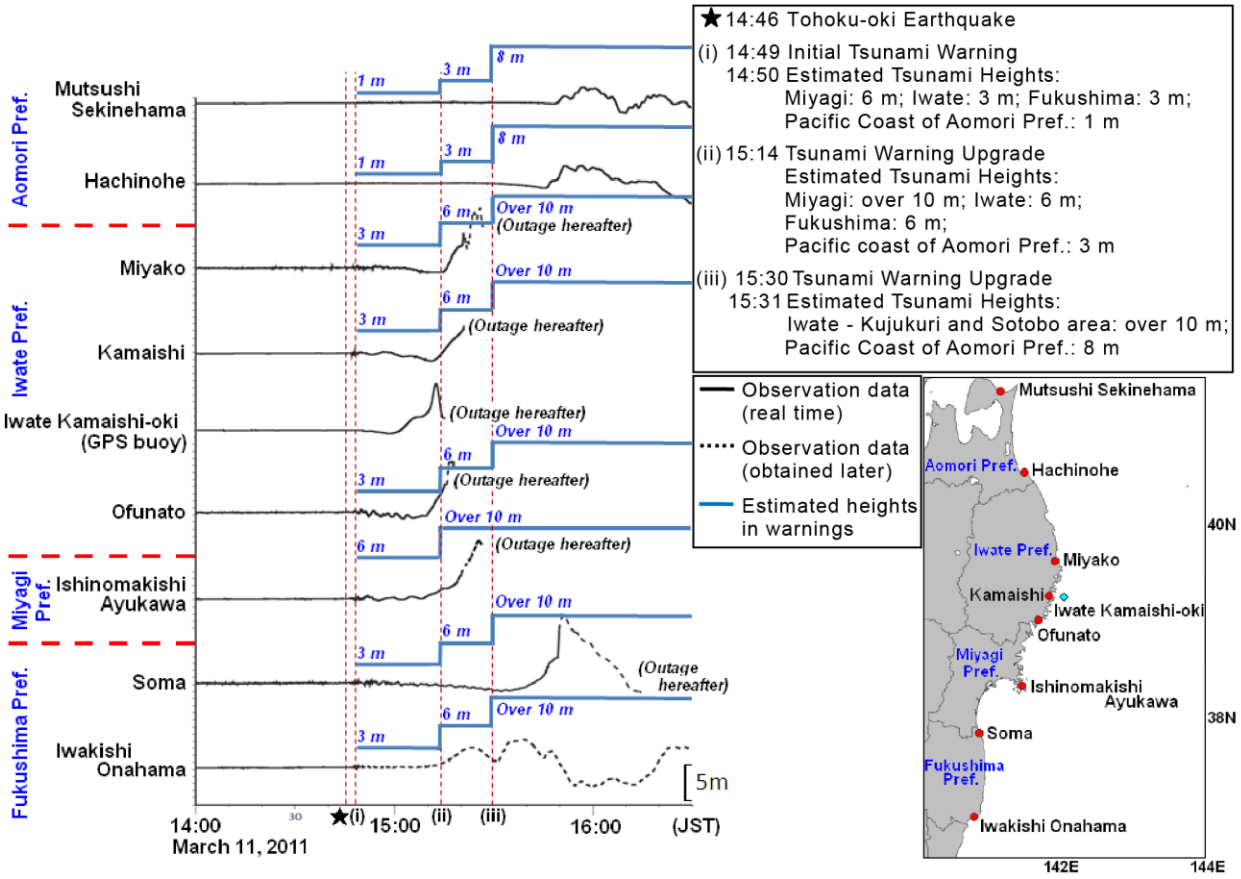

Figure 8 Tsunami observations and issued warnings [after *Japan Meteorological Agency*, 2013]. The black lines show the observed data and blue lines show estimated tsunami heights in the initial warning and two updates. The Iwate Kamaishi-oki GPS buoy 10 km offshore (green diamond) captured the earliest direct evidence of the large tsunami amplitude. A magnitude of Mw 8.8 was determined at around 15:40.

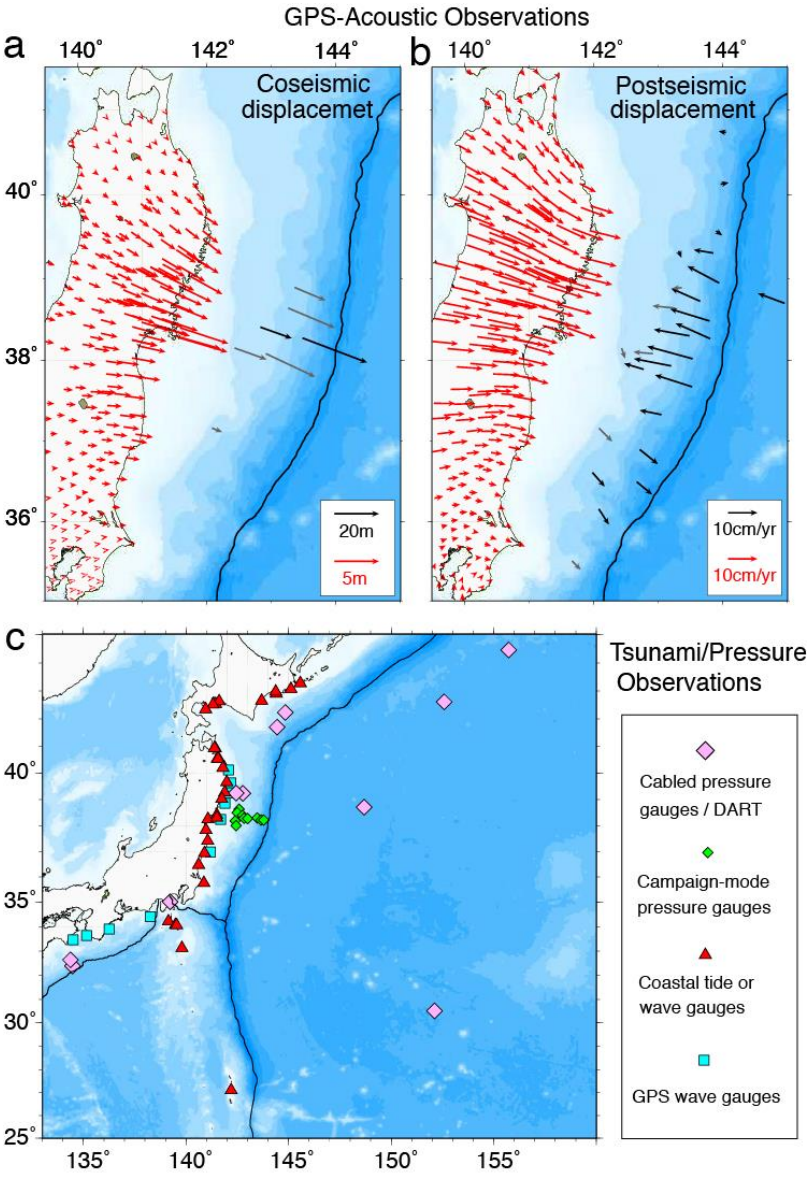

Figure 9 Offshore observations of the coseismic and postseismic phenomena of the Tohoku-oki earthquake. (a) Coseismic displacements from GPS-Acoustic observations (gray arrows from *Sato et al.* [2011a] and black arrows from *Kido et al.* [2011]) and land GPS data after *Iinuma et al.* [2012]. (b) The average postseismic displacement rates determined from 2012 to 2016 (black, from *Honsho et al.* [2019], gray, from *Honsho et al.* [2019] based on *Yokota et al.* [2018]). The on-land velocities during the same period are from *Tomita et al.* [2020]. Note the reversal of postseismic displacement directions above the focal area. (c) Offshore tsunami and pressure observations by campaign-mode pressure sensors (green diamonds), cabled pressure sensors and DART systems (pink diamonds), GPS buoys (cyan squares), and coastal tide or wave gauges (red triangles). The locations of the campaign-mode pressure gauges are from *Y Ito et al.* [2013] and others are from *Satake et al.* [2013].

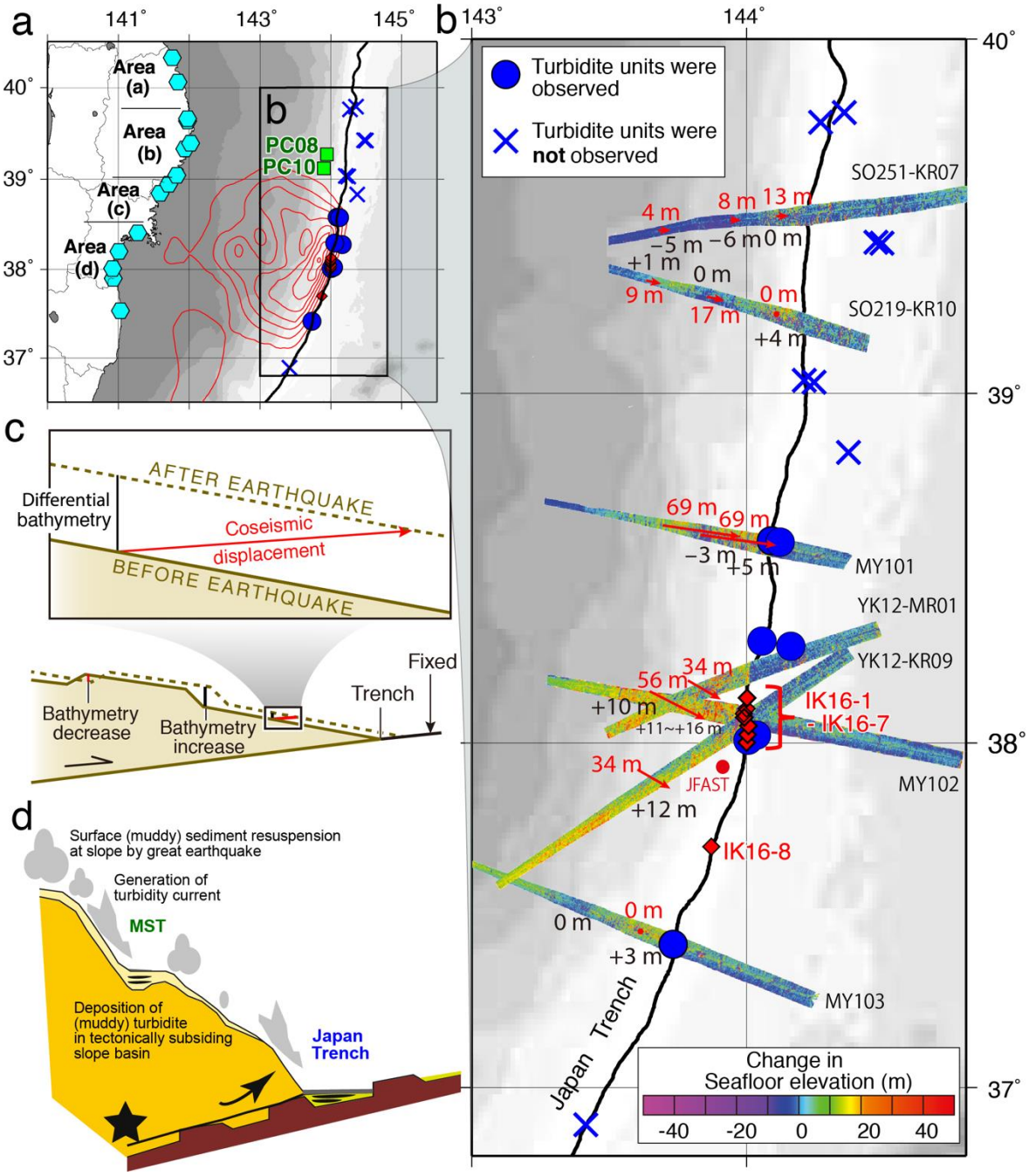

Figure 10 Coseismic change in seafloor elevation and distribution of turbidite deposits from the Tohoku-oki earthquake along the Japan trench axis. (a) Onshore sites of tsunami deposits (cyan hexagons) and offshore survey locations of turbidite units on the mid-slope terrace (green squares [*K Usami et al.*, 2018]) and along the Japan trench (blue crosses and circles [*Ikehara et al.*, 2018]). The circles show the surveyed locations with 2011 turbidites and crosses show locations without 2011 turbidites, showing that no turbidites were found to the north and south of the main coseismic slip area of the Tohoku-oki earthquake (red contour lines, [*Iinuma et al.*, 2012]). (b) Coseismic change in seafloor elevation (color contours) and inferred horizontal (red arrows and labels) and vertical (black labels) movements based on repeated bathymetry

observations (after *Kodaira et al.* [2020]). The data are from *Fujiwara et al.* [2011], *Kodaira et al.* [2012], *Fujiwara et al.* [2017] and *Kodaira et al.* [2020]. Please note large displacements in the middle four traces (MY101, YK12-MR01, YK12-KR09 and MY102) and negligible displacements in the northern two (S0251-KR07) and southern (MY103) traces, considering measurement uncertainties of ~20m in the horizontal and several meters in the vertical component [*Kodaira et al.*, 2020]. Survey site locations shown by blue circles and crosses are the same as those in (a), and the red diamonds show the sites of turbidite observations by *Ikehara et al.* [2016]. (c) Schematic illustration of the relationship between differential bathymetry (coseismic seafloor elevation change) and horizontal displacements (after *Sun et al.* [2017] and *Kodaira et al.* [2020]). Note that both bathymetry increase and decrease may occur due to the lateral offset of raised seafloor features. (d) Schematic showing the mechanism of deposition of turbidites at the mid-slope terrace (MST) and in the Japan trench triggered by the strong ground motion of megathrust earthquakes [after *Ikehara et al.*, 2020]. The strong motion due to the seismic slip below the seaward slope of the Japan trench causes the resuspension of sediment, turbidity current transport and deposition at the MST and Japan trench.

826

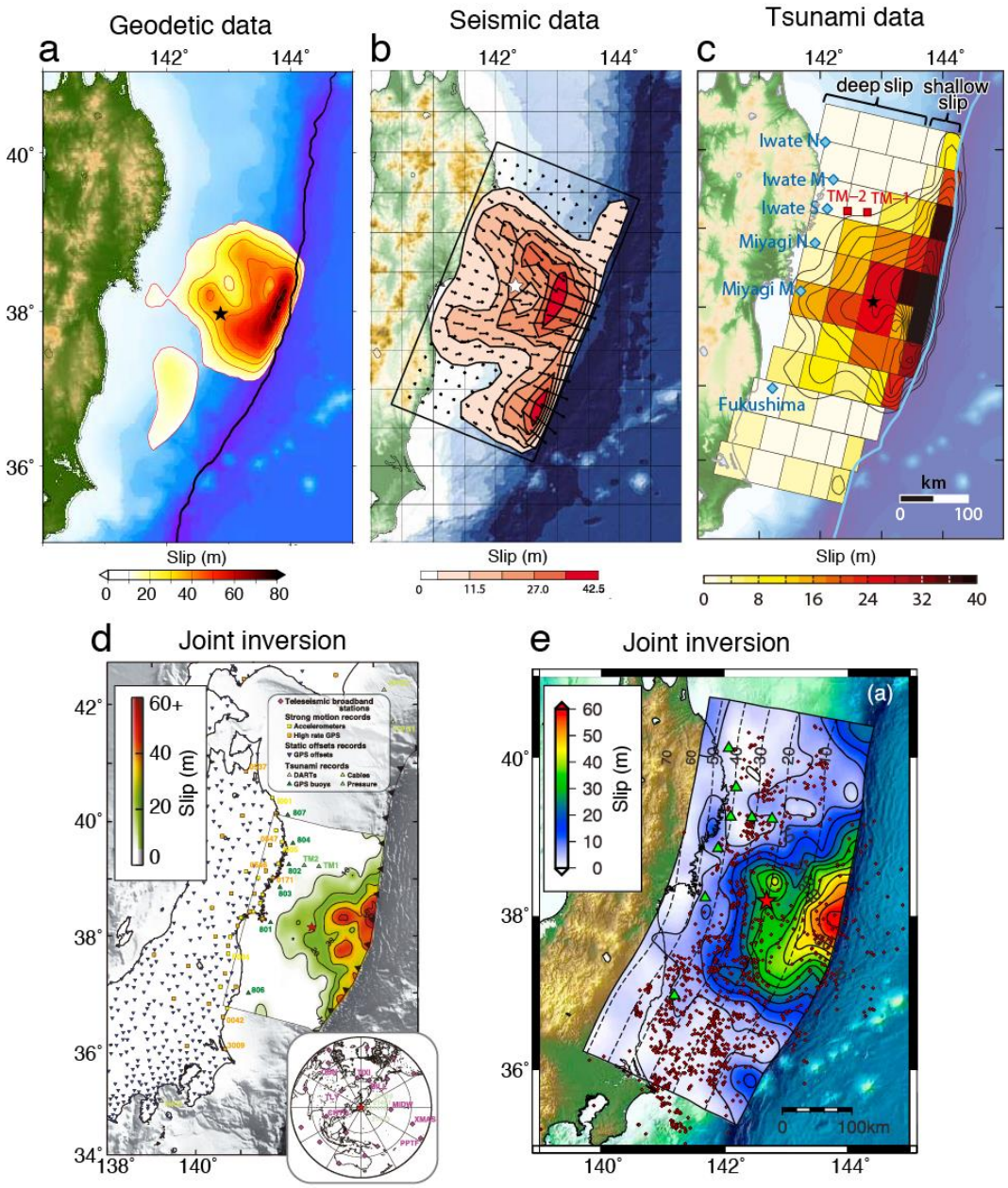

827

828 **Figure 11** Examples of coseismic slip models. (a) Slip model from geodetic displacements
829 [*Iinuma et al.*, 2012]. (b) Slip model from seismic waveforms *Lay et al.* [2011a]. (c) Slip model
830 from and tsunami data [*Satake et al.*, 2013]. (d) Slip model from the joint inversion of
831 teleseismic broadband data, strong motion records, static GPS displacements, and tsunami
832 records [*Bletery et al.*, 2014]. The locations of sensors are shown in the main map and right
833 bottom inset and the symbols are shown in right top inset. (e) Slip model from the joint inversion
834 of high rate (>1 Hz) GPS time series, strong motion, cabled sea floor pressure sensors, and GPS
835 buoys [*Melgar and Bock*, 2015]. The locations of cabled sea floor pressure, and GPS buoys are
836 shown by green triangles.

837

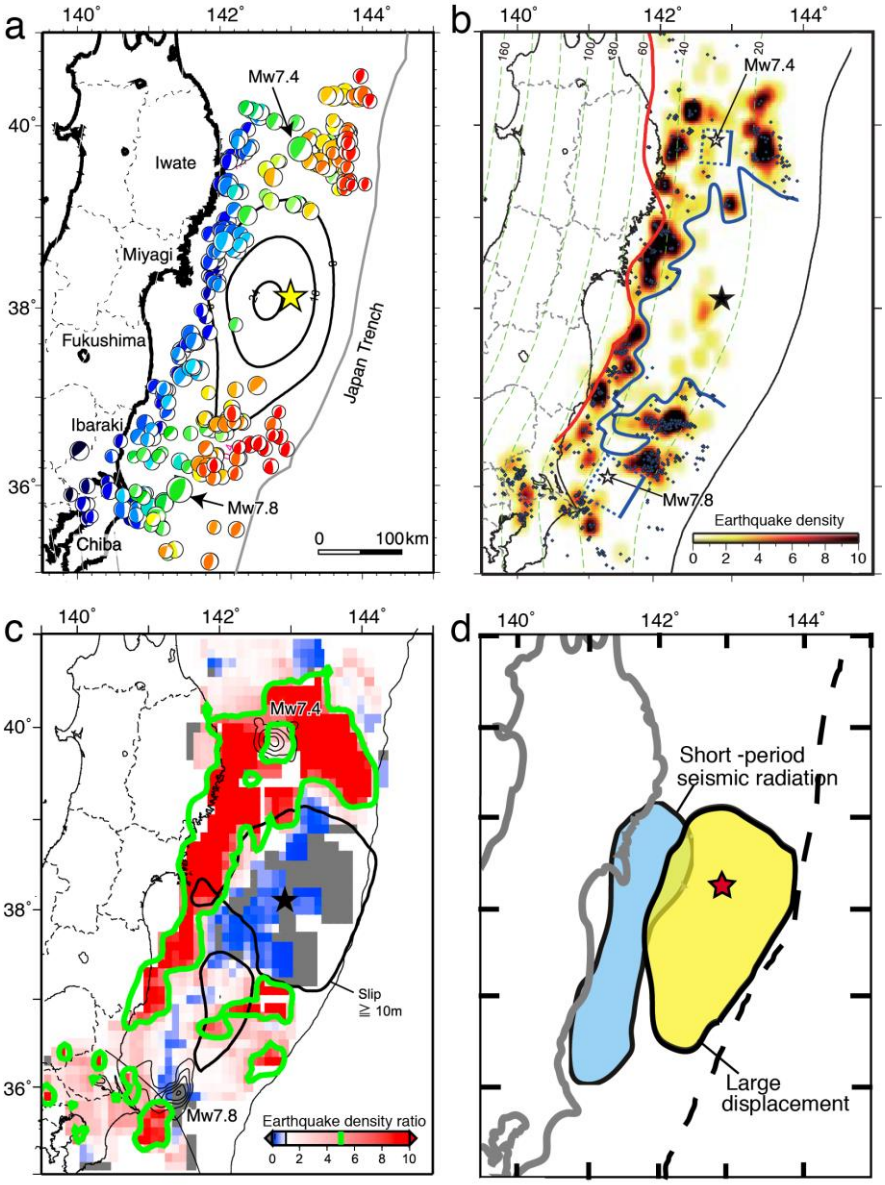

Figure 12 Interplate seismicity after the Tohoku-oki earthquake in relation to coseismic slip area and the distribution of coseimic slip. (a) The distribution of interplate type aftershocks (beach balls showing shallow thrust focal mechanisms from CMT inversion) [after *Asano et al.*, 2011]. The black contours show the coseismic slip model of *Geospatial Information Authority of Japan* [2011]. (b) Density of the interplate type aftershocks from one year of F-net focal mechanisms (color contours) and the distribution of postseismic repeating earthquakes (blue dots) [*Kato and Igarashi*, 2012]. The blue curve outlines the apparent extent of coseismic slip indicated by the seismicity data. The red line shows the downdip limit of interplate earthquakes [*Igarashi et al.*, 2001]. (c) Ratio of rates of interplate earthquakes after the Tohoku-oki earthquake to rates before the mainshock based on a template-matching search for interplate events [after *W Nakamura et al.*, 2016]. The black lines show the coseismic slip model of [*Iinuma et al.*, 2012] and the green lines represent the factor-of-five contour of the seismicity ratio. Note the low interplate seismicity in the slip areas of the mainshock and the two largest aftershocks labeled Mw7.4 and

7.8. (d) Seismic radiation along the fault during the Tohoku-oki earthquake [after *Lay et al.*, 2012]. Yellow patch shows the region of large coseismic fault displacements and the blue area indicates the region of coherent short-period (~ 1s) teleseismic radiation. The stars in (a)-(d) show the mainshock epicenter.

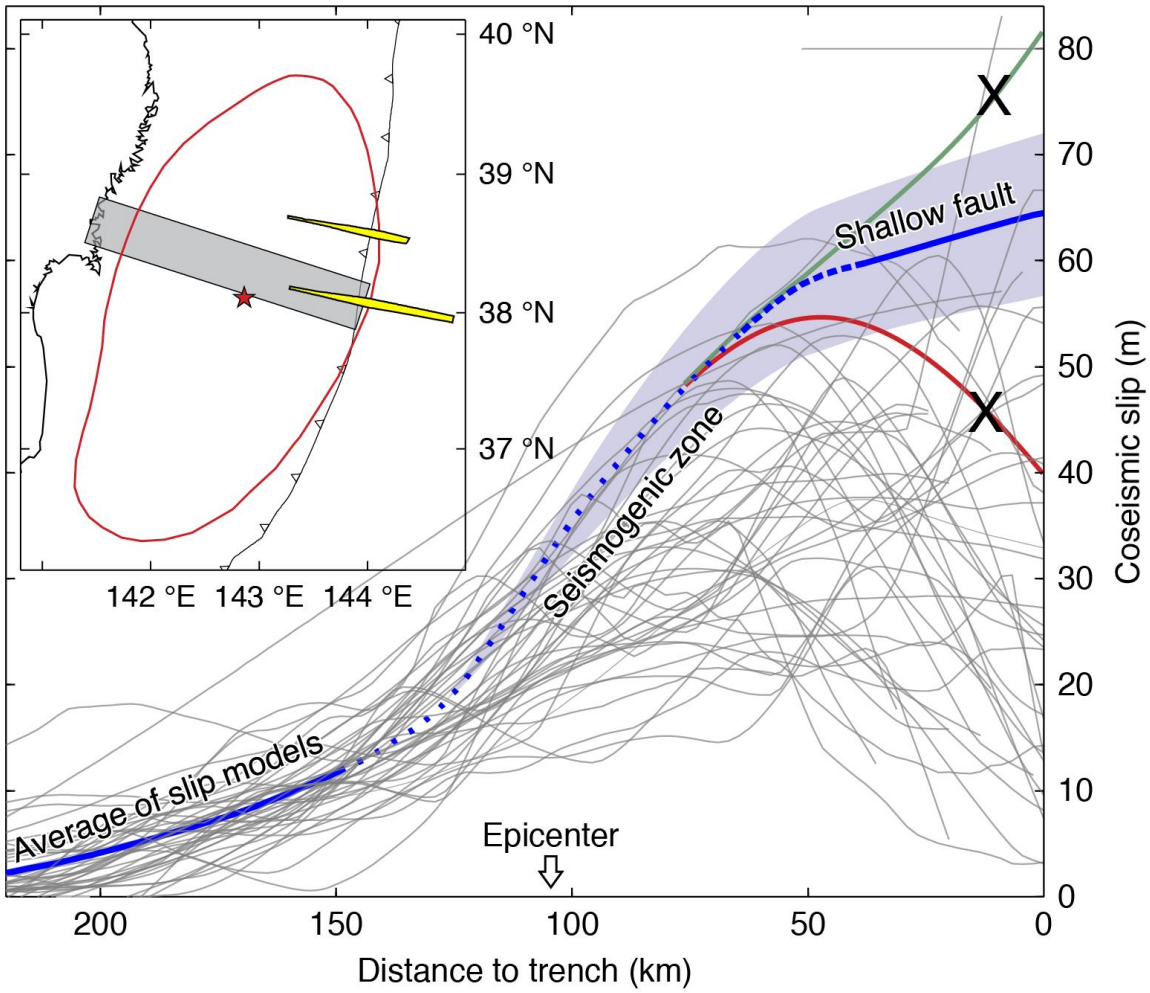

Figure 13 Compilation of 45 published coseismic slip models (gray lines) showing the slip distribution along the gray band in the inset and near-trench slip model (blue line with blue-shaded error ranges estimated from the models with root mean square deviations < 8.55m) based on the modeling of near-trench bathymetry differences at the tracks shown in yellow in the inset [after *Sun et al.*, 2017]. The blue line at distances > 150 km from the trench represents the average of the published slip models and the dotted line represents a poorly constrained interpolation of slip at intermediate depths. In the inset map, the red outline shows the 2-m contour of coseismic slip [*K Wang and Bilek*, 2014] and the red star is the mainshock epicenter. The slip scenarios illustrated by the green and red lines are ruled out by the near-trench bathymetry difference data.

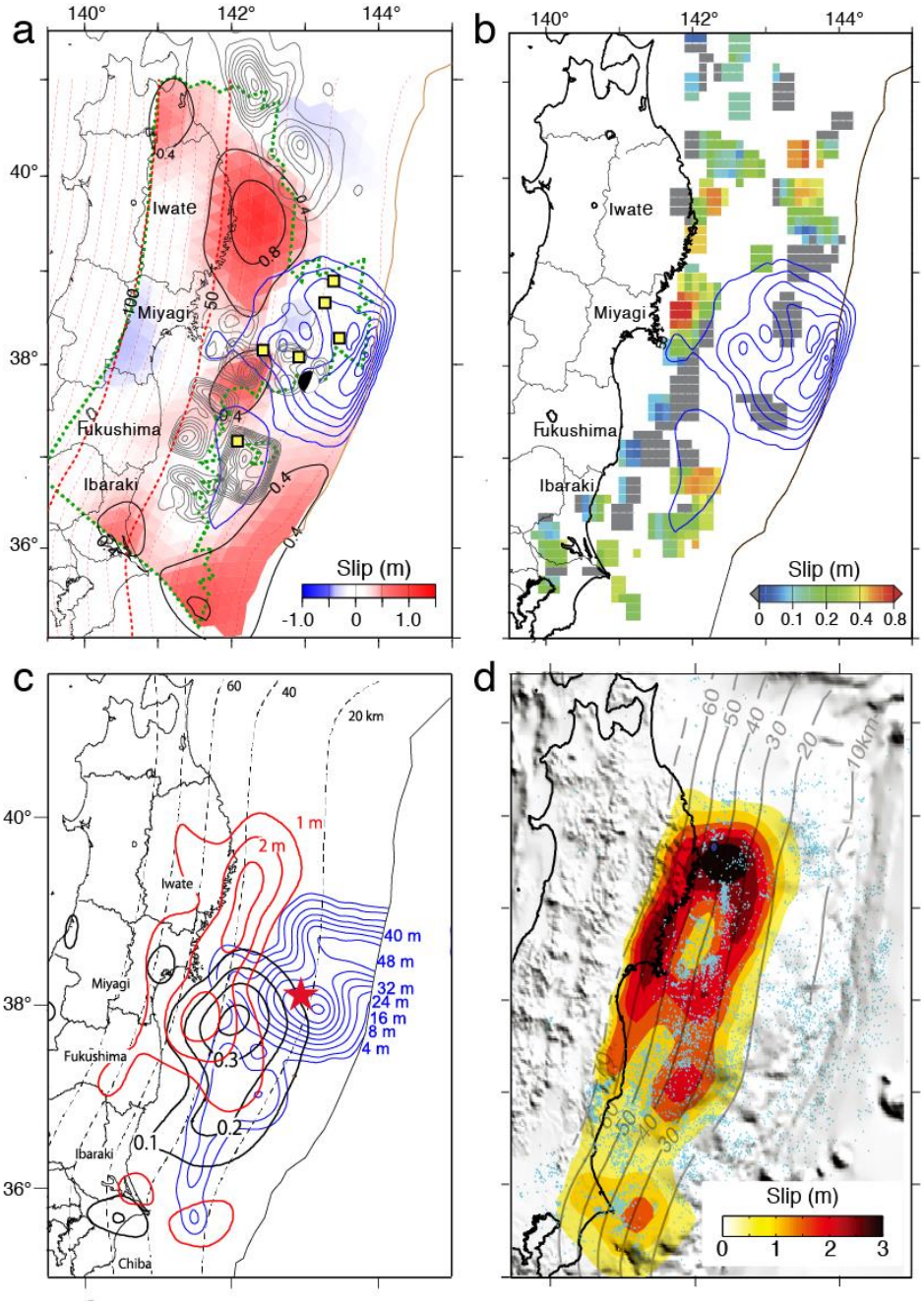

Figure 14 Examples of postseismic afterslip models by (a) *Iinuma et al.* [2016]; (b) *Iinuma et al.* [2016] based on repeating-earthquake data from *Uchida and Matsuzawa* [2013] (c) *Ozawa et al.* [2012]; and (d) *Shirzaei et al.* [2014]. For (a) and (b), the study period of the color-contoured postseismic slip is the same (23 April 2011 to 10 December 2011). The coseismic slip distribution is also shown by the blue contour lines [*Iinuma et al.*, 2016]. In (a), note that the GPS-Acoustic seafloor stations (yellow squares) are distributed only off Miyagi and Fukushima and consequently the uncertainty in the near-trench postseismic slip is large as shown by the green dotted line that surrounds the area with < 0.3m slip uncertainty. In (c), the blue, red and black contours show coseismic slip, 4-month afterslip, and pre-earthquake (January 2003-

January 2011) aseismic slip. In (d) the postseismic slip was inverted from from on-land GPS and repeating earthquake data of the first 15 months following the mainshock. In (c) and (d) no seafloor geodetic data was used.

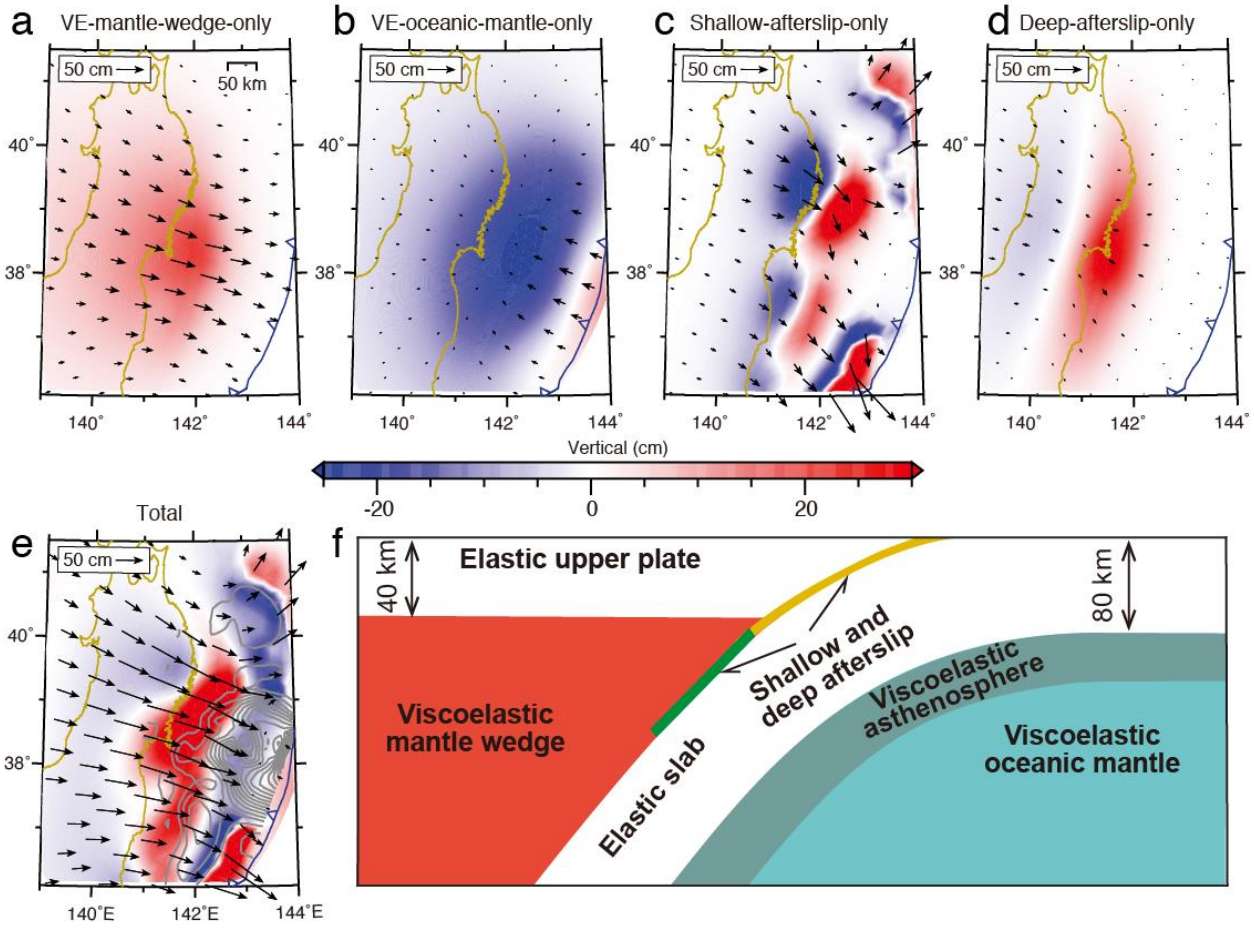

Figure 15 The modeled contribution of different postseismic deformation to the observed postseismic deformation at the surface [after *Hu et al.*, 2016]. Color contours and black arrows show total vertical and horizontal displacements during the first two years after the mainshock. (a) and (b) show contributions from viscoelastic mantle relaxation (VE) above and below the subducting Pacific plate. (c) and (d) show contributions from afterslip in the seismogenic zone (determined from repeating earthquakes) and downdip aseismic shear, respectively. (e) shows the sum of the contributions from viscous relaxation and afterslip in (a) through (d). (f) shows a cross-section through the 3D finite element model showing the locations of the elastic upper plate and elastic subduction slab (white), viscoelastic mantle wedge (red), viscoelastic oceanic mantle (dark and light cyan), and shear zone along the plate interface (green and yellow).

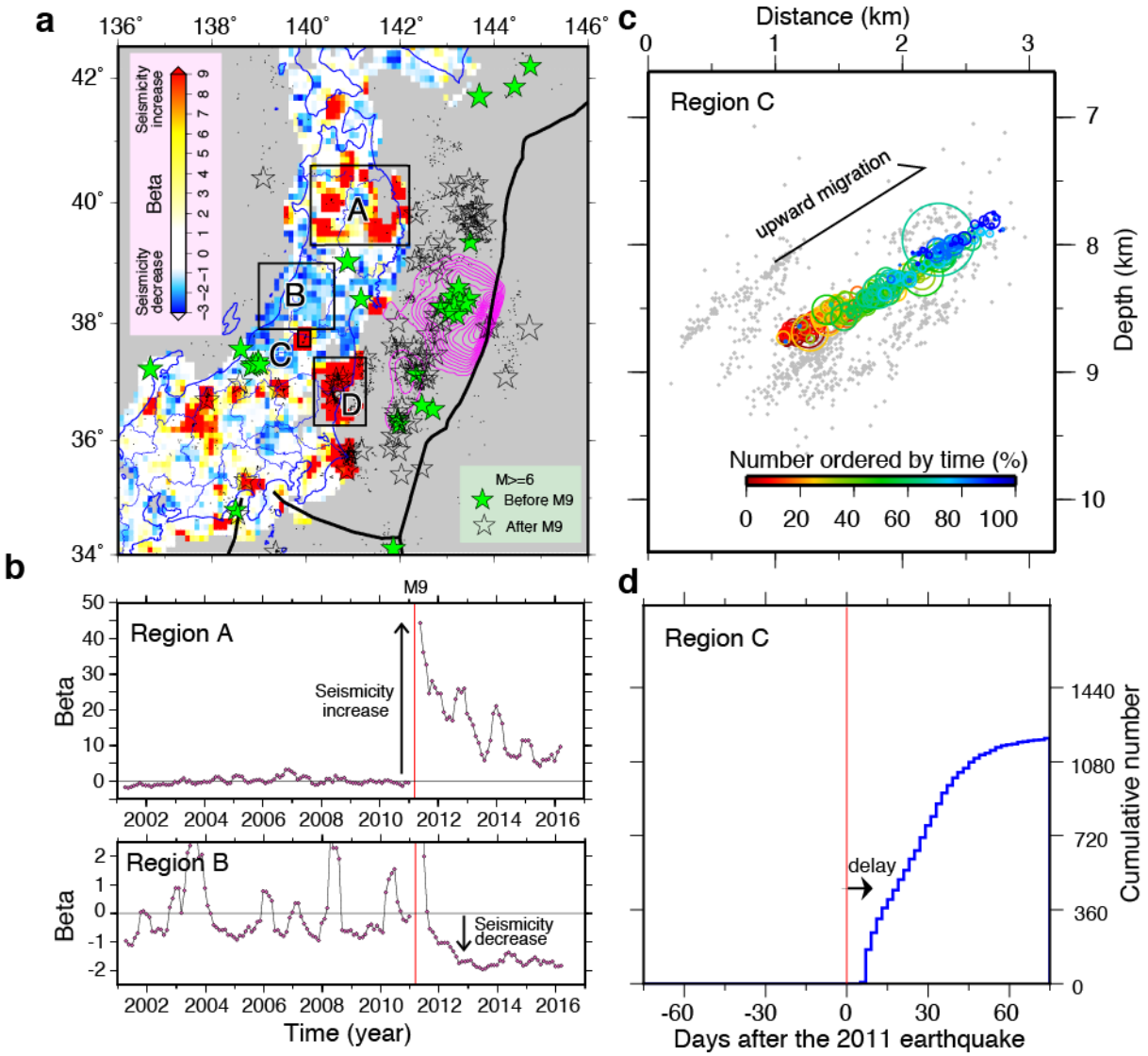

Figure 16 Inland seismicity rate changes after the Tohoku-oki earthquake. (a) Spatial distribution of beta statistic for March 2013 to March 2016, which is the excess rate of crustal earthquakes with respect to the pre-earthquake period from 2001 to March 11, 2011 normalized by the variance [*Reasenberg and Simpson*, 1992]. The value is evaluated for every 0.3 by 0.3 degree spatial window. The values larger (smaller) than 1 (-1) represent significant increases (decreases) in the seismicity. Green and transparent stars denote M6 or larger earthquakes before the Tohoku-oki earthquake (2001 to March 11, 2011) and after the Tohoku-oki earthquake (March 11, 2011 to 2016). (b) Temporal change in beta value for regions A and B outlined in (a), using moving time windows of 0.4 year. (a) and (b) are modified from *Uchida et al.* [2018]. (c) Vertical cross section of earthquakes in a planar structure in the Aizu-swarm in region C shown in (a). The colors show the number ordered in time for a total duration of 800 days from the start of the activity. Sizes of circles correspond to fault diameter assuming a stress drop of 10 MPa. (d) Cumulative number of earthquakes in the earthquake cluster in region C for the first 75 days after the Tohoku-oki earthquake. (c) and (d) are modified from *Keisuke Yoshida et al.* [2019]. The red vertical lines in (b) and (d) are the occurrence time of the

922 Tohoku-oki earthquake. Region D outlined in (a) hosted a pair of M~6 repeating earthquakes
923 discussed in the main text.
924

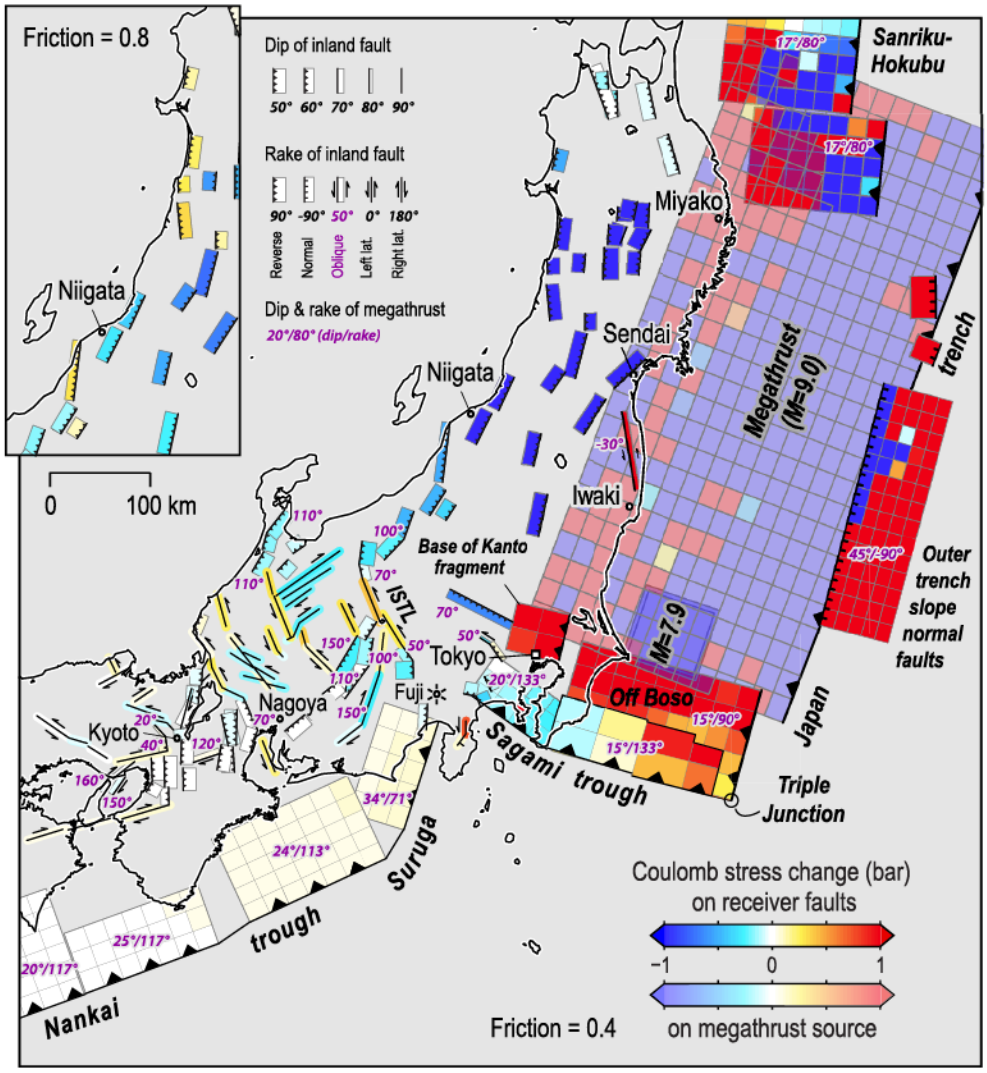

Figure 17 Coulomb stress changes due to the coseismic slip of the 2011 Tohoku-oki earthquake and Mw 7.9 aftershock to the south of the rupture [after *Toda et al.*, 2011a]. The coseismic slip model is from *S. Wei et al.* [2011]. The receiver fault geometries are based on the compilation of active faults from the Research Group for Active Faults in Japan, 1991 and Headquarters for Earthquake Research Promotion, 2011. Top and bottom depths of most of the active faults are set to 0 and 15 km. A friction coefficient of 0.4 was used except for the result shown in top left inset.

4 Earthquake cycle and pre-earthquake processes at various time scales

4.1 Refined geologic evidence of recurrent great earthquakes

After the 2011 Tohoku-oki earthquake, new observations emerged about the prehistoric great earthquake occurrences along the Japan trench. Well-documented tsunami deposits along the coast that were emplaced during the last ~1500 years are summarized by *Sawai* [2017]. The data showed that the 2011 Tohoku-oki earthquake had similar inundation distances (4.5 km maximum) as those indicated by the distribution of the tsunami deposits from the 869 Jyogan earthquake, although the shoreline at the time of the Jyogan earthquake was 1-1.5 km inland from the present shoreline (Fig. 18b). This would suggest a smaller inundation distance for the Jyogan earthquake. However, it was recognized that the actual inundation of the tsunami of the 2011 Tohoku-oki earthquake reached substantially further than the extent of sand deposits (about 1.4-1.6 times larger than the inland limit of sandy tsunami deposit) [*T Abe et al.*, 2012; *K Goto et al.*, 2011; *Shishikura et al.*, 2012]. Therefore, the use of tsunami deposits as a measure of inundation can underestimate the tsunami size. A quantitative re-examination of the size of the 869 Jyogan earthquake, which imposed a minimum flow depth (1m) and flow velocity (0.6m/s) based on the observation of 2011 sand deposit distribution, was performed by *Namegaya and Satake* [2014]. They recalculated the size of the Jyogan earthquake to be >Mw 8.6, which is much larger than the pre-2011 magnitude estimates (Mw 8.3-8.4, see section 2.2). *Satake et al.* [2013] assumed ~25m slip in the deep part of the Tohoku-oki rupture (Mw 8.6) as a Jyogan earthquake's slip model and showed that this model well explains the tsunami inundation of the 869 Jyogan earthquake (Fig. 18). The scenarios of whole-area slip versus deep-only slip do not make a large difference in the simulations of tsunami inundation in the plains (Fig. 18), because the enduring relative coastal sea-level rise due to the long wavelength tsunami from the deep slip is the main cause of the far-reaching inundation. The impulsive tsunami resulting from the shallow slip increases the height of the tsunami, but cannot produce a long inundation distance because of the insufficient duration of the associated sea-level rise. This suggests that the distribution of tsunami deposits on the Sendai and Ishinomaki plains cannot tell whether large slip occurred near the trench at the time of the Jyogan earthquake.

For the events in between the 869 Jyogan and 2011 Tohoku-oki earthquakes, based on tsunami heights from additional historical documents and oral legends pertaining to the 1611 Keicho earthquake [*Ebina and Imai*, 2014], *Imai et al.* [2015] estimated the source of the Keicho earthquake offshore Tohoku with M8.4-8.7 and considered it as a recurrent earthquake that shared the slip area with the 2011 Tohoku-oki earthquake (Fig. 3). On the other hand, [*Sawai et al.*, 2012; *Sawai et al.*, 2015] considered the 1454 Kyotoku earthquake as the penultimate great earthquake from their tsunami deposit data and historical documents [*Namegaya and Yata*, 2014]. Since the 1454 Kyotoku and 1611 Keicho earthquakes are close in time (Fig. 19), it is difficult to discriminate these earthquakes from the tsunami deposits alone [*T Goto et al.*, 2015; *Sawai*, 2017]. However, either way it appears that the recurrence interval of M~9 earthquakes in the Tohoku region is shorter than 1000 years.

The coastal and along-trench geologic data reveal an even longer history of large tsunamigenic earthquakes. Records of coastal tsunami deposits of the last 2000-4000 years suggest average recurrence intervals of 500-750 years from the data collected along the Sanriku coast (Fig. 19, reference 3) [*K Takada et al.*, 2016], ~360-year-long intervals on average at Koyadori on the Sanriku coast [*Ishimura and Miyauchi*, 2015], and 500-800-year-long intervals on the Sendai plain [*Sawai et al.*, 2012] (Fig. 19, reference 2). Many of these deposits along the

Tohoku coast appear to be coincident in time, consistent with their generation by great megathrust earthquakes (Fig. 19).

The observations of offshore turbidite unit along the Japan trench provided new constraints on the recurrence of megathrust earthquakes. [*Ikehara et al.*, 2016; *Ikehara et al.*, 2018] found that along-trench cores off Miyagi recorded two turbidites corresponding to the 1454 Kyotoku and 869 Jyogan earthquakes in addition to deposits associated with the 2011 Tohoku-oki earthquake, suggesting similar events occurred repeatedly. *K Usami et al.* [2018] also used core samples at two sites on the landward mid-slope terrace ~40 km from the Japan trench (Fig. 10 a, d) to find turbidites inferred to be caused by strong shaking. They used radioisotopes, paleomagnetic secular variations and volcanic tephra to date the turbidite deposits and found that only the 2011 Tohoku-oki, 1454 Kyotoku and the 869 Jyogan earthquake are clearly recorded in the upper part of both cores (Fig. 19). At both sites, such turbidites recurred at intervals of 400-900 years in the last 4000 years (Fig. 19). These observations also document that the timing of turbidites is well correlated with the coastal tsunami deposits, providing additional support for the tsunami deposits being due to local great ruptures off NE Japan (Fig. 19).

From these along-coast and near-trench geodetic and historic constraints, the recurrence interval of earthquakes similar to the Tohoku-oki earthquake seems to be 400-900 years. If we consider the 62m maximum slip in 2011 constrained by near-trench bathymetry observations (Fig. 13, *Sun et al.* [2017]), about 730 year of slip-deficit accumulation at 8.5 cm/year plate convergence is needed to rebuild the slip potential for a similar-sized event at the Japan trench. Therefore, the recurrence-interval estimates are consistent with the coseismic slip amount, if the interplate coupling is close to 100% in the maximum-slip area.

4.2 Observations and models of long-term seismicity changes and decadal precursors

There is a long history of discussion regarding seismicity changes leading up to large earthquakes [e.g., *Brodsky and Lay*, 2014; *Hardebeck et al.*, 2008; *Kato and Ben-Zion*, 2020; *Mogi*, 1969]. The 2011 Tohoku-oki earthquake provided a unique opportunity to learn more about seismicity changes over a wide range of time scales before and after the earthquake, inside and outside of the coseismic slip area. The hypocenter distribution of interplate earthquakes in the last ~100 years shows that several previous M~7 earthquakes were located within the 2011 coseismic slip area, as shown in Fig. 5. A number of small repeating earthquake sequences that are typically smaller than M4 were also distributed inside the coseismic slip area based on a record of ~20 years, suggesting the existence of poorly coupled patches within the larger rupture zone (Fig. 20a) [*Uchida and Matsuzawa*, 2011]. For the period after the Tohoku-oki earthquake, however, there is a clear lack of interplate seismicity in the main coseismic slip area [*Asano et al.*, 2011; *Kato and Igarashi*, 2012; *W Nakamura et al.*, 2016] (Fig. 12), and as of 2018 and 2020 respectively, there have been no recurrences of the small repeating earthquakes or occurrences of interplate earthquakes there. This is an important feature of the earthquake, indicating that the seismicity patterns within a future rupture area evolve during the earthquake cycle.

The careful reanalysis of land GPS data showed that the slip rate on the plate boundary increased off central and southern Tohoku, in the decade before the Tohoku-oki earthquake [*Iinuma*, 2018; *Mavrommatis et al.*, 2014; *Ozawa et al.*, 2012; *Yokota and Koketsu*, 2015], as was partly recognized by the monitoring before the earthquake (See section 2.5 and Fig. 7). An independent analysis of repeating earthquakes [*Uchida and Matsuzawa*, 2013] and joint analysis of repeating earthquake sequences and GPS data [*Mavrommatis et al.*, 2015] (Fig. 20b) also

showed unfastening of interplate coupling at decadal time scales in an area that showed relatively large pre-mainshock coupling but did not produce the largest coseismic slip during the 2011 earthquake (Fig. 20a). However, investigation of the long-term (46 years) seismicity suggests there was a seismic quiescence offshore Miyagi between 1978 (M 7.4) and 2005 (M7.2) earthquakes [*Katsumata*, 2011], which suggests there have been more long-term variations in the interplate coupling [*Meade and Loveless*, 2009]. Thus, the progressive interplate uncoupling in the decade preceding the earthquake may represent a preparatory process before the Tohoku-oki earthquake, but it is unclear if this acceleration was unique to just before the eventual rupture.

There are also decadal changes that were newly identified after the earthquake and are not directly related to interplate slip. *Tanaka* [2012] reported enhanced tidal triggering of earthquakes for several to ten years near the epicenter of the Tohoku-oki earthquake. *Nanjo et al.* [2012] and *Tormann et al.* [2015] reported a b-value decrease in the coseismic slip area at a decadal timescale, indicating a relative increase of the number of larger earthquakes relative to smaller events of the Tohoku-oki earthquake. While it has been suggested that b-value decreases may reflect a rise in differential stress, the underlying physical mechanisms for these observations are not well understood [*Bürgmann et al.*, 2016].

The long-term changes in seismicity associated with the earthquake cycle of the Tohoku-oki earthquake can be modeled in earthquake simulations based on frictional failure laws and fault geometry. *Nakata et al.* [2016] simulated the earthquake cycle of M~9 earthquakes offshore Tohoku by considering realistic plate geometry and heterogeneous friction parameters. The model successfully reproduces the overall patterns of seismicity such as frequent recurrences of M ~ 7 earthquakes, as well as the coseismic slip, afterslip, the largest foreshock, and the largest aftershock of the 2011 earthquake. This model also suggests that the asperity of recurrent Miyagi-oki earthquakes (M~7) in the deeper section of the plate boundary will likely rupture at equal or shorter intervals after the Tohoku-oki earthquake. *Barbot* [2020] modeled super-cycles of partial and full ruptures of the Miyagi-oki segment by considering depth-dependent frictional properties that are consistent with the forearc structure. The model can explain the occurrence of smaller size (M~7) 1981 and 2003 earthquakes near the hypocenter of the Tohoku-oki earthquake by introducing a large velocity-weakening fault area with a small nucleation size and also captures other observed features, including slow slip and the development of a foreshock preparatory phase.

4.3 Precursory processes just before the earthquake, real, uncertain and imagined

After many significant earthquakes, attention is being paid to finding potential precursory activity of various kinds, whose recognition might have allowed for anticipating a destructive event. The hope is to better understand physical processes leading up to the nucleation of a mainshock, but also to assess the potential of such precursors for the purpose of improved short-term earthquake forecasting or even prediction. As such studies are generally done retrospectively, it is important to very critically assess if such precursor candidates are real; in the sense that they are based on reliable observations, are statistically significant, and represent plausible physical processes. It is human nature to conjure up anomalous patterns, which after more critical analysis may turn out to be non-unique or imagined [e.g., *Hardebeck et al.*, 2008; *Orihara et al.*, 2019; *Woith et al.*, 2018]. Thanks to improved geophysical monitoring capabilities, apparently meaningful precursors have been recognized preceding several recent large events, including the Tohoku-oki earthquake, leading to renewed interest in such phenomena [*Kato and Ben-Zion*, 2020; *Nakatani*, 2020; *Pritchard et al.*, 2020].

The pressure gauges offshore Miyagi detected temporal changes of sea bottom pressure that are best explained by slow slip on the plate interface near the hypocenters of the M 7.3 foreshock and the mainshock (red rectangle in Fig. 21), extending from the end of January 2011 to March 9 [*Y Ito et al.*, 2013]. The seafloor pressure gauge data also show that a similar event occurred in 2008. In contrast, the pressure gauge data did not show any short-term precursory accelerations at the time scale of hours or minutes [*Hino et al.*, 2014]. From seismicity, a migrating pattern of events propagating from north to south was identified between February and March 9 (magenta circles in Fig. 21) [*Kato et al.*, 2012], culminating in the March 9 M7.3 foreshock of the 2011 Tohoku-oki earthquake (slip area shown by blue in Fig. 21, [*Ohta et al.*, 2012a]). After the large foreshock, a second two-day-long seismicity migration toward the south and the hypocenter of the Tohoku-oki earthquake occurred (yellow circles, [*R Ando and Imanishi*, 2011; *Kato et al.*, 2012], Fig. 21). The migrating seismicity included repeating earthquakes [*Kato et al.*, 2012; *Uchida and Matsuzawa*, 2013], suggesting aseismic slip was involved. The M 7.3 afterslip zone estimated from GPS data (green in Fig. 21) also lies in the earthquake-migration area [*Ohta et al.*, 2012a]). These data suggest a transient slow slip process accompanied by foreshock activity preceded the Tohoku-oki earthquake.

There have also been attempts to capture precursory phenomena at various spatial and temporal scales before the Tohoku-oki earthquake from other space geodetic data. *Kosuke Heki* [2011] reported a positive anomaly of ionospheric total electron content starting ~40 minutes before the Tohoku-oki earthquake using continuous GPS data. *Panet et al.* [2018] reported a gravity field change at the scale of the whole Japanese-islands starting a few months before March 2011 by using time series of GRACE satellite data. *Bedford et al.* [2020] reported surface displacement variations that lasted several months and spanned thousands of kilometers using time series from on-land GPS stations. However, debate continues on the significance of these results. *Kamogawa and Kakinami* [2013], *Masci et al.* [2015] and *Ikuta et al.* [2020] suggest the preseismic disturbance of the total electron content reported by *Kosuke Heki* [2011] and *Kosuke Heki and Enomoto* [2015] represent artifacts associated with the time series analysis and indicate frequent occurrences of similar anomalies in the total-electron-content data, suggesting coincidence by chance. *Lei Wang and Bürgmann* [2019] showed that the proposed precursory changes in gravity [*Panet et al.*, 2018] are not statistically unique, either in time or in space. More research is warranted to thoroughly and critically assess any precursor candidates and to better understand the physical processes that might underly them [*Pritchard et al.*, 2020].

4.4 Could the Tohoku-oki earthquake have been predicted today?

A decade of study since the 2011 Tohoku-oki earthquake established its detailed rupture characteristics, revealed pre- and postseismic deformation processes of the earthquake, and clarified the recurrence history of large megathrust earthquakes in NE Japan. There has also been much discussion addressing why the Tohoku-oki earthquake was not anticipated before the earthquake [e.g., *Hasegawa*, 2011; *Hori et al.*, 2011; *Kagan and Jackson*, 2013; *Toru Matsuzawa*, 2011]. This discussion has led to the establishment of new offshore seismic and geodetic monitoring systems (S-net and GPS-Acoustic stations). In this regard, we now understand the occurrence of the 2011 Tohoku-oki earthquake and the nature of preceding seismicity and deformation much better than before, and we have substantially improved capabilities to monitor the subduction zone. In this section, we try to evaluate the present ability in terms of forecasting or even predicting earthquakes. For this purpose, we envision a scenario in which the Tohoku-

oki earthquake had not yet happened, but the improved technology and geophysical infrastructure, as well as various lessons learned in the last decade were in place.

As for long-term earthquake forecasts of great megathrust earthquakes, which rely on recurrence intervals and the time since the last earthquake, this is now feasible thanks to the new geologic event occurrence data and some evidence of the earlier earthquakes having occurred in the same area (i.e., characteristic earthquakes). However, the recurrence intervals (400-900 years) and the rupture area and size of the previous earthquakes are still not very well constrained (see section 4.1). A retrospective calculation of the long-term probability of a great Tohoku-oki subduction earthquake at the time just before the 2011 mainshock obtained values of 10-20% within 30 years, assuming a 600-year recurrence interval and time of the most recent event about 500-600 years ago [*Headquarters for Earthquake Research Promotion*, 2020]. Just knowing that M>8.5 earthquakes and associated devastating tsunamis are possible along the Japan Trench, and considering the high 30-year occurrence probability, would likely have led to increased earthquake and tsunami hazard mitigation efforts in NE Japan.

The decadal and months-long pre-earthquake slip rate variations and foreshock activity represent candidate observations that have potential to improve the timing accuracy of intermediate-term forecasts. They were largely detected by monitoring from land before the 2011 Tohoku-oki earthquake (section 2.5) and if such changes in megathrust behavior were to occur today, we could more easily detect them both from land and offshore observations. We could also more easily link these phenomena to increased probabilities of an impending earthquake, because we know the large slip deficit area off Tohoku is capable of producing large seismic slip and approaches exist to assess the changes in stress and earthquake probabilities in response to such deformation processes [*Freed*, 2004; *Kano et al.*, 2019; *Kato and Ben-Zion*, 2020; *Mazzotti and Adams*, 2004; *Obara and Kato*, 2016]. However, it is not certain at all that such slow slips or foreshock candidates are prone to occur just before the final rupture of a M~9 earthquake. *Uchida et al.* [2016] found periodic slow slip episodes that were activated before the 2011 Tohoku-oki and other M>7 earthquake, but similar episodic slip transients often did not result in large earthquakes. Near the May 9, 2011 foreshock, there were also similar-sized (M~7) earthquakes with foreshock activity in 2003, 1980, 1962 and 1915 (Fig. 5). In any case, it seems important to use the potential foreshocks and slow slips to develop time-dependent earthquake probability estimates [*Mazzotti and Adams*, 2004] and to enhance efforts aimed at operational earthquake forecasting in subduction zones [e.g., *Field et al.*, 2016; *Jordan et al.*, 2011].

With regards to foreshocks, a global search for successive occurrences of earthquakes suggests that 0.4-0.6% of M~7 earthquakes were followed by M~ 8 or larger earthquakes, within one week [*Fukushima and Nishikawa*, 2020; *T Hashimoto and Yokota*, 2019]. This is a low value but the probability is several to 30 times larger than the average determined in long-term forecasts. For slow slip, there are not many data to evaluate the relationship with, and enhanced probability of large earthquakes, but there are several examples of precursory transients besides the Tohoku-oki earthquake [e.g., *Brodsky and Lay*, 2014; *Obara and Kato*, 2016; *Ruiz et al.*, 2014]. Earthquake cycle simulations and laboratory experiments also suggest that such slow slip events in or near the area of final rupture may be common [e.g., *Barbot*, 2020; *Takanori Matsuzawa et al.*, 2013; *McLaskey*, 2019; *Nakata et al.*, 2016].

In 2019, the Japanese government implemented a procedure that JMA issue forecast information regarding a M8 or larger earthquake, when the Nankai Trough Earthquake Assessment Committee finds that a M7 to 8 earthquake occurred in the wide coupled area along the Nankai trough in SW Japan or a highly anomalous slow slip episode occurred nearby [*Japan*

Meteorological Agency, 2019]. JMA is also to declare a status of "under investigation" even before the final judgement when the committee has convened, given observations of possible partial ruptures of the locked area or notable changes in interplate coupling. It seems reasonable to assume such events are associated with changes in hazard level, and thus to assess the degree to which they may trigger large earthquakes, and to rigorously quantify by how much the probability of earthquakes is raised above background levels.

Compared to the above-mentioned improvements in long-term earthquake forecasts and estimates of time-dependent earthquake probabilities, the short-term (< ~week) precursory processes that were identified retrospectively after the Tohoku-oki earthquake could be more effective to mitigate earthquake disasters if they also reflect a substantial probability gain, thus allowing for meaningful short-term earthquake prediction. However, the debate continues regarding the significance and uniqueness of such precursors as discussed in section 4.3. We consider it is immature to implement them for the purpose of earthquake prediction and more tests are needed to associate the phenomena with the occurrence of large earthquakes and to better understand the underlying physical mechanisms. Our current understanding of the earthquake process suggests that while some earthquakes are preceded by a variety of precursory processes over a wide range of spatial and temporal scales, many and possibly most are not.

In any case, the new offshore real-time seismic and geodetic observations (S-net) can now detect seismic and tsunami signals ~20 sec and ~20 min earlier than the previously available observation networks (Fig. 22). These data have been used since January 2019 to stop the Shinkansen high-speed trains before they experience large shaking [*JR East*, 2019], and have been incorporated in the public earthquake early warning system of JMA, since June 2019. [*JR East*, 2019] The underestimation of initial earthquake size, which was a problem at the time of the Tohoku-oki earthquake (Fig. 8), was also seriously considered. In 2016,the REal-time GEONET Analysis system for Rapid Deformation monitoring (REGARD) [*Ohta et al.*, 2012b], which uses the high-rate displacements of land GPS stations, was implemented at the Geospatial Information Authority of Japan. In March 2019, the use of real-time offshore tsunami data for estimating accurate costal tsunami heights (tsunami Forecasting based on Inversion for initial sea-Surface Height (tFISH)) [*Tsushima et al.*, 2014] was implemented as part of the JMA's official tsunami warning system. Thus, while the prediction of disastrous earthquakes like the 2011 Tohoku-oki event is still impossible, the much improved ability to assess the earthquake potential, and the establishment of offshore real-time observations for earthquake and tsunami warning, have greatly improved the preparation of society and enabled actions immediately after the occurrence of large earthquakes to mitigate the disaster and save human life.

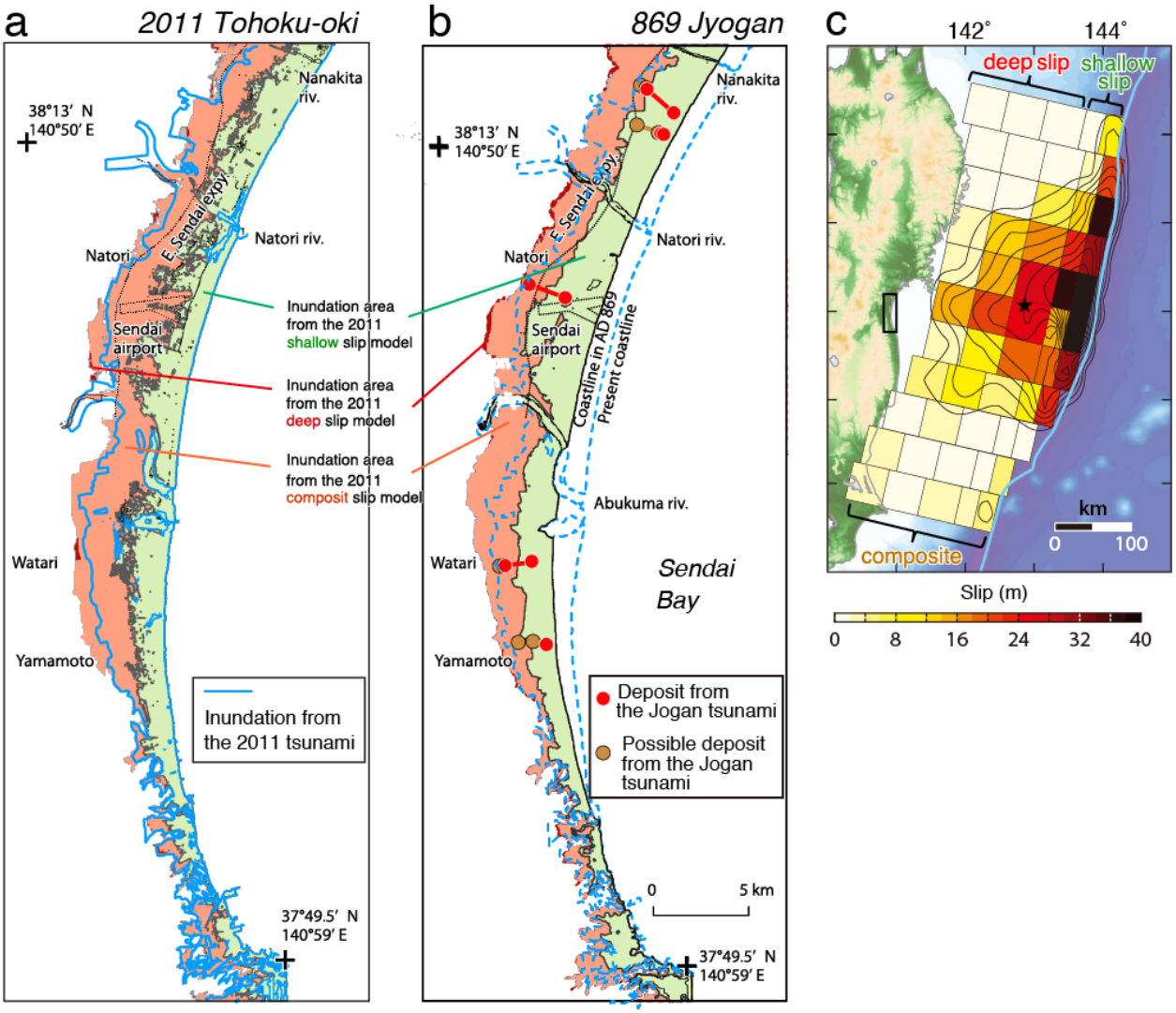

Figure 18 Observed and simulated tsunami inundations due to the 2011 Tohoku-oki (a) and 869 Jyogan (b) earthquakes in the Sendai plane [*Satake et al.*, 2013]. For the simulation the source fault models are the same for both cases but reconstructed near-shore bathymetry and topography are used for the 869 Jyogan earthquake. Three source-fault model scenarios are considered including final (composite) slip model (orange), slip only in shallow near-trench fault area (green), and slip only in the deep area. The slip of composite, deep and near-trench fault areas (the same as Fig. 11c) and the region (black rectangle) shown in (a) and (b) are shown in (c). The inundation area is defined as the land areas where the modeled flow depth is >0.5 m. Note the simulated inundation areas for the deep and composite models are almost identical. The observed inundation from the 2011 Tohoku-oki earthquake is shown by blue lines in (a) [*H Nakajima and Koarai*, 2011] and by blue dashed lines in (b) for reference. The locations of certain and possible 869 tsunami deposits [*Sawai et al.*, 2012; *Sawai et al.*, 2008; *Sawai et al.*, 2007] are shown by red and brown circles, respectively.

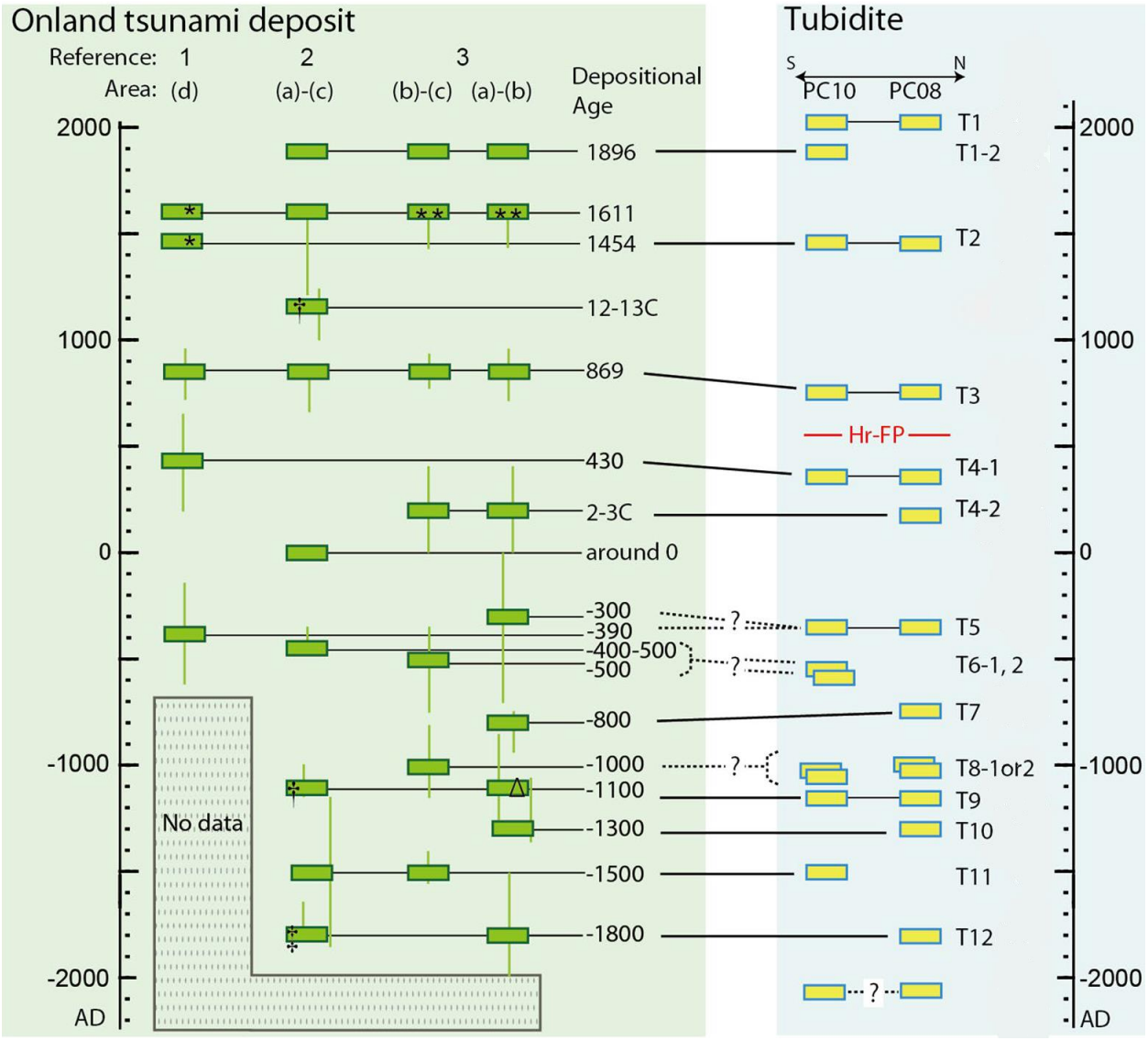

Figure 19 The comparison of dated on-land tsunami deposits and turbidites near the trench [after *K Usami et al.*, 2018]. References 1, 2, and 3 are *Sawai et al.* [2012], *Hirakawa* [2012] and *K Takada et al.* [2016]. Estimated depositional age of the tsunami deposits is shown by green rectangles with error bars (2σ). The locations of areas (a)–(d) , PC08 and PC10 are shown in Fig. 10a. * means northern part of area (d) and ** means that deposits may be associated with the earthquake in A.D. 1454 [*K Takada et al.*, 2016]. † and ‡ mean the northern part of area (b) and Δ means the northern part of area (a). Hr-FP means tephra of Mt. Haruna eruption in the 6th century.

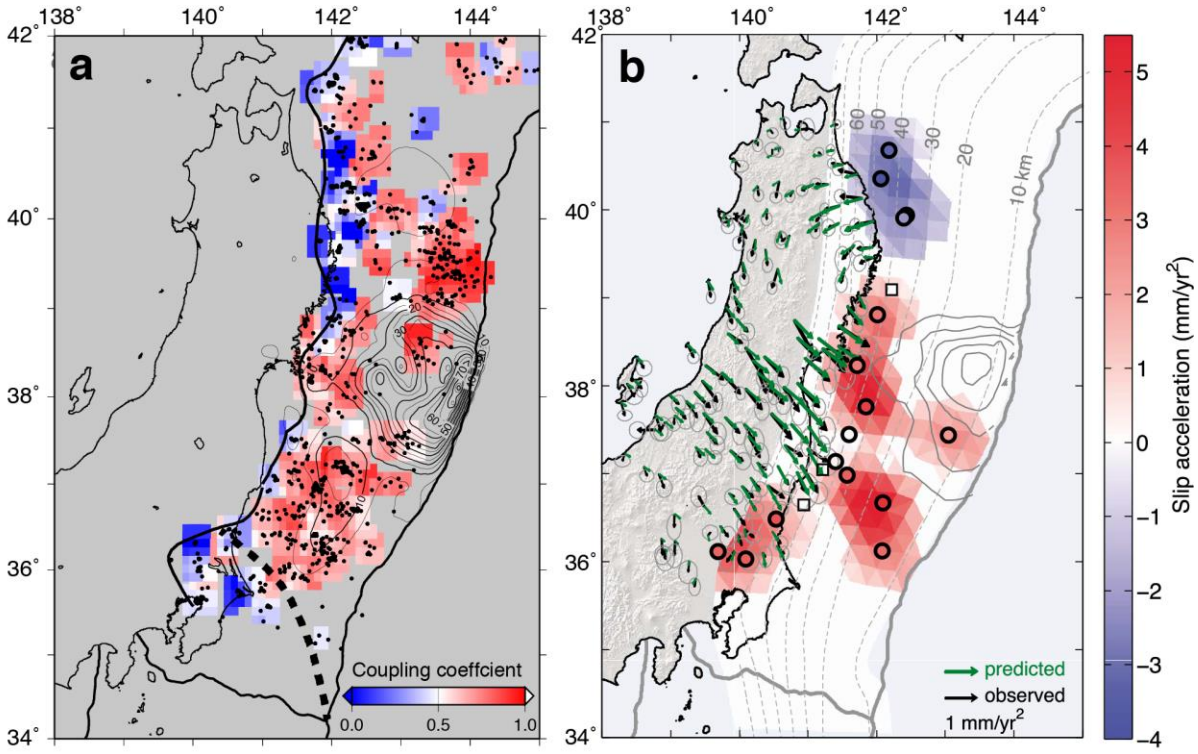

Figure 20 Interplate coupling estimated from (a) repeating earthquakes before the Tohoku-oki earthquake (1993-2007), [after *Uchida and Matsuzawa*, 2011] and (b) decadal acceleration (in mm/yr^2) of interplate slip estimated from the joint inversion of GPS and repeating earthquake data [after *Mavrommatis et al.*, 2015]. The dots in (a) show the locations of repeating earthquake sequences and circles in (b) show the estimated slip accelerations at the locations of the selected repeating earthquake sequences with frequent recurrences. In (a) the black line shows the downdip limit of interplate earthquakes [*Igarashi et al.*, 2001; *Kita et al.*, 2010a; *Uchida et al.*, 2009] and the black dashed line indicates the northeastern limit of the Philippine Sea plate on the Pacific plate [*Uchida et al.*, 2009]. In (b) black arrows on land show observed GPS accelerations with 2σ error ellipses and green arrows show model predicted values.

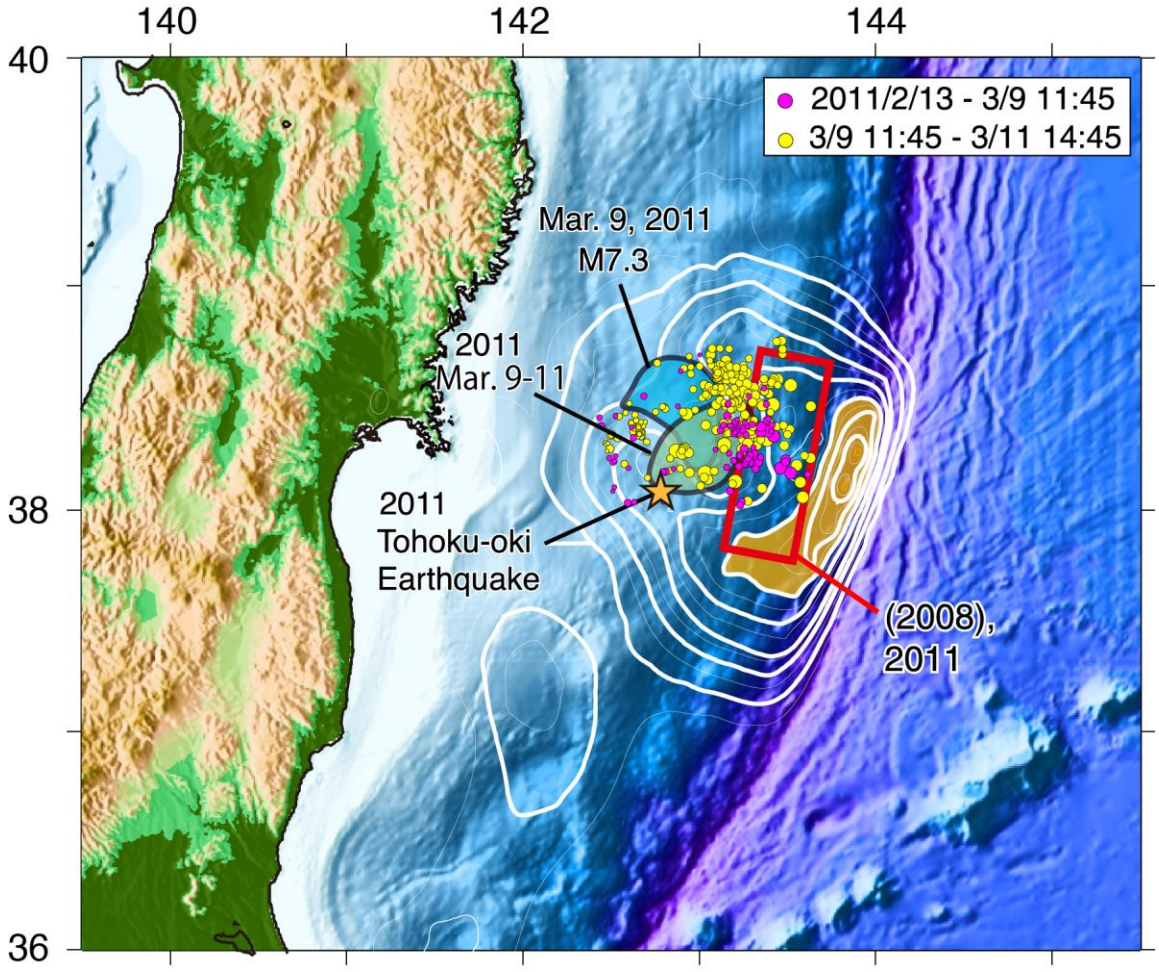

Figure 21 Various phenomena that occurred before the 2011 Tohoku-oki earthquake in the final slip area. The white contour lines show the coseismic slip model by *Iinuma et al.* [2012] with 10 m contour intervals for thick white lines. The area with >50m slip is filled with orange color. The inferred area of the slow slip events detected in 2008 and 2011 from pressure gauge data are shown by red bold rectangle [*Y Ito et al.*, 2013]. Slip areas of the M7.3 foreshock on March 9, 2011 and its afterslip are shown by blue and green polygons, respectively [*Ohta et al.*, 2012a]. The seismicity that showed migration toward the M9 mainshock hypocenter from Feb. 13, 2011 to March 9 (before the foreshock) and from March 9 (after the foreshock) to March 11 (before the M9 mainshock) are shown by magenta and yellow circles, respectively [*Kato et al.*, 2012].

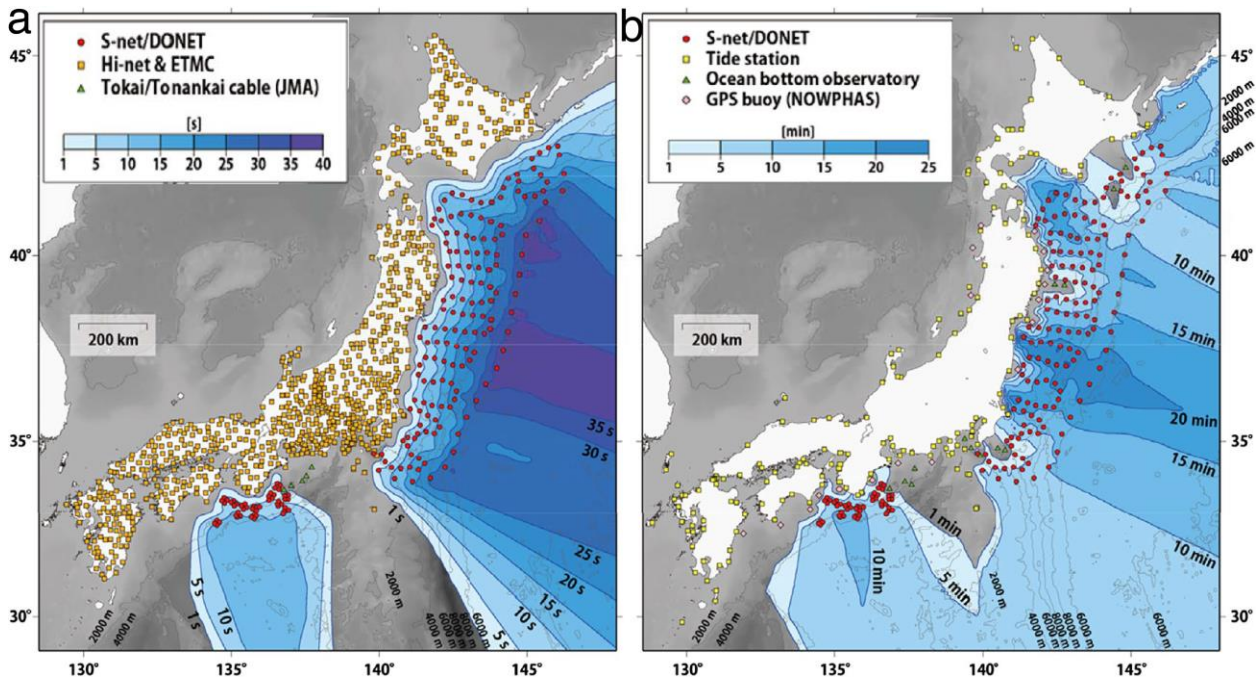

Figure 22. The time advancement of (a) seismic and (b) tsunami wave detection thanks to the seafloor observation network for earthquakes and tsunami along the Japan trench (S-net, small red circles off NE Japan) and Dense Oceanfloor Network system for Earthquakes and Tsunamis (DONET, small red circles off SW Japan). The labeled blue color contours indicate the time advance over the warning times from the land seismic networks alone (yellow squares), if an earthquake occurred in a given location in the offshore area [after *Aoi et al.*, 2020].

5 Summary of the lessons learned and implications for future megathrust earthquakes

The 2011 Tohoku-oki earthquake occurred where geodetic data showed large interplate coupling (slip deficit) along the Japan trench (Fig. 3), which confirms that interseismically locked areas are the likely source areas of future earthquakes. However, the zone of strong geodetic coupling inferred before the earthquake did not extend to the near-trench area that produced the largest slip during the earthquake. The incorrect shallow geodetic coupling was due to poor model resolution in the near-trench area from the land deformation data, and offshore sea-bottom displacements from GPS-Acoustic observations are key to better resolving the near-trench coupling. Seismic data, including slip rate estimates from small repeating earthquakes (Fig. 20a), and the pattern of focal mechanisms in the upper plate, are also useful to discriminate the main coupling areas that produced the megathrust earthquake. The characterization of interplate coupling is fundamental to assessing the potential of megathrust earthquakes in subduction zones.

Geological observations of tsunami deposits along the coast and historical documents and legends provid further indication of great megathrust earthquakes that occurred before the instrumental era (Fig. 4a and 18b). The evidence of recurrent great earthquakes similar to the 2011 earthquake comes not only from the coastal tsunami deposits and historical accounts, but also from earthquake-induced turbidites near the trench axis (Figs. 10 and 19). One important lesson from these results is the reminder that instrumentally observed seismic data easily miss the rare largest events in an area and that it is fundamentally important to find evidence of large previous earthquakes from a variety of data to recognize the possibility of such events. The geological data document a recurrence history of great off-Tohoku ruptures with 400-900 year intervals (Fig. 19), characterizing the earthquake cycle and further quantifying the hazard of great ruptures.

Examination of near-fault materials and structural anomalies (e.g, Fig. 2b) can also improve our understanding of the fault behavior and inform computational models of subduction zone mechanics. Increasingly advanced earthquake cycle simulations can also contribute to assessing the earthquake hazard, constrained by the observed coupling, large-earthquake recurrence history, distribution of seismicity and slow slip in space and time, fault geometry, and frictional properties. Since most observations are inherently incomplete, it is important to integrate the knowledge from many scientific fields to better understand the likelihood of an impending great earthquake and optimally prepare for it.

The aftershocks and postseismic deformation processes that occurred in response to the large coseismic slip helped advance of understanding of earthquake mechanisms and the subduction system. Coseismic and postseismic slip showed complementary distribution (Fig. 14), and interplate aftershocks (Fig. 12), repeating earthquakes and tremors, and very low frequency earthquakes (Fig. 2b) were activated in the afterslip zone, driven by the coseismic stress concentration. Within the coseismic slip zone, the seismic activity diminished (Fig. 12), probably indicating a nearly full stress drop and long-term interplate seismicity changes through the earthquake cycle. The widespread triggered earthquakes away from the plate interface and postseismic deformation document the far reach of the mainshock and the enduring viscoelastic relaxation in the mantle (Fig. 15). The post-mainshock observations provided new insights on earthquake generation processes including static and dynamic triggering (Fig. 16a and Fig. 17), have illuminated the role of fluid pressure and migration (Fig. 16c and d), highlighted the

heterogeneous pre-Tohoku-oki stress and structure, contributed to the better understanding of the rheological structure beneath the arc, and revealed the low ambient stress levels and low fault strength in the subduction zone.

The Tohoku-oki earthquake also illuminated the importance of real-time observation and processing of earthquake data. The offshore GPS tsunami buoy contributed to recognizing the large tsunami earlier than is possible with only the coastal tsunami observations (Fig. 8). Many more offshore cabled pressure gauges (S-net) are now deployed based on this lesson and contribute to the time advancement of earthquake early warning and tsunami forecasts (Fig. 22). Another lesson regarding the real-time processing of earthquake data is the difficulty of rapid estimation of earthquake size for very large earthquakes. In 2011, the delay caused initial underestimation of the area affected by strong earthquake shaking and tsunami heights. Improved real-time analysis methods of the complementary data types, including on-land geodetic data and offshore tsunami data assimilation, will contribute to a more rapid and more accurate source-size determination.

Offshore geophysical and geological observations provided crucial information about the interplate coupling, evidence of previous great megathrust earthquakes, fault-zone to asperity-size characterization of structure and fault behavior, and real-time observation and warning of the earthquake and tsunami. The data include sea-bottom GPS-Acoustic displacements (Fig. 9a and b), pressure and tsunami observations (Figs. 9c and 22), coseismic differential bathymetry (Fig. 10b) and seismic imaging, near-trench, earthquake-induced turbidites (Fig. 10c), cored fault-zone material and near-fault borehole observations, and seismometers just above the shallow subduction zone (Fig. 22).

The decadal evolution of seismicity and changes in megathrust coupling (e.g., Fig. 20b) are new observations, which appear related to the physical state of the plate boundary approaching the final stage of the earthquake cycle. The accumulation of such observations, also in other subduction zones, will promote improved understanding of the whole earthquake cycle and nature of earthquakes. However, it is uncertain if this apparent preparation process observed before the Tohoku-oki earthquake occurred only before the final rupture or if it is a recurring feature; thus, uncertainty remains with regards to its relevance for earthquake forecasting.

Finally, the apparent short-term precursors of the Tohoku-oki earthquake, including foreshocks and slow slip transients (e.g., Fig. 21), represent important phenomena that have been intensively investigated. These observations have contributed to better understanding of the earthquake generation process and can potentially lead to improved time-dependent operational earthquake forecasting. However, similar fault slip anomalies have been observed without being followed by large ruptures, and there is little evidence of a unique nucleation or preparation process that is diagnostic of the size and time of an eventual mainshock. Other intriguing observations, including changes in b-values and tidal modulation, regional-scale deformation and gravity anomalies, and ionospheric perturbations, have been put forward as potential precursor candidates, but neither the observations themselves nor the physics of underlying processes are well established. In the next decade, we have the opportunity to further improve our understanding of the complex dynamics of subduction zones and to implement that knowledge for the assessment of probability gains in increasingly accurate time-dependent earthquake forecasts.

6 Future Issues

1. Due to the centuries-long intervals between ~M9 interplate earthquakes offshore Tohoku, more accurate paleoseismic information is key to confirming the existence, recurrence pattern and hazard of such great earthquakes.
2. The coseismic rupture, afterslip, aftershocks, slow earthquakes, and viscoelastic deformation are all related to each other. Further examining their interactions will contribute to more advanced modeling of these phenomena and will improve our overall understanding of this dynamic system.
3. Further improvements of a wide range of geophysical observations and the development of more advanced computational models are necessary to gain a deeper understanding of the megathrust earthquake cycle and physical processes associated with the spectrum of fault slip processes in subduction zones.
4. Comparative studies illuminating the variety of fault system environments, properties and mechanical behaviors will be important to better understand the factors underlying variable behaviors among the world's subduction zones.
5. Offshore observations greatly improve the monitoring capabilities in subduction systems and enable more accurate earthquake hazard assessment. Such capabilities should be developed in other subduction zones to improve our knowledge of the range of fault system behaviors.
6. It is important to make optimal use of real-time observations and to further develop the methodologies and accuracy of earthquake and tsunami early warning systems.
7. Although the Tohoku-oki earthquake provided unprecedented observations of active processes leading up to, during and following the megathrust rupture, it is important to understand which features are likely to be applicable only to the Tohoku subduction zone or even just this one particular rupture.
8. While it remains a daunting challenge, we should not rule out the possibility of much improved short-term forecasting of large earthquakes based on the careful analysis and interpretation of high-quality geophysical observations.

Glossary

Coulomb stress change: Coulomb stress change is the stress change on a fault that determines the degree to which fault slip is encouraged or suppressed. Increasing shear stress in the slip direction and decreasing fault-normal stress cause positive Coulomb stress changes that promote earthquakes. It depends on the imparted stress change, the geometry and slip direction of a fault, the friction coefficient, and the pore pressure [*Freed*, 2004].

Double seismic zone: Double seismic zones feature two planar earthquake concentrations in the subducted plate in subduction zones that are near-parallel to the plate surface. One is located near the surface and the other is located ~30km below in the case of the NE Japan subduction zone [*Hasegawa et al.*, 1978].

Dynamic weakening: Dynamic weakening of faults is a transient decrease in the friction of faults during the slip [*Di Toro et al.*, 2011].

GPS-Acoustic observation: GPS-Acoustic systems estimate water (sea) bottom displacements by combining repeated GPS measurements of the position of a platform at the sea surface and acoustic ranging between the surface and acoustic transponders on the seafloor [*Bürgmann and Chadwell*, 2014].

GRACE: GRACE (Gravity Recovery and Climate Experiment) is a system that measure Earth's gravity field at ~350 km resolution by using accurate distance measurements between a pair of satellites [*Tapley et al.*, 2004].

Poroelastic rebound: Poroelastic rebound is a postseismic deformation process that is caused by the movement of fluids within poroelastic media induced by coseismic pressure changes [*Peltzer et al.*, 1996].

Repeating earthquakes: Repeating earthquakes are effectively identical earthquakes that occur at the same place but different time. The overlapping events suggest the existence of fault creep in the surrounding area. Multiple repeating earthquake sequences provide information about the spatio-temporal distribution of fault creep [*Uchida and Bürgmann*, 2019].

Seafloor pressure gauge: Seafloor pressure gauges measure the ocean bottom pressure that can be transformed into the water thickness above the site. It can thus measure vertical displacements of the seafloor and temporal changes of sea height (e.g., tsunami) [*Bürgmann and Chadwell*, 2014].

Slip deficit: Slip deficit is the amount of fault displacement that is not released by earthquakes or other types of slip. Slip deficit on a fault builds up due to plate motion across faults and will be compensated by future slip [*Lifeng Wang et al.*, 2015].

Tremor: Tremors and low frequency earthquakes represent a type of slow earthquake on a fault. They are dominated by shaking at several Hz and do not have clear P and S phases that are observed for regular earthquakes [*Beroza and Ide*, 2011].

Very low frequency earthquakes: Very low frequency earthquakes are a type of slow earthquake that are dominated by low-frequency seismic waves (below 0.1 Hz) [*Beroza and Ide*, 2011].

Acknowledgments, Samples, and Data

We thank Yukitoshi Fukahata and Tatsuhiko Saito for discussions regarding the significance of the Tohoku-oki earthquake, Toru Matsuzawa, Ryota Hino and Akira Hasegawa for comment on the manuscript. We also thank Keisuke Yoshida, Takeshi Iinuma and Fumiaki Tomita for original data for figures. Data were not used, nor created for this research. This work was supported in part by JSPS KAKENHI 16H06473, 17KK0081, and 19H05596 and MEXT of Japan, under its Earthquake and Volcano Hazards Observation and Research Program. RB

acknowledges support by NSF award EAR-1801720. This work is dedicated to the people affected by the Tohoku-oki earthquake on March 11, 2011.

References

Abe, H., Y. Sugeno, and A. Chigama (1990), Estimation of the Height of the Sanriku Jogan 11 Earthquake-Tsunami (A. D. 869) in the Sendai Plain, *Zisin 2*, *43*(4), 513-525, doi:10.4294/zisin1948.43.4_513.

Abe, T., K. Goto, and D. Sugawara (2012), Relationship between the maximum extent of tsunami sand and the inundation limit of the 2011 Tohoku-oki tsunami on the Sendai Plain, Japan, *Sedimentary Geology*, *282*, 142-150, doi:https://doi.org/10.1016/j.sedgeo.2012.05.004.

Ammon, C. J., T. Lay, H. Kanamori, and M. Cleveland (2011), A rupture model of the 2011 off the Pacific coast of Tohoku Earthquake, *Earth, Planets and Space*, *63*(7), 33, doi:10.5047/eps.2011.05.015.

Ando, M. (1975), Source mechanisms and tectonic significance of historical earthquakes along the nankai trough, Japan, *Tectonophysics*, *27*(2), 119-140, doi:http://dx.doi.org/10.1016/0040-1951(75)90102-X.

Ando, R., and K. Imanishi (2011), Possibility of Mw 9.0 mainshock triggered by diffusional propagation of after-slip from Mw 7.3 foreshock, *Earth, Planets and Space*, *63*(7), 47, doi:10.5047/eps.2011.05.016.

Aoi, S., Y. Asano, T. Kunugi, T. Kimura, K. Uehira, N. Takahashi, H. Ueda, K. Shiomi, T. Matsumoto, and H. Fujiwara (2020), MOWLAS: NIED observation network for earthquake, tsunami and volcano, *Earth, Planets and Space*, *72*(1), 126, doi:10.1186/s40623-020-01250-x.

Asano, Y., T. Saito, Y. Ito, K. Shiomi, H. Hirose, T. Matsumoto, S. Aoi, S. Hori, and S. Sekiguchi (2011), Spatial distribution and focal mechanisms of aftershocks of the 2011 off the Pacific coast of Tohoku Earthquake, *Earth Planets and Space*, *63*(7), 669-673, doi:10.5047/eps.2011.06.016.

Baba, S., A. Takeo, K. Obara, T. Matsuzawa, and T. Maeda (2020), Comprehensive Detection of Very Low Frequency Earthquakes Off the Hokkaido and Tohoku Pacific Coasts, Northeastern Japan, *Journal of Geophysical Research: Solid Earth*, *125*(1), e2019JB017988, doi:https://doi.org/10.1029/2019JB017988.

Barbot, S. (2020), Frictional and structural controls of seismic super-cycles at the Japan trench, *Earth, Planets and Space*, *72*(1), 63, doi:10.1186/s40623-020-01185-3.

Bassett, D., D. T. Sandwell, Y. Fialko, and A. B. Watts (2016), Upper-plate controls on co-seismic slip in the 2011 magnitude 9.0 Tohoku-oki earthquake, *Nature*, *531*(7592), 92-96, doi:10.1038/nature16945.

Bedford, J. R., M. Moreno, Z. Deng, O. Oncken, B. Schurr, T. John, J. C. Báez, and M. Bevis (2020), Months-long thousand-kilometre-scale wobbling before great subduction earthquakes, *Nature*, *580*(7805), 628-635, doi:10.1038/s41586-020-2212-1.

Beroza, G. C., and S. Ide (2011), Slow Earthquakes and Nonvolcanic Tremor, *Annual Review of Earth and Planetary Sciences*, *39*(1), 271-296, doi:10.1146/annurev-earth-040809-152531.

Bilek, S. L., and T. Lay (2002), Tsunami earthquakes possibly widespread manifestations of frictional conditional stability, *Geophysical Research Letters*, *29*(14), 18-11-18-14, doi:doi:10.1029/2002GL015215.

Bletery, Q., A. Sladen, B. Delouis, M. Vallée, J.-M. Nocquet, L. Rolland, and J. Jiang (2014), A detailed source model for the Mw9.0 Tohoku-Oki earthquake reconciling geodesy, seismology, and tsunami records, *Journal of Geophysical Research: Solid Earth*, *119*(10), 7636-7653, doi:10.1002/2014JB011261.

Brodsky, E. E., and T. Lay (2014), Recognizing Foreshocks from the 1 April 2014 Chile Earthquake, *Science*, *344*(6185), 700, doi:10.1126/science.1255202.

Brodsky, E. E., et al. (2020), The State of Stress on the Fault Before, During, and After a Major Earthquake, *Annual Review of Earth and Planetary Sciences*, *48*(1), 49-74, doi:10.1146/annurev-earth-053018-060507.

Brodsky, E. E., D. Saffer, P. Fulton, F. Chester, M. Conin, K. Huffman, J. C. Moore, and H.-Y. Wu (2017), The postearthquake stress state on the Tohoku megathrust as constrained by reanalysis of the JFAST breakout data, *Geophysical Research Letters*, *44*(16), 8294-8302, doi:https://doi.org/10.1002/2017GL074027.

Brown, L., K. Wang, and T. Sun (2015), Static stress drop in the Mw 9 Tohoku-oki earthquake: Heterogeneous distribution and low average value, *Geophysical Research Letters*, *42*(24), 10,595-510,600, doi:10.1002/2015GL066361.

Bürgmann, R., and D. Chadwell (2014), Seafloor Geodesy, *Annual Review of Earth and Planetary Sciences*, *42*(1), 509-534, doi:10.1146/annurev-earth-060313-054953.

Bürgmann, R., N. Uchida, Y. Hu, and T. Matsuzawa (2016), Tohoku rupture reloaded?, *Nature Geosci*, *9*(3), 183-184, doi:10.1038/ngeo2649

http://www.nature.com/ngeo/journal/v9/n3/abs/ngeo2649.html#supplementary-information.
Chagué-Goff, C., A. Andrew, W. Szczuciński, J. Goff, and Y. Nishimura (2012), Geochemical signatures up to the maximum inundation of the 2011 Tohoku-oki tsunami — Implications for the 869AD Jogan and other palaeotsunamis, *Sedimentary Geology*, *282*, 65-77, doi:https://doi.org/10.1016/j.sedgeo.2012.05.021.
Chao, K., Z. Peng, H. Gonzalez - Huizar, C. Aiken, B. Enescu, H. Kao, A. A. Velasco, K. Obara, and T. Matsuzawa (2013), A Global Search for Triggered Tremor Following the 2011 Mw 9.0 Tohoku Earthquake, *B Seismol Soc Am*, *103*(2B), 1551-1571, doi:10.1785/0120120171.
Chester, F. M., et al. (2013), Structure and Composition of the Plate-Boundary Slip Zone for the 2011 Tohoku-Oki Earthquake, *Science*, *342*(6163), 1208, doi:10.1126/science.1243719.
Chiba, K., Y. Iio, and Y. Fukahata (2013), Detailed stress fields in the focal region of the 2011 off the Pacific coast of Tohoku Earthquake—Implication for the distribution of moment release—, *Earth, Planets and Space*, *64*(12), 10, doi:10.5047/eps.2012.07.008.
Delbridge, B. G., S. Kita, N. Uchida, C. W. Johnson, T. Matsuzawa, and R. Bürgmann (2017), Temporal variation of intermediate-depth earthquakes around the time of the M9.0 Tohoku-oki earthquake, *Geophysical Research Letters*, *44*(8), 3580-3590, doi:10.1002/2017GL072876.
Di Toro, G., R. Han, T. Hirose, N. De Paola, S. Nielsen, K. Mizoguchi, F. Ferri, M. Cocco, and T. Shimamoto (2011), Fault lubrication during earthquakes, *Nature*, *471*(7339), 494-498, doi:10.1038/nature09838.
Diao, F., X. Xiong, R. Wang, Y. Zheng, T. R. Walter, H. Weng, and J. Li (2014), Overlapping post-seismic deformation processes: afterslip and viscoelastic relaxation following the 2011 Mw 9.0 Tohoku (Japan) earthquake, *Geophysical Journal International*, *196*(1), 218-229, doi:10.1093/gji/ggt376.
Ebina, Y., and K. Imai (2014), Tsunami traces survey of the 1611 Keicho Ohsyu earthquake tsunami based on historucal documents and traditions, *Report of Tsunami Engineering*, *31*, 139-148.
Field, E. H., T. H. Jordan, L. M. Jones, A. J. Michael, M. L. Blanpied, and P. Other Workshop (2016), The Potential Uses of Operational Earthquake Forecasting, *Seismological Research Letters*, *87*(2A), 313-322, doi:10.1785/0220150174.
Fire and disaster management agancy, Japan, (2020), On the 2011 off the Pacific coast of Tohoku earthquake (report no. 160), *https://www.fdma.go.jp/disaster/higashinihon/items/160.pdf*.
Freed, A. M. (2004), EARTHQUAKE TRIGGERING BY STATIC, DYNAMIC, AND POSTSEISMIC STRESS TRANSFER, *Annual Review of Earth and Planetary Sciences*, *33*(1), 335-367, doi:10.1146/annurev.earth.33.092203.122505.
Fujii, Y., K. Satake, S. i. Sakai, M. Shinohara, and T. Kanazawa (2011), Tsunami source of the 2011 off the Pacific coast of Tohoku Earthquake, *Earth, Planets and Space*, *63*(7), 55, doi:10.5047/eps.2011.06.010.
Fujiwara, T., C. dos Santos Ferreira, A. K. Bachmann, M. Strasser, G. Wefer, T. Sun, T. Kanamatsu, and S. Kodaira (2017), Seafloor Displacement After the 2011 Tohoku-oki Earthquake in the Northern Japan Trench Examined by Repeated Bathymetric Surveys, *Geophysical Research Letters*, *44*(23), 11,833-811,839, doi:10.1002/2017GL075839.
Fujiwara, T., S. Kodaira, T. No, Y. Kaiho, N. Takahashi, and Y. Kaneda (2011), The 2011 Tohoku-Oki Earthquake: Displacement Reaching the Trench Axis, *Science*, *334*(6060), 1240, doi:10.1126/science.1211554.
Fukushima, Y., and T. Nishikawa (2020), New Earthquake Warning Framework in the Nankai Trough Subduction Zone in Japan and Scientific Rationale that the Society Need to Know for Effective Countermeasures, *AGU 2020 Fall Meeting*.
Fukushima, Y., S. Toda, S. Miura, D. Ishimura, J. i. Fukuda, T. Demachi, and K. Tachibana (2018), Extremely early recurrence of intraplate fault rupture following the Tohoku-Oki earthquake, *Nature Geoscience*, doi:10.1038/s41561-018-0201-x.
Fukuyama, E., and S. Hok (2015), Dynamic Overshoot Near Trench Caused by Large Asperity Break at Depth, *Pure and Applied Geophysics*, *172*(8), 2157-2165, doi:10.1007/s00024-013-0745-z.
Fulton, P. M., E. E. Brodsky, Y. Kano, J. Mori, F. Chester, T. Ishikawa, R. N. Harris, W. Lin, N. Eguchi, and S. Toczko (2013), Low Coseismic Friction on the Tohoku-Oki Fault Determined from Temperature Measurements, *Science*, *342*(6163), 1214, doi:10.1126/science.1243641.
Gao, X., and K. Wang (2014), Strength of stick-slip and creeping subduction megathrusts from heat flow observations, *Science*, *345*(6200), 1038, doi:10.1126/science.1255487.
Geospatial Information Authority of Japan (2011), The 2011 off the Pacific coast of Tohoku Earthquake, Coseismic and postseismic
slip distribution on the plate interface (preliminary result), *http://www.gsi.go.jp/cais/topic110315.2-index-e.html*.

Gonzalez-Huizar, H., A. A. Velasco, Z. Peng, and R. R. Castro (2012), Remote triggered seismicity caused by the 2011, M9.0 Tohoku-Oki, Japan earthquake, *Geophysical Research Letters*, *39*(10), doi:https://doi.org/10.1029/2012GL051015.

Goto, K., et al. (2011), New insights of tsunami hazard from the 2011 Tohoku-oki event, *Marine Geology*, *290*(1), 46-50, doi:https://doi.org/10.1016/j.margeo.2011.10.004.

Goto, T., K. Satake, T. Sugai, T. Ishibe, T. Harada, and S. Murotani (2015), Historical tsunami and storm deposits during the last five centuries on the Sanriku coast, Japan, *Marine Geology*, *367*, 105-117, doi:https://doi.org/10.1016/j.margeo.2015.05.009.

Gusman, A. R., Y. Tanioka, S. Sakai, and H. Tsushima (2012), Source model of the great 2011 Tohoku earthquake estimated from tsunami waveforms and crustal deformation data, *Earth and Planetary Science Letters*, *341-344*, 234-242, doi:https://doi.org/10.1016/j.epsl.2012.06.006.

Hara, T. (2011), Magnitude determination using duration of high frequency energy radiation and displacement amplitude: application to the 2011 off the Pacific coast of Tohoku Earthquake, *Earth, Planets and Space*, *63*(7), 3, doi:10.5047/eps.2011.05.014.

Hardebeck, J. L. (2012), Coseismic and postseismic stress rotations due to great subduction zone earthquakes, *39*(21), doi:https://doi.org/10.1029/2012GL053438.

Hardebeck, J. L. (2015), Stress orientations in subduction zones and the strength of subduction megathrust faults, *Science*, *349*(6253), 1213, doi:10.1126/science.aac5625.

Hardebeck, J. L., K. R. Felzer, and A. J. Michael (2008), Improved tests reveal that the accelerating moment release hypothesis is statistically insignificant, *Journal of Geophysical Research: Solid Earth*, *113*(B8), doi:10.1029/2007JB005410.

Hardebeck, J. L., and T. Okada (2018), Temporal Stress Changes Caused by Earthquakes: A Review, *Journal of Geophysical Research: Solid Earth*, *123*(2), 1350-1365, doi:https://doi.org/10.1002/2017JB014617.

Hasegawa, A. (2011), Social function of seismologiost and seismology community - on the relationship with government, *The report of special committee for the Tohoku-oki earthquake, Seismological Society of Japan*, 18-22, https://www.zisin.jp/publications/pdf/SSJ_final_report.pdf.

Hasegawa, A., J. Nakajima, N. Uchida, T. Okada, D. Zhao, T. Matsuzawa, and N. Umino (2009), Plate subduction, and generation of earthquakes and magmas in Japan as inferred from seismic observations: An overview, *Gondwana Research*, *16*, 370-400.

Hasegawa, A., N. Umino, and A. Takagi (1978), Double-planed structure of the deep seismic zone in the northeastern Japan arc, *Tectonophysics*, *47*(1–2), 43-58, doi:http://dx.doi.org/10.1016/0040-1951(78)90150-6.

Hasegawa, A., N. Umino, and A. Takagi (1985), Seismicity in the Northeastern Japan Arc and Seismicity Patterns before Large Earthquakes, *Kisslinger C., Rikitake T. (eds) Practical Approaches to Earthquake Prediction and Warning*, doi:10.1007/978-94-017-2738-9_23.

Hasegawa, A., and K. Yoshida (2015), Preceding seismic activity and slow slip events in the source area of the 2011 Mw 9.0 Tohoku-Oki earthquake: a review, *Geoscience Letters*, *2*(1), 6, doi:10.1186/s40562-015-0025-0.

Hasegawa, A., K. Yoshida, Y. Asano, T. Okada, T. Iinuma, and Y. Ito (2012), Change in stress field after the 2011 great Tohoku-Oki earthquake, *Earth and Planetary Science Letters*, *355–356*, 231-243, doi:http://dx.doi.org/10.1016/j.epsl.2012.08.042.

Hasegawa, A., K. Yoshida, and T. Okada (2011), Nearly complete stress drop in the 2011 Mw 9.0 off the Pacific coast of Tohoku Earthquake, *Earth, Planets and Space*, *63*(7), 35, doi:10.5047/eps.2011.06.007.

Hashimoto, C., A. Noda, and M. Matsu′ ura (2012), The M w 9.0 northeast Japan earthquake: total rupture of a basement asperity, *Geophysical Journal International*, *189*(1), 1-5.

Hashimoto, C., A. Noda, T. Sagiya, and M. Matsu/'ura (2009), Interplate seismogenic zones along the Kuril-Japan trench inferred from GPS data inversion, *Nature Geosci*, *2*(2), 141-144, doi:http://www.nature.com/ngeo/journal/v2/n2/suppinfo/ngeo421_S1.html.

Hashimoto, T., and T. Yokota (2019), Successively occurring large earthquakes in the world –comparison of real cases with expectations by the space-time ETAS, *JpGU 2019 meeting*, SSS10-P02.

Hatori, T. (1972), The Tsunamis generated off Cape Erimo on August 2, 1971 and off Hachijo Island on February 29, 1972: Tsunami source and distribution of the initial motion of Tsunami, *Zisin 2*, *25*(4), 362-370, doi:10.4294/zisin1948.25.4_362.

Hatori, T. (1974), Tsunami sources on the Pacific side in norsteast Japan, *Zisin(2)*, *27*, 321-337.

Hatori, T. (1975), Sources of Tsunamis generated off Boso Peninsula, *Bulletin of the Earthquake Research Institute, University of Tokyo*, *50*(1), 83-91.

Hatori, T. (1976), Source Mechanisms of Tsunamis Associated with the Fukushima-oki Earthquake Swarm in 1938, *Zisin 2*, *29*(2), 179-190.

Hatori, T. (1978), The Tsunami Generated off Miyagi Prefecture in 1978 and Tsunami Activity in the Region, *Bulletin of the Earthquake Research Institute, University of Tokyo*, *53*(4), 1177-1189.

Hatori, T. (1989), Characteristic of Tsunamis Associated with Aftershock and Swarm near Japan, *Zisin 2*, *42*, 183-188.

Hatori, T. (1996), The 1994 Sanriku-Oki Tsunami and Distribution of the Radiating Tsunami Energy in the Sanriku Region, *Zisin 2*, *49*(1), 19-26.

Hatori, T. (2012), The size of the Tsunami of the 2011 Tohoku-oki earthquake, *Report of Tsunami Engineering*, *31*, 325-328.

Hayes, G. P. (2011), Rapid source characterization of the 2011 Mw 9.0 off the Pacific coast of Tohoku Earthquake, *Earth, Planets and Space*, *63*(7), 4, doi:10.5047/eps.2011.05.012.

Headquarters for Earthquake Research Promotion (2020), The catalogue of long-term foracast of active faults and subduction zone earthquakes, https://www.jishin.go.jp/main/choukihyoka/ichiran.pdf.

Headquarters for Earthquake Research Promotion, Ministry of Education, Culture, Sports, Science and Technology, Japan (2011), The Evaluation of Seismic Activities in Japan, February 2011, *https://www.static.jishin.go.jp/resource/monthly/2011/2011_02.pdf*.

Headquarters for Earthquake Research Promotion, Ministry of Education, Culture, Sports, Science and Technology, Japan,, (2009), Summary report of the Research and Observation of the Miyagi-Oki Earthquake conducted in 2005-2009, *https://www.jishin.go.jp/database/project_report/miyagi_juten/*.

Headquarters of Earthquake Research Promotion, M. o. E., Culture, Sports, Science and Technology, Japan (2000), The long-term earthquake forecast of the Miyagi-ken-oki earthquake, *https://www.jishin.go.jp/main/chousa/00nov4/miyagi.htm*.

Headquarters of Earthquake Research Promotion, M. o. E., Culture, Sports, Science and Technology, Japan (2002), Longterm forecast of earthquakes from Sanriku-oki to Boso-oki, https://www.jishin.go.jp/main/chousa/kaikou_pdf/sanriku_boso.pdf.

Heki, K. (2011), Ionospheric electron enhancement preceding the 2011 Tohoku-Oki earthquake, *Geophysical Research Letters*, *38*(17), doi:10.1029/2011GL047908.

Heki, K., and Y. Enomoto (2015), Mw dependence of the preseismic ionospheric electron enhancements, *Journal of Geophysical Research: Space Physics*, *120*(8), 7006-7020, doi:10.1002/2015JA021353.

Heki, K., S. Miyazaki, and H. Tsuji (1997), Silent fault slip following an interplate thrust earthquake at the Japan Trench, *Nature*, *386*(6625), 595-598.

Hino, R. (2015), An overview of the Mw 9, 11 March 2011, Tohoku earthquake, *Summary of the Bulletin of the International Seismological Centre*, *48*(1-6), 100-132, doi:10.5281/zenodo.998789.

Hino, R., D. Inazu, Y. Ohta, Y. Ito, S. Suzuki, T. Iinuma, Y. Osada, M. Kido, H. Fujimoto, and Y. Kaneda (2014), Was the 2011 Tohoku-Oki earthquake preceded by aseismic preslip? Examination of seafloor vertical deformation data near the epicenter, *Mar Geophys Res*, *35*(3), 181-190, doi:10.1007/s11001-013-9208-2.

Hino, R., T. Tanioka, T. Kanazawa, S. Sakai, M. Nishino, and K. Suyehiro (2001), Micro-tsunami from a local interplate earthquake detected by cabled offshore tsunami observation in northeastern Japan, *Geophys. Res. Lett.*, *28*, 3533-3536.

Hirakawa, K. (2012), Outsize tsunami sediments since last years along the Japan and Kuril-Trench: a tentative idea on source and supercycle, *Kagaku*, *82*, 172-181.

Hirono, T., K. Tsuda, W. Tanikawa, J.-P. Ampuero, B. Shibazaki, M. Kinoshita, and J. J. Mori (2016), Near-trench slip potential of megaquakes evaluated from fault properties and conditions, *Scientific Reports*, *6*(1), 28184, doi:10.1038/srep28184.

Honsho, C., M. Kido, F. Tomita, and N. Uchida (2019), Offshore Postseismic Deformation of the 2011 Tohoku Earthquake Revisited: Application of an Improved GPS-Acoustic Positioning Method Considering Horizontal Gradient of Sound Speed Structure, *124*(6), 5990-6009, doi:10.1029/2018jb017135.

Hooper, A., J. Pietrzak, W. Simons, H. Cui, R. Riva, M. Naeije, A. Terwisscha van Scheltinga, E. Schrama, G. Stelling, and A. Socquet (2013), Importance of horizontal seafloor motion on tsunami height for the 2011 Mw=9.0 Tohoku-Oki earthquake, *Earth and Planetary Science Letters*, *361*, 469-479, doi:https://doi.org/10.1016/j.epsl.2012.11.013.

Hori, T., T. Matsuzawa, and Y. Yagi (2011), Why the Tohoku-oki was not assumed - identifying problems for new seismology, *The report of special committee for the Tohoku-oki earthquake, Seismological Society of Japan*, 125-130, https://www.zisin.jp/publications/pdf/SSJ_final_report.pdf.

Hori, T., and S. i. Miyazaki (2010), Hierarchical asperity model for multiscale characteristic earthquakes: A numerical study for the off-Kamaishi earthquake sequence in the NE Japan subduction zone, *Geophys. Res. Lett.*, *37*(10), L10304, doi:10.1029/2010gl042669.

Hoshiba, M., and K. Iwakiri (2011), Initial 30 seconds of the 2011 off the Pacific coast of Tohoku Earthquake (Mw 9.0)—amplitude and τcfor magnitude estimation for Earthquake Early Warning—, *Earth, Planets and Space*, *63*(7), 8, doi:10.5047/eps.2011.06.015.

Hossen, M. J., P. R. Cummins, J. Dettmer, and T. Baba (2015), Tsunami waveform inversion for sea surface displacement following the 2011 Tohoku earthquake: Importance of dispersion and source kinematics, *Journal of Geophysical Research: Solid Earth*, *120*(9), 6452-6473, doi:10.1002/2015JB011942.

Hu, Y., R. Bürgmann, N. Uchida, P. Banerjee, and J. T. Freymueller (2016), Stress-driven relaxation of heterogeneous upper mantle and time-dependent afterslip following the 2011 Tohoku earthquake, *Journal of Geophysical Research: Solid Earth*, 2015JB012508, doi:10.1002/2015JB012508.

Hua, Y., D. Zhao, G. Toyokuni, and Y. Xu (2020), Tomography of the source zone of the great 2011 Tohoku earthquake, *Nature Communications*, *11*(1), 1163, doi:10.1038/s41467-020-14745-8.

Hyndman, R. D., and K. Wang (1993), Thermal Constraints on the Zone of Major Thrust Earthquake Failure - the Cascadia Subduction Zone, *J Geophys Res-Sol Ea*, *98*(B2), 2039-2060.

Ide, S., and H. Aochi (2005), Earthquakes as multiscale dynamic ruptures with heterogeneous fracture surface energy, *Journal of Geophysical Research: Solid Earth*, *110*(B11), doi:doi:10.1029/2004JB003591.

Ide, S., A. Baltay, and G. C. Beroza (2011), Shallow dynamic overshoot and energetic deep rupture in the 2011 Mw 9.0 Tohoku-oki earthquake, *Science*, *332*, 1427-1429.

Igarashi, T., T. Matsuzawa, and A. Hasegawa (2003), Repeating earthquakes and interplate aseismic slip in the northeastern Japan subduction zone, *J. Geophys. Res.*, *108*, 10.1029/2002JB001920.

Igarashi, T., T. Matsuzawa, N. Umino, and A. Hasegawa (2001), Spatial distribution of focal mechanisms for interplate and intraplate earthquakes associated with the subducting Pacific plate beneath the northeastern Japan arc: A triple-plated deep seismic zone, *J. Geophys. Res.*, *106*, 2177-2191.

Iinuma, T. (2018), Monitoring of the spatio-temporal change in the interplate coupling at northeastern Japan subduction zone based on the spatial gradients of surface velocity field, *Geophysical Journal International*, *213*(1), 30-47, doi:10.1093/gji/ggx527.

Iinuma, T., et al. (2012), Coseismic slip distribution of the 2011 off the Pacific Coast of Tohoku Earthquake (M9.0) refined by means of seafloor geodetic data, *J. Geophys. Res.*, *117*, doi:10.1029/2012JB009186.

Iinuma, T., R. Hino, N. Uchida, W. Nakamura, M. Kido, Y. Osada, and S. Miura (2016), Seafloor observations indicate spatial separation of coseismic and postseismic slips in the 2011 Tohoku earthquake, *Nature Communications*, *7*, 13506, doi:10.1038/ncomms13506 http://www.nature.com/articles/ncomms13506#supplementary-information.

Ikeda, Y. (1996), Implications of active fault study for the present-day tectonics of the Japan arc, *Active Fault Research (Katsudanso Kenkyu)*, *15*, 93–99.

Ikehara, K., T. Kanamatsu, Y. Nagahashi, M. Strasser, H. Fink, K. Usami, T. Irino, and G. Wefer (2016), Documenting large earthquakes similar to the 2011 Tohoku-oki earthquake from sediments deposited in the Japan Trench over the past 1500 years, *Earth and Planetary Science Letters*, *445*, 48-56, doi:https://doi.org/10.1016/j.epsl.2016.04.009.

Ikehara, K., K. Usami, and T. Kanamatsu (2020), Repeated occurrence of surface-sediment remobilization along the landward slope of the Japan Trench by great earthquakes, *Earth, Planets and Space*, *72*(1), 114, doi:10.1186/s40623-020-01241-y.

Ikehara, K., K. Usami, T. Kanamatsu, K. Arai, A. Yamaguchi, and R. Fukuchi (2018), Spatial variability in sediment lithology and sedimentary processes along the Japan Trench: use of deep-sea turbidite records to reconstruct past large earthquakes, *Geological Society, London, Special Publications*, *456*(1), 75, doi:10.1144/SP456.9.

Ikuta, R., T. Hisada, G. Karakama, and O. Kuwano *Was the observed pre-seismic total electron content enhancement a true precursor of the 2011 Tohoku-Oki Earthquake? %J Earth and Space Science Open Archive*, 33 pp., doi:doi:10.1002/essoar.10502392.2.

Imai, K., T. Maeda, T. Iinuma, Y. Ebina, D. Sugawara, F. Imamura, and A. Hirakawa (2015), Paleo tsunami source estimation by using combination optimization algorithm - Case study of The 1611 Keicho earthquake tsunami, *Tohoku Journal of Natural Disaster Science*, *51*, 139-144.

Imanishi, K., R. Ando, and Y. Kuwahara (2012), Unusual shallow normal-faulting earthquake sequence in compressional northeast Japan activated after the 2011 off the Pacific coast of Tohoku earthquake, *Geophysical Research Letters*, *39*(9), L09306, doi:10.1029/2012GL051491.

Ishimura, D., and T. Miyauchi (2015), Historical and paleo-tsunami deposits during the last 4000 years and their correlations with historical tsunami events in Koyadori on the Sanriku Coast, northeastern Japan, *Progress in Earth and Planetary Science*, *2*(1), 16, doi:10.1186/s40645-015-0047-4.

Ito, T., K. Ozawa, T. Watanabe, and T. Sagiya (2011a), Slip distribution of the 2011 off the Pacific coast of Tohoku Earthquake inferred from geodetic data, *Earth, Planets and Space*, *63*(7), 21, doi:10.5047/eps.2011.06.023.

Ito, Y., et al. (2013), Episodic slow slip events in the Japan subduction zone before the 2011 Tohoku-Oki earthquake, *Tectonophysics*, *600*(0), 14-26, doi:http://dx.doi.org/10.1016/j.tecto.2012.08.022.

Ito, Y., T. Tsuji, Y. Osada, M. Kido, D. Inazu, Y. Hayashi, H. Tsushima, R. Hino, and H. Fujimoto (2011b), Frontal wedge deformation near the source region of the 2011 Tohoku-Oki earthquake, *Geophysical Research Letters*, *38*(7), doi:10.1029/2011GL048355.

Japan Meteorological Agency (2013), Lessons learned from the tsunami disaster caused by the 2011 Great East Japan Earthquake and improvements in JMA's tsunami warning system, https://www.jma.go.jp/jma/en/Publications/publications.html.

Japan Meteorological Agency (2019), On the launch of the Nankai trough earthquake extra information *https://www.jma.go.jp/jma/press/1905/31a/20190531_nteq_name.html*.

Johnson, K. M., J. i. Fukuda, and P. Segall (2012), Challenging the rate-state asperity model: Afterslip following the 2011 M9 Tohoku-oki, Japan, earthquake, *Geophysical Research Letters*, *39*(20), n/a-n/a, doi:10.1029/2012GL052901.

Jordan, T. H., Y.-T. Chen, P. Gasparini, R. Madariaga, I. Main, W. Marzocchi, G. Papadopoulos, G. Sobolev, K. Yamaoka, and J. Zschau (2011), Operational earthquake forecasting. State of knowledge and guidelines for utilization, *Annals of Geophysics*, *54*(4).

JR East (2019), On the addition of sea-bottom seismometers to the Shinkansen Early Earthquake Detection System, *https://www.jreast.co.jp/press/2018/20190110.pdf*.

Kagan, Y. Y. (1997), Seismic moment-frequency relation for shallow earthquakes: Regional comparison, *Journal of Geophysical Research: Solid Earth*, *102*(B2), 2835-2852, doi:10.1029/96JB03386.

Kagan, Y. Y., and D. D. Jackson (2013), Tohoku Earthquake: A Surprise?, *B Seismol Soc Am*, *103*(2B), 1181-1194, doi:10.1785/0120120110.

Kahoku-shinpo (2011), The relationship between the Sanriku-oki M7.3 earthquake and Miyagi-ken-oki earthquake - the possibility of a multisegment rupture decreased?, *March 10, 2011, Kahoku-shinpo (news paper)*.

Kaizuka, S., and T. Imaizumi (1984), Horizontal strain rates of the japanese islands estimated from quaternary fault data, *Geographical Reports of Tokyo Metropolitan University*, *19*, 43-65.

Kamogawa, M., and Y. Kakinami (2013), Is an ionospheric electron enhancement preceding the 2011 Tohoku-Oki earthquake a precursor?, *Journal of Geophysical Research: Space Physics*, *118*(4), 1751-1754, doi:10.1002/jgra.50118.

Kanamori, H. (1972), Mechanism of tsunami earthquakes, *Physics of the Earth and Planetary Interiors*, *6*(5), 346-359, doi:https://doi.org/10.1016/0031-9201(72)90058-1.

Kanamori, H., M. Miyazawa, and J. Mori (2006), Investigation of the earthquake sequence off Miyagi prefecture with historical seismograms, *Earth, Planets and Space*, *58*(12), 1533-1541, doi:10.1186/BF03352657.

Kano, M., A. Kato, and K. Obara (2019), Episodic tremor and slip silently invades strongly locked megathrust in the Nankai Trough, *Scientific Reports*, *9*(1), 9270, doi:10.1038/s41598-019-45781-0.

Katakami, S., Y. Ito, K. Ohta, R. Hino, S. Suzuki, and M. Shinohara (2018), Spatiotemporal Variation of Tectonic Tremor Activity Before the Tohoku-Oki Earthquake, *Journal of Geophysical Research: Solid Earth*, *123*(11), 9676-9688, doi:10.1029/2018JB016651.

Kato, A., and Y. Ben-Zion (2020), The generation of large earthquakes, *Nature Reviews Earth & Environment*, doi:10.1038/s43017-020-00108-w.

Kato, A., J. i. Fukuda, and K. Obara (2013), Response of seismicity to static and dynamic stress changes induced by the 2011 M9.0 Tohoku-Oki earthquake, *Geophysical Research Letters*, *40*(14), 3572-3578, doi:https://doi.org/10.1002/grl.50699.

Kato, A., and T. Igarashi (2012), Regional extent of the large coseismic slip zone of the 2011 Mw 9.0 Tohoku-Oki earthquake delineated by on-fault aftershocks, *Geophysical Research Letters*, *39*(15), n/a-n/a, doi:10.1029/2012gl052220.

Kato, A., K. Obara, T. Igarashi, H. Tsuruoka, S. Nakagawa, and N. Hirata (2012), Propagation of Slow Slip Leading Up to the 2011 Mw 9.0 Tohoku-Oki Earthquake, *Science*, *335*(6069), 705-708, doi:10.1126/science.1215141.

Katsumata, K. (2011), A long-term seismic quiescence started 23 years before the 2011 off the Pacific coast of Tohoku Earthquake (M = 9.0), *Earth, Planets and Space*, *63*(7), 36, doi:10.5047/eps.2011.06.033.

Kawasaki, I., Y. Asai, and Y. Tamura (2001), Space–time distribution of interplate moment release including slow earthquakes and the seismo-geodetic coupling in the Sanriku-oki region along the Japan trench, *Tectonophysics*, *330*(3), 267-283, doi:https://doi.org/10.1016/S0040-1951(00)00245-6.

Kido, M., Y. Osada, H. Fujimoto, R. Hino, and Y. Ito (2011), Trench-normal variation in observed seafloor displacements associated with the 2011 Tohoku-Oki earthquake, *Geophysical Research Letters*, *38*(24), doi:10.1029/2011GL050057.

Kiser, E., and M. Ishii (2013), Hidden aftershocks of the 2011 Mw 9.0 Tohoku, Japan earthquake imaged with the backprojection method, *Journal of Geophysical Research: Solid Earth*, *118*(10), 5564-5576, doi:10.1002/2013JB010158.

Kita, S., T. Okada, A. Hasegawa, J. Nakajima, and T. Matsuzawa (2010a), Anomalous deepening of a seismic belt in the upper-plane of the double seismic zone in the Pacific slab beneath the Hokkaido corner : Possible evidence for thermal shielding caused by subducted forearc crust materials, *Earth Planet. Sci. Lett.*, *290*, 415-426.

Kita, S., T. Okada, A. Hasegawa, J. Nakajima, and T. Matsuzawa (2010b), Existence of interplane earthquakes and neutral stress boundary between the upper and lower planes of the double seismic zone beneath Tohoku and Hokkaido, northeastern Japan, *Tectonophysics*, *496*(1–4), 68-82, doi:http://dx.doi.org/10.1016/j.tecto.2010.10.010.

Kobayashi, T., M. Tobita, T. Nishimura, A. Suzuki, Y. Noguchi, and M. Yamanaka (2011), Crustal deformation map for the 2011 off the Pacific coast of Tohoku Earthquake, detected by InSAR analysis combined with GEONET data, *Earth, Planets and Space*, *63*(7), 20, doi:10.5047/eps.2011.06.043.

Kodaira, S., T. Fujiwara, G. Fujie, Y. Nakamura, and T. Kanamatsu (2020), Large Coseismic Slip to the Trench During the 2011 Tohoku-Oki Earthquake, *Annual Review of Earth and Planetary Sciences*, *48*(1), 321-343, doi:10.1146/annurev-earth-071719-055216.

Kodaira, S., T. No, Y. Nakamura, T. Fujiwara, Y. Kaiho, S. Miura, N. Takahashi, Y. Kaneda, and A. Taira (2012), Coseismic fault rupture at the trench axis during the 2011 Tohoku-oki earthquake, *Nature Geoscience*, *5*(9), 646-650, doi:10.1038/ngeo1547.

Koketsu, K., et al. (2011), A unified source model for the 2011 Tohoku earthquake, *Earth and Planetary Science Letters*, *310*(3–4), 480-487, doi:10.1016/j.epsl.2011.09.009.

Konca, A. O., et al. (2008), Partial rupture of a locked patch of the Sumatra megathrust during the 2007 earthquake sequence, *Nature*, *456*(7222), 631-635, doi:10.1038/nature07572.

Kozdon, J. E., and E. M. Dunham (2013), Rupture to the Trench: Dynamic Rupture Simulations of the 11 March 2011 Tohoku Earthquake, *B Seismol Soc Am*, *103*(2B), 1275-1289, doi:10.1785/0120120136.

Kubo, H., K. Asano, and T. Iwata (2013), Source-rupture process of the 2011 Ibaraki-oki, Japan, earthquake (Mw 7.9) estimated from the joint inversion of strong-motion and GPS Data: Relationship with seamount and Philippine Sea Plate, *Geophysical Research Letters*, *40*(12), 3003-3007, doi:10.1002/grl.50558.

Kubo, H., and Y. Kakehi (2013), Source Process of the 2011 Tohoku Earthquake Estimated from the Joint Inversion of Teleseismic Body Waves and Geodetic Data Including Seafloor Observation Data: Source Model with Enhanced Reliability by Using Objectively Determined Inversion Settings, *B Seismol Soc Am*, *103*(2B), 1195-1220, doi:10.1785/0120120113.

Kubo, H., and T. Nishikawa (2020), Relationship of preseismic, coseismic, and postseismic fault ruptures of two large interplate aftershocks of the 2011 Tohoku earthquake with slow-earthquake activity, *Scientific Reports*, *10*(1), 12044, doi:10.1038/s41598-020-68692-x.

Kubota, T., R. Hino, D. Inazu, and S. Suzuki (2019), Fault model of the 2012 doublet earthquake, near the up-dip end of the 2011 Tohoku-Oki earthquake, based on a near-field tsunami: implications for intraplate stress state, *Progress in Earth and Planetary Science*, *6*(1), 67, doi:10.1186/s40645-019-0313-y.

Kurahashi, S., and K. Irikura (2011), Source model for generating strong ground motions during the 2011 off the Pacific coast of Tohoku Earthquake, *Earth, Planets and Space*, *63*(7), 11, doi:10.5047/eps.2011.06.044.

Kyriakopoulos, C., T. Masterlark, S. Stramondo, M. Chini, and C. Bignami (2013), Coseismic slip distribution for the Mw 9 2011 Tohoku-Oki earthquake derived from 3-D FE modeling, *Journal of Geophysical Research: Solid Earth*, *118*(7), 3837-3847, doi:10.1002/jgrb.50265.

Lay, T. (2018), A review of the rupture characteristics of the 2011 Tohoku-oki Mw 9.1 earthquake, *Tectonophysics*, *733*, 4-36, doi:https://doi.org/10.1016/j.tecto.2017.09.022.

Lay, T., C. J. Ammon, H. Kanamori, M. J. Kim, and L. Xue (2011a), Outer trench-slope faulting and the 2011 Mw 9.0 off the Pacific coast of Tohoku Earthquake, *Earth, planets and space*, *63*(7), 713-718.

Lay, T., C. J. Ammon, H. Kanamori, L. Rivera, K. D. Koper, and A. R. Hutko (2010), The 2009 Samoa-Tonga great earthquake triggered doublet, *Nature*, *466*(7309), 964-968, doi:http://www.nature.com/nature/journal/v466/n7309/abs/nature09214.html#supplementary-information.

Lay, T., C. J. Ammon, H. Kanamori, L. Xue, and M. J. Kim (2011b), Possible large near-trench slip during the 2011 M(w) 9.0 off the Pacific coast of Tohoku Earthquake, *Earth Planets and Space*, *63*(7), 687-692, doi:10.5047/eps.2011.05.033.

Lay, T., H. Kanamori, C. J. Ammon, K. D. Koper, A. R. Hutko, L. Ye, H. Yue, and T. M. Rushing (2012), Depth-varying rupture properties of subduction zone megathrust faults, *Journal of Geophysical Research: Solid Earth*, *117*(B4), doi:10.1029/2011JB009133.

Lee, S.-J., B.-S. Huang, M. Ando, H.-C. Chiu, and J.-H. Wang (2011), Evidence of large scale repeating slip during the 2011 Tohoku-Oki earthquake, *Geophys. Res. Lett.*, *38*(19), L19306, doi:10.1029/2011gl049580.

Lengliné, O., B. Enescu, Z. Peng, and K. Shiomi (2012), Decay and expansion of the early aftershock activity following the 2011, Mw9.0 Tohoku earthquake, *Geophysical Research Letters*, *39*(18), doi:https://doi.org/10.1029/2012GL052797.

Lin, W., M. Conin, J. C. Moore, F. M. Chester, Y. Nakamura, J. J. Mori, L. Anderson, E. E. Brodsky, and N. Eguchi (2013), Stress State in the Largest Displacement Area of the 2011 Tohoku-Oki Earthquake, *Science*, *339*(6120), 687, doi:10.1126/science.1229379.

Loveless, J. P., and B. J. Meade (2010), Geodetic imaging of plate motions, slip rates, and partitioning of deformation in Japan, *Journal of Geophysical Research: Solid Earth*, *115*(B2), B02410, doi:10.1029/2008jb006248.

Maeda, T., T. Furumura, S. i. Sakai, and M. Shinohara (2011), Significant tsunami observed at ocean-bottom pressure gauges during the 2011 off the Pacific coast of Tohoku Earthquake, *Earth, Planets and Space*, *63*(7), 53, doi:10.5047/eps.2011.06.005.

Masci, F., J. N. Thomas, F. Villani, J. A. Secan, and N. Rivera (2015), On the onset of ionospheric precursors 40 min before strong earthquakes, *Journal of Geophysical Research: Space Physics*, *120*(2), 1383-1393, doi:10.1002/2014JA020822.

Matsuo, K., and K. Heki (2011), Coseismic gravity changes of the 2011 Tohoku-Oki earthquake from satellite gravimetry, *Geophysical Research Letters*, *38*(7), doi:https://doi.org/10.1029/2011GL049018.

Matsuzawa, T. (2011), Why could the M9 earthquake occur in the northeastern Japan subduction zone?: Why did we believe it would not occur there?, *Kagaku*, *81(10)*, 1020-1026.

Matsuzawa, T., Y. Asano, and K. Obara (2015), Very low frequency earthquakes off the Pacific coast of Tohoku, Japan, *Geophysical Research Letters*, *42*(11), 4318-4325, doi:https://doi.org/10.1002/2015GL063959.

Matsuzawa, T., B. Shibazaki, K. Obara, and H. Hirose (2013), Comprehensive model of short- and long-term slow slip events in the Shikoku region of Japan, incorporating a realistic plate configuration, *Geophysical Research Letters*, *40*(19), 5125-5130, doi:10.1002/grl.51006.

Mavrommatis, A. P., P. Segall, and K. M. Johnson (2014), A decadal-scale deformation transient prior to the 2011 Mw 9.0 Tohoku-oki earthquake, *Geophysical Research Letters*, *41*(13), 4486-4494, doi:10.1002/2014gl060139.

Mavrommatis, A. P., P. Segall, N. Uchida, and K. M. Johnson (2015), Long-term acceleration of aseismic slip preceding the Mw 9 Tohoku-oki earthquake: Constraints from repeating earthquakes, *Geophysical Research Letters*, 2015GL066069, doi:10.1002/2015GL066069.

Mazzotti, S. p., and J. Adams (2004), Variability of Near-Term Probability for the Next Great Earthquake on the Cascadia Subduction Zone, *B Seismol Soc Am*, *94*(5), 1954-1959, doi:10.1785/012004032.

McCaffrey, R. (2008), Global frequency of magnitude 9 earthquakes, *Geology*, *36*(3), 263-266, doi:10.1130/G24402A.1.

McHugh, C. M., T. Kanamatsu, L. Seeber, R. Bopp, M.-H. Cormier, and K. Usami (2016), Remobilization of surficial slope sediment triggered by the A.D. 2011 Mw 9 Tohoku-Oki earthquake and tsunami along the Japan Trench, *Geology*, *44*(5), 391-394, doi:10.1130/G37650.1.

McLaskey, G. C. (2019), Earthquake Initiation From Laboratory Observations and Implications for Foreshocks, *Journal of Geophysical Research: Solid Earth*, *124*(12), 12882-12904, doi:https://doi.org/10.1029/2019JB018363.

Meade, B. J., and J. P. Loveless (2009), Predicting the geodetic signature of MW ≥ 8 slow slip events, *Geophysical Research Letters*, *36*(1), doi:https://doi.org/10.1029/2008GL036364.

Melgar, D., and Y. Bock (2015), Kinematic earthquake source inversion and tsunami runup prediction with regional geophysical data, *Journal of Geophysical Research: Solid Earth*, *120*(5), 3324-3349, doi:10.1002/2014JB011832.

Meneses-Gutierrez, A., and T. Sagiya (2016), Persistent inelastic deformation in central Japan revealed by GPS observation before and after the Tohoku-oki earthquake, *Earth and Planetary Science Letters*, *450*, 366-371, doi:https://doi.org/10.1016/j.epsl.2016.06.055.

Minoura, K., F. Imamura, D. Sugawara, Y. Kono, and T. J. J. o. N. D. S. Iwashita (2001), The 869 Jogan tsunami deposit and recurrence interval of large-scale tsunami on the Pacific coast of northeast Japan, *23*, 83-88.

Minoura, K., and S. Nakaya (1991), Traces of Tsunami preserved in inter-tidal lacustrine and marsh deposits - Some examples from northeast Japan, *J. Geol.*, *99*(2), 265-287.

Minson, S. E., M. Simons, J. L. Beck, F. Ortega, J. Jiang, S. E. Owen, A. W. Moore, A. Inbal, and A. Sladen (2014), Bayesian inversion for finite fault earthquake source models – II: the 2011 great Tohoku-oki, Japan earthquake, *Geophysical Journal International*, *198*(2), 922-940, doi:10.1093/gji/ggu170.

Miyazawa, M. (2011), Propagation of an earthquake triggering front from the 2011 Tohoku-Oki earthquake, *Geophysical Research Letters*, *38*(23), doi:10.1029/2011GL049795.
Mogi, K. (1969), Some Features of Recent Seismic Activity in and near Japan (2) : Activity before and after Great Earthquakes, *Bulletin of the Earthquake Research Institute, University of Tokyo*, *47(3)*, 395 - 417.
Molenaar, A., J. Moernaut, G. Wiemer, N. Dubois, and M. Strasser (2019), Earthquake Impact on Active Margins: Tracing Surficial Remobilization and Seismic Strengthening in a Slope Sedimentary Sequence, *Geophysical Research Letters*, *46*(11), 6015-6023, doi:10.1029/2019GL082350.
Mori, N., T. Takahashi, T. Yasuda, and H. Yanagisawa (2011), Survey of 2011 Tohoku earthquake tsunami inundation and run-up, *Geophysical Research Letters*, *38*(7), doi:10.1029/2011GL049210.
Murotani, T., M. Kikuchi, and Y. Yamanaka (2003), Rupture processes of large Fukushima-Oki Earthquakes in 1938, *presented at the 2003 Japan Geoscience Union, Chiba, Japan*, S052-004.
Murray, J., and J. Langbein (2006), Slip on the San Andreas Fault at Parkfield, California, over Two Earthquake Cycles, and the Implications for Seismic Hazard, *B Seismol Soc Am*, *96*(4B), S283-S303, doi:10.1785/0120050820.
Muto, J., B. Shibazaki, T. Iinuma, Y. Ito, Y. Ohta, S. Miura, and Y. Nakai (2016), Heterogeneous rheology controlled postseismic deformation of the 2011 Tohoku-Oki earthquake, *Geophysical Research Letters*, *43*(10), 4971-4978, doi:https://doi.org/10.1002/2016GL068113.
Nakajima, H., and M. Koarai (2011), Assessment of tsunami flood situation from the Great East Japan Earthquake, *Bulletin of the Geospatial Information Authority of Japan*, *59*.
Nakajima, J., A. Hasegawa, and S. Kita (2011), Seismic evidence for reactivation of a buried hydrated fault in the Pacific slab by the 2011 M9.0 Tohoku earthquake, *Geophysical Research Letters*, *38*(7), doi:https://doi.org/10.1029/2011GL048432.
Nakamura, W., N. Uchida, and T. Matsuzawa (2016), Spatial distribution of the faulting types of small earthquakes around the 2011 Tohoku - oki earthquake: A comprehensive search using template events, *Journal of Geophysical Research: Solid Earth*, *121*(4), 2591-2607, doi:doi:10.1002/2015JB012584.
Nakamura, Y., T. Fujiwara, S. Kodaira, S. Miura, and K. Obana (2020), Correlation of frontal prism structures and slope failures near the trench axis with shallow megathrust slip at the Japan Trench, *Scientific Reports*, *10*(1), 11607, doi:10.1038/s41598-020-68449-6.
Nakata, R., T. Hori, M. Hyodo, and K. Ariyoshi (2016), Possible scenarios for occurrence of M ~ 7 interplate earthquakes prior to and following the 2011 Tohoku-Oki earthquake based on numerical simulation, *Scientific Reports*, *6*(1), 25704, doi:10.1038/srep25704.
Nakatani, M. (2020), Evaluation of Phenomena Preceding Earthquakes and Earthquake Predictability, *Journal of Disaster Research*, *15*(2), 112-143, doi:10.20965/jdr.2020.p0112.
Namegaya, Y., and K. Satake (2014), Reexamination of the A.D. 869 Jogan earthquake size from tsunami deposit distribution, simulated flow depth, and velocity, *Geophysical Research Letters*, *41*(7), 2297-2303, doi:10.1002/2013GL058678.
Namegaya, Y., K. Satake, and S. Yamaki (2010), Numerical simulation of the AD 869 Jogan tsunami in Ishinomaki and Sendai
plains and Ukedo river-mouth lowland, *Annu. Rep. Active Fault Paleoearthquake Res.*, *10*, 1-21.
Namegaya, Y., and T. Yata (2014), Tsunamis which affected the Pacific coast of eastern Japan in medieval times inferrred from historical documents, *Zisin (Journal of the Seismological Society of Japan. 2nd ser.)*, *66*, 73-81, doi:10.4249/zisin.66.73.
Nanayama, F., K. Satake, R. Furukawa, K. Shimokawa, B. F. Atwater, K. Shigeno, and S. Yamaki (2003), Unusually large earthquakes inferred from tsunami deposits along the Kuril trench, *Nature*, *424*(6949), 660-663, doi:10.1038/nature01864.
Nanjo, K. Z., N. Hirata, K. Obara, and K. Kasahara (2012), Decade-scale decrease inb value prior to the M9-class 2011 Tohoku and 2004 Sumatra quakes, *Geophysical Research Letters*, *39*(20), doi:doi:10.1029/2012GL052997.
Nanjo, K. Z., H. Tsuruoka, N. Hirata, and T. H. Jordan (2011), Overview of the first earthquake forecast testing experiment in Japan, *Earth, Planets and Space*, *63*(3), 1, doi:10.5047/eps.2010.10.003.
National Research Institute for Earth Science and Disaster Resilience (2019), NIED S-net, *National Research Institute for Earth Science and Disaster Resilience*, 10.17598/NIED.10007
Nishikawa, T., T. Matsuzawa, K. Ohta, N. Uchida, T. Nishimura, and S. Ide (2019), The slow earthquake spectrum in the Japan Trench illuminated by the S-net seafloor observatories, *Science*, *365*, 808-813, doi:doi:10.1126/science.aax5618.
Nishimura, T., S. Miura, K. Tachibana, K. Hashimoto, T. Sato, S. Hori, E. Murakami, T. Kono, and M. M. K. Nida, T. Hirasawa, S. Miyazaki (2000), Distribution of seismic coupling on the subducting plate boundary in northeastern Japan inferred from GPS observations, *Tectonophysics*, *323*, 217-238.

Nishimura, T., M. Sato, and T. Sagiya (2014), Global Positioning System (GPS) and GPS-Acoustic Observations: Insight into Slip Along the Subduction Zones Around Japan, *Annual Review of Earth and Planetary Sciences*, *42*(1), 653-674, doi:10.1146/annurev-earth-060313-054614.

Noda, H., and N. Lapusta (2013), Stable creeping fault segments can become destructive as a result of dynamic weakening, *Nature*, *493*(7433), 518-521, doi:http://www.nature.com/nature/journal/v493/n7433/abs/nature11703.html#supplementary-information.

Obana, K., G. Fujie, T. Takahashi, Y. Yamamoto, Y. Nakamura, S. Kodaira, N. Takahashi, Y. Kaneda, and M. Shinohara (2012), Normal-faulting earthquakes beneath the outer slope of the Japan Trench after the 2011 Tohoku earthquake: Implications for the stress regime in the incoming Pacific plate, *Geophysical Research Letters*, *39*(7), L00G24, doi:10.1029/2011gl050399.

Obara, K., and A. Kato (2016), Connecting slow earthquakes to huge earthquakes, *Science*, *353*(6296), 253-257, doi:10.1126/science.aaf1512.

Ohta, Y., et al. (2012a), Geodetic constraints on afterslip characteristics following the March 9, 2011, Sanriku-oki earthquake, Japan, *Geophysical Research Letters*, *39*(16), doi:10.1029/2012GL052430.

Ohta, Y., et al. (2012b), Quasi real-time fault model estimation for near-field tsunami forecasting based on RTK-GPS analysis: Application to the 2011 Tohoku-Oki earthquake (Mw 9.0), *117*(B2), doi:10.1029/2011jb008750.

Ohzono, M., Y. Yabe, T. Iinuma, Y. Ohta, S. Miura, K. Tachibana, T. Sato, and T. Demachi (2013), Strain anomalies induced by the 2011 Tohoku Earthquake (Mw 9.0) as observed by a dense GPS network in northeastern Japan, *Earth, Planets and Space*, *64*(12), 17, doi:10.5047/eps.2012.05.015.

Okada, T., et al. (2015), Hypocenter migration and crustal seismic velocity distribution observed for the inland earthquake swarms induced by the 2011 Tohoku-Oki earthquake in NE Japan: implications for crustal fluid distribution and crustal permeability, *Geofluids*, *15*(1-2), 293-309, doi:10.1111/gfl.12112.

Okada, T., K. Yoshida, S. Ueki, J. Nakajima, N. Uchida, T. Matsuzawa, N. Umino, A. Hasegawa, and E. Group for the aftershock observations of the off the Pacific coast of Tohoku (2011), Shallow inland earthquakes in NE Japan possibly triggered by the 2011 off the Pacific coast of Tohoku Earthquake, *Earth, Planets and Space*, *63*(7), 44, doi:10.5047/eps.2011.06.027.

Oleskevich, D. A., R. D. Hyndman, and K. Wang (1999), The updip and downdip limits to great subduction earthquakes: Thermal and structural models of Cascadia, south Alaska, SW Japan, and Chile, *Journal of Geophysical Research: Solid Earth*, *104*(B7), 14965-14991, doi:10.1029/1999JB900060.

Orihara, Y., M. Kamogawa, Y. Noda, and T. Nagao (2019), Is Japanese Folklore Concerning Deep - Sea Fish Appearance a Real Precursor of Earthquakes?, *B Seismol Soc Am*, *109*(4), 1556-1562, doi:10.1785/0120190014.

Ozawa, S., T. Nishimura, H. Munekane, H. Suito, T. Kobayashi, M. Tobita, and T. Imakiire (2012), Preceding, coseismic, and postseismic slips of the 2011 Tohoku earthquake, Japan, *J Geophys Res*, doi:10.1029/2011JB009120.

Ozawa, S., T. Nishimura, H. Suito, T. Kobayashi, M. Tobita, and T. Imakiire (2011), Coseismic and postseismic slip of the 2011 magnitude 9 Tohoku-oki earthquake, *Nature*, 10.1038/nature10227.

Pacheco, J. F., L. R. Sykes, and C. H. Scholz (1993), Nature of seismic coupling along simple plate boundaries of the subduction type, *Journal of Geophysical Research: Solid Earth*, *98*(B8), 14133-14159, doi:10.1029/93jb00349.

Panet, I., S. Bonvalot, C. Narteau, D. Remy, and J.-M. Lemoine (2018), Migrating pattern of deformation prior to the Tohoku-Oki earthquake revealed by GRACE data, *Nature Geoscience*, *11*(5), 367-373, doi:10.1038/s41561-018-0099-3.

Pararas-Carayannis, G. (2014), The Great Tohoku-Oki Earthquake and Tsunami of March 11, 2011 in Japan: A Critical Review and Evaluation of the Tsunami Source Mechanism, *Pure and Applied Geophysics*, *171*(12), 3257-3278, doi:10.1007/s00024-013-0677-7.

Peltzer, G., P. Rosen, F. Rogez, and K. Hudnut (1996), Postseismic Rebound in Fault Step-Overs Caused by Pore Fluid Flow, *Science*, *273*(5279), 1202-1204, doi:10.1126/science.273.5279.1202.

Perfettini, H., and J. P. Avouac (2014), The seismic cycle in the area of the 2011 Mw9.0 Tohoku-Oki earthquake, *Journal of Geophysical Research: Solid Earth*, *119*(5), 4469-4515, doi:10.1002/2013JB010697.

Peterson, E. T., and T. Seno (1984), Factors affecting seismic moment release rates in subduction zones, *Journal of Geophysical Research: Solid Earth*, *89*(B12), 10233-10248.

Pollitz, F. F., R. Bürgmann, and P. Banerjee (2011), Geodetic slip model of the 2011 M9.0 Tohoku earthquake, *Geophys. Res. Lett.*, *38*, L00G08, doi:10.1029/2011gl048632.

Pritchard, M. E., et al. (2020), New Opportunities to Study Earthquake Precursors, *Seismological Research Letters*, *91*(5), 2444-2447, doi:10.1785/0220200089.

Reasenberg, P. A., and R. W. Simpson (1992), Response of Regional Seismicity to the Static Stress Change Produced by the Loma Prieta Earthquake, *Science*, *255*(5052), 1687, doi:10.1126/science.255.5052.1687.

Research Center for Prediction of Earthquakes and Volcanic Eruptions, Graduate School of Science, Tohoku University (2011), On the M7.3 earthquake off-Sanriku on March 9, 2011, *https://www.aob.gp.tohoku.ac.jp/info/topics/topics-110309/*.

Romano, F., A. Piatanesi, S. Lorito, N. D'Agostino, K. Hirata, S. Atzori, Y. Yamazaki, and M. Cocco (2012), Clues from joint inversion of tsunami and geodetic data of the 2011 Tohoku-oki earthquake, *Scientific Reports*, *2*(1), 385, doi:10.1038/srep00385.

Romano, F., E. Trasatti, S. Lorito, C. Piromallo, A. Piatanesi, Y. Ito, D. Zhao, K. Hirata, P. Lanucara, and M. Cocco (2014), Structural control on the Tohoku earthquake rupture process investigated by 3D FEM, tsunami and geodetic data, *Scientific Reports*, *4*(1), 5631, doi:10.1038/srep05631.

Ruff, L., and H. Kanamori (1980), Seismicity and the subduction process, *Physics of the Earth and Planetary Interiors*, *23*(3), 240-252, doi:https://doi.org/10.1016/0031-9201(80)90117-X.

Ruiz, S., M. Metois, A. Fuenzalida, J. Ruiz, F. Leyton, R. Grandin, C. Vigny, R. Madariaga, and J. Campos (2014), Intense foreshocks and a slow slip event preceded the 2014 Iquique Mw 8.1 earthquake, *Science*, doi:10.1126/science.1256074.

Saito, T., Y. Ito, D. Inazu, and R. Hino (2011), Tsunami source of the 2011 Tohoku-Oki earthquake, Japan: Inversion analysis based on dispersive tsunami simulations, *Geophysical Research Letters*, *38*(7), doi:10.1029/2011GL049089.

Satake, K., and Y. Fujii (2014), Review: Source Models of the 2011 Tohoku Earthquake and Long-Term Forecast of Large Earthquakes, *Journal of Disaster Research*, *9*(3), 272-280, doi:10.20965/jdr.2014.p0272.

Satake, K., Y. Fujii, T. Harada, and Y. Namegaya (2013), Time and Space Distribution of Coseismic Slip of the 2011 Tohoku Earthquake as Inferred from Tsunami Waveform Data, *B Seismol Soc Am*, *103*(2B), 1473-1492, doi:10.1785/0120120122.

Satake, K., Y. Namegaya, and S. Yamaki (2008), Numerical simulation of the AD 869 Jogan tsunami in Ishinomaki and Sendai plains, *Annual Report on Active Fault and Paleoearthquake Researches*, *8*, 71-89.

Sato, M., T. Ishikawa, N. Ujihara, S. Yoshida, M. Fujita, M. Mochizuki, and A. Asada (2011a), Displacement Above the Hypocenter of the 2011 Tohoku-Oki Earthquake, *Science*, 1207401, doi:10.1126/science.1207401.

Sato, M., H. Saito, T. Ishikawa, Y. Matsumoto, M. Fujita, M. Mochizuki, and A. Asada (2011b), Restoration of interplate locking after the 2005 Off-Miyagi Prefecture earthquake, detected by GPS/acoustic seafloor geodetic observation, *38*(1), doi:10.1029/2010gl045689.

Satriano, C., V. Dionicio, H. Miyake, N. Uchida, J.-P. Vilotte, and P. Bernard (2014), Structural and thermal control of seismic activity and megathrust rupture dynamics in subduction zones: Lessons from the Mw 9.0, 2011 Tohoku earthquake, *Earth and Planetary Science Letters*, *403*, 287-298, doi:https://doi.org/10.1016/j.epsl.2014.06.037.

Sawai, Y. (2017), Paleotsunami research along the Pacific coast of Tohoku region, *The Journal of the Geological Society of Japan*, *123*(10), 819-830, doi:10.5575/geosoc.2017.0055.

Sawai, Y., Y. Namegaya, Y. Okamura, K. Satake, and M. Shishikura (2012), Challenges of anticipating the 2011 Tohoku earthquake and tsunami using coastal geology, *Geophysical Research Letters*, *39*(21), L21309, doi:10.1029/2012gl053692.

Sawai, Y., Y. Namegaya, T. Tamura, R. Nakashima, and K. Tanigawa (2015), Shorter intervals between great earthquakes near Sendai: Scour ponds and a sand layer attributable to A.D. 1454 overwash, *Geophysical Research Letters*, *42*(12), 4795-4800, doi:10.1002/2015GL064167.

Sawai, Y., M. Shishikura, and J. Komatsubara (2008), A study on paleotsunami using hand corer in Sendai plain (Sendai City, Natori City, Iwanuma City, Watari Town, Yamamoto Town), Miyagi, Japan, *Annual report on active fault and paleoearthquake researches*, *8*, 17-70.

Sawai, Y., et al. (2007), A study on paleotsunami using handy geoslicer in Sendai Plain (Sendai, Natori, Iwanuma, Watari, and Yamamoto), Miyagi, Japan, *Annual report on active fault and paleoearthquake researches*, *7*, 47-80.

Sawazaki, K., H. Kimura, K. Shiomi, N. Uchida, R. Takagi, and R. Snieder (2015), Depth-dependence of seismic velocity change associated with the 2011 Tohoku earthquake, Japan, revealed from repeating earthquake analysis and finite-difference wave propagation simulation, *Geophysical Journal International*, *201*(2), 741-763, doi:10.1093/gji/ggv014.

Scholz, C. H., and J. Campos (2012), The seismic coupling of subduction zones revisited, *117*(B5), doi:10.1029/2011jb009003.

Schwartz, D. P., and K. J. Coppersmith (1984), Fault behavior and characteristic earthquakes: Examples from the Wasatch and San Andreas fault zones, *J. Geophys. Res.*, *89*, doi:10.1029/JB089iB07p05681.

Shao, G., X. Li, C. Ji, and T. Maeda (2011), Focal mechanism and slip history of the 2011 Mw 9.1 off the Pacific coast of Tohoku Earthquake, constrained with teleseismic body and surface waves, *Earth Planets Space*, *63*(7), 559-564.

2072 Shennan, I., R. Bruhn, and G. Plafker (2009), Multi-segment earthquakes and tsunami potential of the Aleutian
2073 megathrust, *Quaternary Science Reviews*, *28*(1), 7-13, doi:https://doi.org/10.1016/j.quascirev.2008.09.016.
2074 Shibazaki, B., T. Matsuzawa, A. Tsutsumi, K. Ujiie, A. Hasegawa, and Y. Ito (2011), 3D modeling of the cycle of a
2075 great Tohoku-oki earthquake, considering frictional behavior at low to high slip velocities, *Geophysical Research*
2076 *Letters*, *38*(21), L21305, doi:10.1029/2011gl049308.
2077 Shibazaki, B., H. Noda, and M. J. Ikari (2019), Quasi-Dynamic 3D Modeling of the Generation and Afterslip of a
2078 Tohoku-oki Earthquake Considering Thermal Pressurization and Frictional Properties of the Shallow Plate
2079 Boundary, *Pure and Applied Geophysics*, *176*(9), 3951-3973, doi:10.1007/s00024-018-02089-w.
2080 Shirzaei, M., R. Bürgmann, N. Uchida, Y. Hu, F. Pollitz, and T. Matsuzawa (2014), Seismic versus aseismic slip:
2081 Probing mechanical properties of the northeast Japan subduction zone, *Earth and Planetary Science Letters*, *406*(0),
2082 7-13, doi:http://dx.doi.org/10.1016/j.epsl.2014.08.035.
2083 Shishikura, M., O. Fujiwara, Y. Sawai, Y. Namegaya, and K. Tanigawa (2012), Inland-limit of the tsunami deposit
2084 associated with the 2011 Off-Tohoku Earthquake in the Sendai and Ishinomaki Plains, Northeastern Japan, *Annu.*
2085 *Rep. Active Fault Paleoearthquake Res.*, *12*, 45-61.
2086 Shishikura, M., Y. Sawai, Y. Okamura, J. Komatsubara, T. T. Aung, T. Ishiyama, O. Fujiwara, and S. Fujino (2007),
2087 Age and distribution of tsunami deposit in the Ishinomaki Plain, Northeastern Japan, *Annual Report on Active Fault*
2088 *and Paleoearthquake Researches*, *7*, 31-46.
2089 Silverii, F., D. Cheloni, N. D'Agostino, G. Selvaggi, and E. Boschi (2014), Post-seismic slip of the 2011 Tohoku-
2090 Oki earthquake from GPS observations: implications for depth-dependent properties of subduction megathrusts,
2091 *Geophysical Journal International*, *198*(1), 580-596, doi:10.1093/gji/ggu149.
2092 Somerville, P. G. (2014), A post-Tohoku earthquake review of earthquake probabilities in the Southern Kanto
2093 District, Japan, *Geoscience Letters*, *1*(1), 10, doi:10.1186/2196-4092-1-10.
2094 Strasser, M., et al. (2013), A slump in the trench: Tracking the impact of the 2011 Tohoku-Oki earthquake, *Geology*,
2095 *41*(8), 935-938, doi:10.1130/G34477.1.
2096 Sugawara, D., F. Imamura, K. Goto, H. Matsumoto, and K. Minoura (2013), The 2011 Tohoku-oki Earthquake
2097 Tsunami: Similarities and Differences to the 869 Jogan Tsunami on the Sendai Plain, *Pure and Applied Geophysics*,
2098 *170*(5), 831-843, doi:10.1007/s00024-012-0460-1.
2099 Sugawara, D., F. Imamura, H. Matsumoto, K. Goto, and K. Minoura (2010), Quantitative reconstruction of
2100 historical tsunami: On the investigation of tsunami trace of the Jyogan earthquake and estimation of
2101 palaeotopography, *Res. Rep. Tsunami Eng.*, *27*, 103-132.
2102 Sugawara, D., F. Imamura, H. Matsumoto, K. Goto, and K. Munoura (2011), Reconstruction of the AD869 Jogan
2103 earthquake induced tsunami by using the geological da, *Journal of Japan Society for Natural Disaster Science*,
2104 *29*(4), 501-516.
2105 Sugawara, D., K. Minoura, and F. Imamura (2001), Sedimentation associated with the AD 869 Jogan tsunami and
2106 its numerical reconstruction, *Res. Rep. Tsunami Eng.*, *18*, 1-10.
2107 Sun, T., and K. Wang (2015), Viscoelastic relaxation following subduction earthquakes and its effects on afterslip
2108 determination, *Journal of Geophysical Research: Solid Earth*, *120*(2), 2014JB011707, doi:10.1002/2014JB011707.
2109 Sun, T., K. Wang, T. Fujiwara, S. Kodaira, and J. He (2017), Large fault slip peaking at trench in the 2011 Tohoku-
2110 oki earthquake, *Nature Communications*, *8*(1), 14044, doi:10.1038/ncomms14044.
2111 Sun, T., et al. (2014), Prevalence of viscoelastic relaxation after the 2011 Tohoku-oki earthquake, *Nature*,
2112 *514*(7520), 84-87, doi:10.1038/nature13778.
2113 Suwa, Y., S. Miura, A. Hasegawa, T. Sato, and K. Tachibana (2006), Interplate coupling beneath NE Japan inferred
2114 from three dimensional displacement field, *J. Geophys. Res.*, *111*(B04402), doi:101029/102004JB003203.
2115 Suzuki, W., S. Aoi, H. Sekiguchi, and T. Kunugi (2011), Rupture process of the 2011 Tohoku-Oki mega-thrust
2116 earthquake (M9.0) inverted from strong-motion data, *Geophys. Res. Lett.*, *38*, L00G16, doi:10.1029/2011gl049136.
2117 Tajima, F., J. Mori, and B. L. N. Kennett (2013), A review of the 2011 Tohoku-Oki earthquake (Mw 9.0): Large-
2118 scale rupture across heterogeneous plate coupling, *Tectonophysics*, *586*, 15-34,
2119 doi:https://doi.org/10.1016/j.tecto.2012.09.014.
2120 Takada, K., et al. (2016), Distribution and ages of tsunami deposits along the Pacific Coast of the Iwate Prefecture,
2121 *Annu. Rep. Active Fault Paleoearthquake Res.*, *16*, 1-52.
2122 Takada, Y., and Y. Fukushima (2013), Volcanic subsidence triggered by the 2011 Tohoku earthquake in Japan,
2123 *Nature Geoscience*, *6*(8), 637-641, doi:10.1038/ngeo1857.
2124 Takagi, R., and T. Okada (2012), Temporal change in shear velocity and polarization anisotropy related to the
2125 2011 M9.0 Tohoku-Oki earthquake examined using KiK-net vertical array data, *Geophysical Research Letters*,
2126 *39*(9), doi:10.1029/2012GL051342.

Takahashi, H., R. Hino, N. Uchida, K. Ohta, and M. Shinohara (2020), Low-frequency tremor activity along northern Japan Trench before the 2011 Tohoku-Oki earthquake, *AGU 2020 Fall Meeting*, T003-0013.

Tanaka, S. (2012), Tidal triggering of earthquakes prior to the 2011 Tohoku-Oki earthquake (Mw 9.1), *Geophysical Research Letters*, *39*(7), L00G26, doi:10.1029/2012gl051179.

Tanioka, Y., and K. Satake (1996), Fault parameters of the 1896 Sanriku Tsunami Earthquake estimated from Tsunami Numerical Modeling, *Geophysical Research Letters*, *23*(13), 1549-1552, doi:10.1029/96gl01479.

Tapley, B. D., S. Bettadpur, J. C. Ries, P. F. Thompson, and M. M. Watkins (2004), GRACE Measurements of Mass Variability in the Earth System, *Science*, *305*(5683), 503, doi:10.1126/science.1099192.

Tappin, D. R., S. T. Grilli, J. C. Harris, R. J. Geller, T. Masterlark, J. T. Kirby, F. Shi, G. Ma, K. K. S. Thingbaijam, and P. M. Mai (2014), Did a submarine landslide contribute to the 2011 Tohoku tsunami?, *Marine Geology*, *357*, 344-361, doi:https://doi.org/10.1016/j.margeo.2014.09.043.

Toda, S., J. Lin, and R. S. Stein (2011a), Using the 2011 Mw 9.0 off the Pacific coast of Tohoku Earthquake to test the Coulomb stress triggering hypothesis and to calculate faults brought closer to failure, *Earth, Planets and Space*, *63*(7), 39, doi:10.5047/eps.2011.05.010.

Toda, S., R. S. Stein, and J. Lin (2011b), Widespread seismicity excitation throughout central Japan following the 2011 M=9.0 Tohoku earthquake and its interpretation by Coulomb stress transfer, *Geophysical Research Letters*, *38*(7), doi:10.1029/2011GL047834.

Tomita, F., T. Iinuma, Y. Ohta, R. Hino, M. Kido, and N. Uchida (2020), Improvement on spatial resolution of a coseismic slip distribution using postseismic geodetic data through a viscoelastic inversion, *Earth, Planets and Space*, *72*(1), 84, doi:10.1186/s40623-020-01207-0.

Tomita, F., M. Kido, Y. Ohta, T. Iinuma, and R. Hino (2017), Along-trench variation in seafloor displacements after the 2011 Tohoku earthquake, *Science Advances*, *3*(7), e1700113, doi:10.1126/sciadv.1700113.

Tormann, T., B. Enescu, J. Woessner, and S. Wiemer (2015), Randomness of megathrust earthquakes implied by rapid stress recovery after the Japan earthquake, *Nature Geosci*, *8*(2), 152-158, doi:10.1038/ngeo2343 http://www.nature.com/ngeo/journal/v8/n2/abs/ngeo2343.html#supplementary-information.

Tsuji, Y., K. Imai, Y. Mabuchi, T. Oie, K. Okada, Y. Iwabuchi, and F. Imamura (2012), Field Survey of the Tsunami of the 1677 Empo Boso-Oki and the 1611 Keicho Sanriku-Oki Earthquake, *Tsunami engineering technical report*, *29*, 189-207.

Tsuji, Y., Y. Mabuchi, T. Oie, and F. Imamura (2011), The tsunami record survey for the Keicho 16 Sanriku earthquake at the Iwate prefecture, *Tsunami engineering technical report*, *28*, 173-180.

Tsuji, Y., and K. Ueda (1995), The investigation of Keicho 16 (1611), Enpo 5 (1677), Houreki 12 (1768), Kansei 5 (1793) and Ansei 3 (1856) earthquake tsunami, *Historical Earthquakes*, *11*.

Tsunami Joint Survey Group, The Tohoku Earthquake (2011), NATIONWIDE FIELD SURVEY OF THE 2011 OFF THE PACIFIC COAST OF TOHOKU EARTHQUAKE TSUNAMI, *Journal of Japan Society of Civil Engineers, Ser. B2 (Coastal Engineering)*, *67*(1), 63-66, doi:10.2208/kaigan.67.63.

Tsushima, H., R. Hino, Y. Ohta, T. Iinuma, and S. Miura (2014), tFISH/RAPiD: Rapid improvement of near-field tsunami forecasting based on offshore tsunami data by incorporating onshore GNSS data, *Geophysical Research Letters*, *41*(10), 3390-3397, doi:10.1002/2014GL059863.

Uchida, N., and R. Bürgmann (2019), Repeating earthquakes, *Annual Review of Earth and Planetary Sciences*, *47*, 10.1146/annurev-earth-053018-060119.

Uchida, N., Y. Hu, and R. Bürgmann (2018), Co- and Postseismic Changes in Inland Seismicity and its Relationship with Transient Stress by the 2011 Tohoku-Oki Earthquake, *AOGS 2018*, SE28-A049.

Uchida, N., T. Iinuma, R. M. Nadeau, R. Bürgmann, and R. Hino (2016), Periodic slow slip triggers megathrust zone earthquakes in northeastern Japan, *Science*, *351*(6272), 488-492, doi:10.1126/science.aad3108.

Uchida, N., and T. Matsuzawa (2011), Coupling coefficient, hierarchical structure, and earthquake cycle for the source area of the 2011 off the Pacific coast of Tohoku earthquake inferred from small repeating earthquake data, *Earth Planets and Space*, *63*(7), 675-679, doi:10.5047/eps.2011.07.006.

Uchida, N., and T. Matsuzawa (2013), Pre- and postseismic slow slip surrounding the 2011 Tohoku-oki earthquake rupture, *Earth and Planetary Science Letters*, *374*(0), 81-91, doi:http://dx.doi.org/10.1016/j.epsl.2013.05.021.

Uchida, N., T. Matsuzawa, W. L. Ellsworth, K. Imanishi, T. Okada, and A. Hasegawa (2007), Source parameters of a M4.8 and its accompanying repeating earthquakes off Kamaishi, NE Japan - implications for the hierarchical structure of asperities and earthquake cycle, *Geophys. Res. Lett.*, *34*, doi:10.1029/2007GL031263.

Uchida, N., J. Nakajima, A. Hasegawa, and T. Matsuzawa (2009), What controls interplate coupling?: Evidence for abrupt change in coupling across a border between two overlying plates in the NE Japan subduction zone, *Earth Planet. Sci. Lett.*, *283*, 111-121.

Uchide, T. (2013), High-speed rupture in the first 20 s of the 2011 Tohoku earthquake, Japan, *Geophysical Research Letters*, *40*(12), 2993-2997, doi:10.1002/grl.50634.

Ujiie, K., H. Tanaka, T. Saito, A. Tsutsumi, J. J. Mori, J. Kameda, E. E. Brodsky, F. M. Chester, N. Eguchi, and S. Toczko (2013), Low Coseismic Shear Stress on the Tohoku-Oki Megathrust Determined from Laboratory Experiments, *Science*, *342*(6163), 1211, doi:10.1126/science.1243485.

Usami, K., K. Ikehara, T. Kanamatsu, and C. M. McHugh (2018), Supercycle in great earthquake recurrence along the Japan Trench over the last 4000 years, *Geoscience Letters*, *5*(1), 11, doi:10.1186/s40562-018-0110-2.

Usami, T. (1996), Materials for Comprehensive List of De- structive Earthquakes in Japan 416-1995, *University of Tokyo Press, (in Japanese)*, pp. 493.

Wang, C., X. Ding, X. Shan, L. Zhang, and M. Jiang (2012a), Slip distribution of the 2011 Tohoku earthquake derived from joint inversion of GPS, InSAR and seafloor GPS/acoustic measurements, *Journal of Asian Earth Sciences*, *57*, 128-136, doi:https://doi.org/10.1016/j.jseaes.2012.06.019.

Wang, K., and S. L. Bilek (2014), Invited review paper: Fault creep caused by subduction of rough seafloor relief, *Tectonophysics*, *610*(0), 1-24, doi:http://dx.doi.org/10.1016/j.tecto.2013.11.024.

Wang, K., L. Brown, Y. Hu, K. Yoshida, J. He, and T. Sun (2019), Stable Forearc Stressed by a Weak Megathrust: Mechanical and Geodynamic Implications of Stress Changes Caused by the M = 9 Tohoku-Oki Earthquake, *Journal of Geophysical Research: Solid Earth*, *124*(6), 6179-6194, doi:10.1029/2018JB017043.

Wang, L., and R. Bürgmann (2019), Statistical Significance of Precursory Gravity Changes Before the 2011 Mw 9.0 Tohoku-Oki Earthquake, *Geophysical Research Letters*, *46*(13), 7323-7332, doi:10.1029/2019GL082682.

Wang, L., S. Hainzl, and P. M. Mai (2015), Quantifying slip balance in the earthquake cycle: Coseismic slip model constrained by interseismic coupling, *Journal of Geophysical Research: Solid Earth*, *120*(12), 8383-8403, doi:https://doi.org/10.1002/2015JB011987.

Wang, L., C. K. Shum, F. J. Simons, B. Tapley, and C. Dai (2012b), Coseismic and postseismic deformation of the 2011 Tohoku-Oki earthquake constrained by GRACE gravimetry, *Geophysical Research Letters*, *39*(7), doi:https://doi.org/10.1029/2012GL051104.

Wang, R., S. Parolai, M. Ge, M. Jin, T. R. Walter, and J. Zschau (2013), The 2011 Mw 9.0 Tohoku Earthquake: Comparison of GPS and Strong - Motion Data, *B Seismol Soc Am*, *103*(2B), 1336-1347, doi:10.1785/0120110264.

Wang, Z., T. Kato, X. Zhou, and J. i. Fukuda (2016), Source process with heterogeneous rupture velocity for the 2011 Tohoku-Oki earthquake based on 1-Hz GPS data, *Earth, Planets and Space*, *68*(1), 193, doi:10.1186/s40623-016-0572-4.

Watanabe, H. (2001), Is it possible to clarify the real state of past earthquakes and tsunamis on the basis of legends ? -as an example of the 869 Jogan earthquake and tsunami -, *Historical Earthquakes*, *17*, 130-146.

Watanabe, S.-i., M. Sato, M. Fujita, T. Ishikawa, Y. Yokota, N. Ujihara, and A. Asada (2014), Evidence of viscoelastic deformation following the 2011 Tohoku-Oki earthquake revealed from seafloor geodetic observation, *Geophysical Research Letters*, *41*(16), 5789-5796, doi:10.1002/2014GL061134.

Wei, S., R. Graves, D. Helmberger, J.-P. Avouac, and J. Jiang (2012), Sources of shaking and flooding during the Tohoku-Oki earthquake: A mixture of rupture styles, *Earth and Planetary Science Letters*, *333-334*, 91-100, doi:https://doi.org/10.1016/j.epsl.2012.04.006.

Wei, S., A. Sladen, and t. A. group (2011), Updated Result 3/11/2011 (Mw 9.0), Tohoku-oki, Japan, *http://www.tectonics.caltech.edu/slip_history/2011_taiheiyo-oki/index.html, last accessed December 4, 2020*.

Woith, H., G. M. Petersen, S. Hainzl, and T. Dahm (2018), Review: Can Animals Predict Earthquakes?, *B Seismol Soc Am*, *108*(3A), 1031-1045, doi:10.1785/0120170313.

Yagi, Y., and Y. Fukahata (2011), Rupture process of the 2011 Tohoku-oki earthquake and absolute elastic strain release, *Geophysical Research Letters*, *38*(19), L19307, doi:10.1029/2011GL048701.

Yamagiwa, S., S. i. Miyazaki, K. Hirahara, and Y. Fukahata (2015), Afterslip and viscoelastic relaxation following the 2011 Tohoku-oki earthquake (Mw9.0) inferred from inland GPS and seafloor GPS/Acoustic data, *Geophysical Research Letters*, *42*(1), 66-73, doi:10.1002/2014GL061735.

Yamanaka, Y., and M. Kikuchi (2004), Asperity map along the subduction zone in northeastern Japan inferred from regional seismic data, *J. Geophys. Res.*, *109*(B7), B07307, doi:10.1029/2003jb002683.

Yamazaki, Y., K. F. Cheung, and T. Lay (2018), A Self-Consistent Fault Slip Model for the 2011 Tohoku Earthquake and Tsunami, *Journal of Geophysical Research: Solid Earth*, *123*(2), 1435-1458, doi:10.1002/2017JB014749.

Yokota, Y., T. Ishikawa, and S.-i. Watanabe (2018), Seafloor crustal deformation data along the subduction zones around Japan obtained by GNSS-A observations, *Scientific Data*, *5*(1), 180182, doi:10.1038/sdata.2018.182.

Yokota, Y., and K. Koketsu (2015), A very long-term transient event preceding the 2011 Tohoku earthquake, *Nat Commun*, *6*, doi:10.1038/ncomms6934.

Yokota, Y., K. Koketsu, Y. Fujii, K. Satake, S. i. Sakai, M. Shinohara, and T. Kanazawa (2011), Joint inversion of strong motion, teleseismic, geodetic, and tsunami datasets for the rupture process of the 2011 Tohoku earthquake, *Geophysical Research Letters*, *38*(7), doi:10.1029/2011GL050098.

Yoshida, K., and A. Hasegawa (2018), Hypocenter Migration and Seismicity Pattern Change in the Yamagata-Fukushima Border, NE Japan, Caused by Fluid Movement and Pore Pressure Variation, *Journal of Geophysical Research: Solid Earth*, *123*(6), 5000-5017, doi:10.1029/2018JB015468.

Yoshida, K., A. Hasegawa, T. Yoshida, and T. Matsuzawa (2019), Heterogeneities in Stress and Strength in Tohoku and Its Relationship with Earthquake Sequences Triggered by the 2011 M9 Tohoku-Oki Earthquake, *Pure and Applied Geophysics*, *176*(3), 1335-1355, doi:10.1007/s00024-018-2073-9.

Yoshida, K., K. Miyakoshi, and K. Irikura (2011), Source process of the 2011 off the Pacific coast of Tohoku Earthquake inferred from waveform inversion with long-period strong-motion records, *Earth, Planets and Space*, *63*(7), 12, doi:10.5047/eps.2011.06.050.

Yue, H., and T. Lay (2011), Inversion of high-rate (1 sps) GPS data for rupture process of the 11 March 2011 Tohoku earthquake (Mw 9.1), *Geophys. Res. Lett.*, *38*, L00G09, doi:10.1029/2011gl048700.

Yue, H., and T. Lay (2013), Source Rupture Models for the Mw 9.0 2011 Tohoku Earthquake from Joint Inversions of High - Rate Geodetic and Seismic Data, *B Seismol Soc Am*, *103*(2B), 1242-1255, doi:10.1785/0120120119.

Zhao, D., Z. Huang, N. Umino, A. Hasegawa, and H. Kanamori (2011), Structural heterogeneity in the megathrust zone and mechanism of the 2011 Tohoku-oki earthquake (Mw 9.0), *Geophysical Research Letters*, *38*(17), L17308, doi:10.1029/2011gl048408.

Zhou, X., G. Cambiotti, W. Sun, and R. Sabadini (2014), The coseismic slip distribution of a shallow subduction fault constrained by prior information: the example of 2011 Tohoku (Mw 9.0) megathrust earthquake, *Geophysical Journal International*, *199*(2), 981-995, doi:10.1093/gji/ggu310.